UTILIZING *DROSOPHILA* S2 CELLS AS A MODEL SYSTEM TO DETERMINE UNDERLYING MECHANISMS OF ER-ASSOCIATED DEGRADATION

APPROVED BY SUPERVISORY COMMITTEE

_____
Russell DeBose-Boyd, Ph.D.

_____
Joachim Seemann, Ph.D.

_____
Dean Smith, M.D., Ph.D.

_____
Philip Thomas, Ph.D.

DEDICATION

I dedicate this work to my parents, Brian and Deborah, and to my husband Chris, whom have been a constant source of encouragement and support throughout my education.

ACKNOWLEDGEMENT

I thank Dr. Russell DeBose-Boyd for the opportunity to be a part of his lab and providing an encouraging, yet challenging research environment. He has been a phenomenal mentor throughout my years in his lab, and I appreciate the time and effort he spent training me in numerous areas including experimental design, data analysis, and scientific writing. I am grateful for his willingness to allow me to take part in annual scientific meetings, and collaborate with other scientists. Most importantly, Russell has taught me to perform high quality research with scientific integrity.

I want to acknowledge the entire DeBose-Boyd lab for creating a collaborative lab environment. I particularly want to thank Youngah for her willingness to always answer my many questions, assisting me with sequencing, and teaching me all her tricks and techniques over the years. Kristi and Tammy, for their daily assistance, hundreds of gels they have provided, antibodies purified, and anything else I needed. I want to thank other past and present lab members who have provided experimental advice and insight including Dong-Jae, Rania, Isamu, Andy, and Marc. I especially want to thank Lindsey for her constant support, her encouragement throughout our graduate school courses, and for being an amazing friend. Additionally, I thank Lisa Beatty for her invaluable tissue culture expertise and assistance in generating stable cells lines.

I acknowledge the American Heart Association for funding my project and awarding me a SouthWest Affiliate Summer 2012 Predoctoral Fellowship 13PRE13980007.

Lastly, I want to acknowledge my committee members, Joachim Seemann, Dean Smith, and Philip Thomas. Thank you for providing constructive insight and suggestions at committee meetings and on this dissertation, and for the time you all spent evaluating my work. Joachim, I appreciate your collaboration and the time spent assisting me with immunofluorescence.

UTILIZING *DROSOPHILA* S2 CELLS AS A MODEL SYSTEM TO DETERMINE UNDERLYING MECHANISMS OF ER-ASSOCIATED DEGRADATION

by

REBECCA ANN FAULKNER

DISSERTATION

Presented to the Faculty of the Graduate School of Biomedical Sciences
The University of Texas Southwestern Medical Center
In Partial Fulfillment of the Requirements
For the Degree of

DOCTOR OF PHILOSOPHY

The University of Texas Southwestern Medical Center

Dallas, Texas

May 2014

UTILIZING *DROSOPHILA* S2 CELLS AS A MODEL SYSTEM TO DETERMINE UNDERLYING MECHANISMS OF ER-ASSOCIATED DEGRADATION

REBECCA ANN FAULKNER

The University of Texas Southwestern Medical Center at Dallas, 2014

RUSSELL DEBOSE-BOYD, Ph.D.

Proper folding of nascent polypeptides is vital to maintain cellular homeostasis; proteins that adopt aberrant confirmations are selectively degraded through a multi-step process known as endoplasmic reticulum-associated degradation (ERAD). Underlying mechanisms for ERAD of membrane proteins, especially those with multiple membrane-spanning segments, are poorly understood. There are currently many unknown aspects of ERAD including mechanisms for selection of polytopic substrates, whether dislocation from ER membranes into the cytosol requires a protein conducting channel, how solubility of the transmembrane domains are maintained during dislocation and

delivery to proteasomes for degradation. I have begun to address these questions by examining the ERAD of integral membrane proteins, HMG CoA reductase and Insig-1. These are ideal model substrates since their ERAD is strictly regulated by lipids, which helps guard against artifacts when various aspects of the reactions are reconstituted in model systems or *in vitro*. I utilized *Drosophila* S2 cells as a model system to identify proteins required for ERAD and cytosolic dislocation of HMG CoA reductase and Insig-1. S2 cells offer several advantages over mammalian cells, i.e., ease of transgene overexpression, simpler genome, and robust execution of RNA interference.

Previously, my laboratory reconstituted sterol-regulated ERAD of mammalian reductase in S2 cells and identified dHrd1 as the ubiquitin ligase required for the reaction. Using tandem affinity purification of dHrd1 and mass spectrometry, I identified components of the *Drosophila* ERAD pathway that associate with dHrd1. A role for dHrd1-associated proteins in cytosolic dislocation and ERAD of HMG CoA reductase was subsequently established using RNA interference. I also defined a role for dSel1, a dHrd1 complex component, in selection of reductase for ERAD, and identified the region of dSel1 required to bridge reductase to Insig-1. Finally, I demonstrated that physiologic conditions for Insig-1 ERAD in S2 cells are consistent with those in mammalian cells and identified dTeb4 as the ubiquitin ligase required for the reaction. Data indicate dHrd1 and dTeb4 share common ERAD components. Surprisingly, genetic and pharmacologic experiments indicate that Insig-1 and reductase are degraded through distinct mechanisms mediated by different ubiquitin ligase complexes in S2 cells.

TABLE OF CONTENTS

CHAPTER ONE: INTRODUCTION

PRIOR PUBLICATIONS

Faulkner, R.A., W. McAlpine, R.A. DeBose-Boyd. A role for dSel1 in selection of HMG CoA reductase for lipid-regulated ER-associated degradation in insect cells. (in preparation)

Faulkner, R.A., A.D. Nguyen, Y. Jo, R.A. DeBose-Boyd. 2013. Lipid-regulated degradation of HMG-CoA reductase and Insig-1 through distinct mechanisms in insect cells. *J. Lipid Res.* 54:1011-1022. PMID: 23403031

LIST OF FIGURES

LIST OF TABLES

LIST OF APPENDICES

LIST OF ABBREVIATIONS

BAP, biotin acceptor peptide

dsRNA, double-stranded RNA

ER, endoplasmic reticulum

ERAD, endoplasmic reticulum-associated degradation

HA, hemagglutinin

25-HC, 25-hydroxycholesterol

HI-FCS, heat-inactivated fetal calf serum

HI-DFCS, heat-inactivated delipidated fetal calf serum

HI-LPDS, heat-inactivated lipoprotein-deficient serum

LPDS, lipoprotein-deficient serum

RNAi, RNA interference

SREBP, sterol regulatory element-binding protein

TAP, tandem affinity purification

TEV, tobacco etch virus

UBA, ubiquitin-associated

UBL, ubiquitin-like

Ubx, ubiquitin regulatory X

Ubxd8, ubiquitin regulatory X domain containing protein 8

CHAPTER ONE:

Introduction

1.1 Importance of ER-associated degradation

The endoplasmic reticulum (ER) is a major site of protein biosynthesis, ensuring their delivery into the secretory pathway. Approximately 30% of newly synthesized proteins are translocated into the lumen of the ER, which houses a battery of molecular chaperones that assist in folding and assembly of nascent polypeptides (1, 2). While in the lumen, proteins are subjected to modifications including N-linked glycosylation and disulfide bond formation, which promote proper folding (3, 4). Proteins that adopt aberrant confirmations are targeted for degradation by 26S proteasomes through a process called ER-associated degradation (ERAD) (5, 6). Efficient degradation of defective proteins through ERAD is instrumental in maintaining homeostasis in the ER since they are prone to form insoluble aggregates that can substantially reduce cell viability by triggering apoptosis (7).

Understanding the molecular mechanisms of ERAD is essential because the accumulation of defective ERAD substrates has been linked to a number of human diseases (8). These diseases stem from loss-of-function mutations in polypeptide sequences resulting in either disposal or retention of misfolded proteins. A loss-of-function condition results in protein disposal and occurs when a protein that is usually secreted becomes misfolded and is retained in the ER lumen and disposed by ERAD. For example, mutated α1-antitrypsin is degraded rather than secreted and delivered to

the lungs resulting in lung emphysema (9, 10). Many other diseases are caused in a similar manner including cystic fibrosis, Alzheimer's disease, polycystic kidney disease, diabetes mellitus, and familial hypercholesterolemia (11-17). In contrast, gain-of-toxic function mutations lead to retention of misfolded proteins triggering the unfolded protein response and leading to tissue damage. This effect causes many diseases including Parkinson's disease, Charcot-Marie-Tooth syndrome, Wilson disease, X-linked autism, and Asperger syndrome (18-21). Understanding the underlying mechanisms of ERAD is vital to development of therapies targeting components of the ERAD pathway to treat these diseases.

1.2 Understanding ERAD Pathways

The ERAD pathway is a highly conserved, multistep process; substrates of the pathway include both soluble proteins within the ER lumen and integral membrane proteins with one or more membrane-spanning helices (**Figure 1-1**). Cytosolic and lumenal chaperones survey potential substrates for the presence of misfolded domains and engage specific ERAD pathways depending on the location of the misfolded region. For instance, cytosolic chaperones engage the ERAD-C pathway whereas lumenal chaperones engage the ERAD-L pathway (22, 23). Misfolded integral membrane proteins engage ERAD-M; however, chaperones involved in selection of these substrates are unknown. These pathways have been primarily characterized in the yeast system where there are two E3 ligases, Hrd1 and Doa10. Hrd1 engages substrates through the ERAD-L and –M pathways where as Doa10 is responsible for

the ERAD-C pathway (22). However, higher organisms have many more E3 ligases as well as a larger repertoire of substrates resulting in a much more complex ERAD system that has yet to be fully understood.

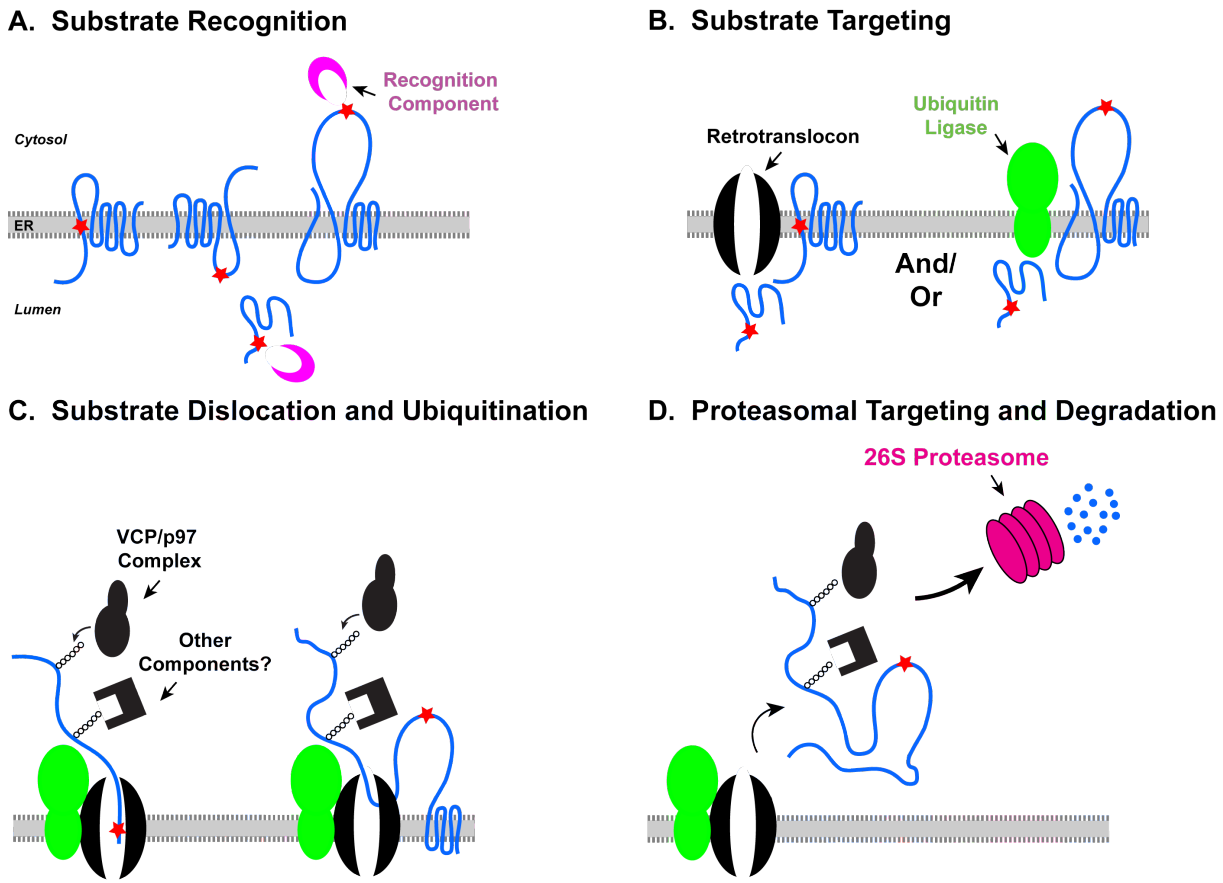

Figure 1-1. Schematic representation of the ERAD pathway. ERAD substrates can be either soluble proteins in the ER lumen, or integral membrane proteins with misfolded regions in the lumen, cytosol, or intramembrane regions. Lumenal and cytosolic chaperones recognize misfolded domains (A) and target them to either ubiquitin ligases or retrotranslocation machinery (B). The substrate is ubiquitinated and dislocated to the cytosol through an unknown mechanism that requires the AAA-ATPase VCP/p97 (C). Then the protein is targeted to the 26S proteasome for degradation (D).

The key events in the ERAD pathway include substrate recognition, polyubiquitination, membrane extraction/dislocation from ER membranes into the cytosol, and delivery to proteasomes for degradation (24). Much has been learned about ERAD through studies of soluble substrates such as mutant forms of the

Saccharomyces cerevisiae proteins carboxypeptidase Y and alpha-factor precursor. It is widely accepted that these misfolded proteins are selected for ERAD by lumenal chaperones including heat shock protein homologs (e.g., Hsp40, Hsp70, Hsp90). Once selected, soluble ERAD substrates are transported across the ER membrane into the cytosol (retrotranslocation) through a protein-conducting channel. Candidates for this channel are the polytopic Derlin-1 protein and Sec61, the major component of the translocation channel that imports polypeptides into the ER (5, 25, 26). Following retrotranslocation into the cytosol the substrate becomes ubiquitinated through the action of ubiquitin ligating enzymes, which transfer activated ubiquitin from ubiquitin-conjugating enzymes (27). Ubiquitination triggers delivery of substrates to the proteasomes through a mechanism that appears to be mediated by p97, a cytosolic AAA-ATPase (28). Ubiquitin regulatory X (UBX) domain containing proteins such as Ubxd8 and Ubxd2 recruit p97 to the ER membrane (29). The p97 protein associates with ubiquitinated substrates through Npl4 and Ufd1, two substrate recruitment cofactors that both bind polyubiquitin chains. Biochemical studies suggest a model in which the ATPase activity of p97 drives extraction of the ubiquitinated substrate from the ER membrane into the cytosol (30). Following this extraction, substrates are delivered to proteasomes through an unclear mechanism involving a variety of ubiquitin-associated (UBA) and ubiquitin-like (UBL) domain-containing proteins. For example, Ufd2, an E4 enzyme that extends polyubiquitin chains (31), the deubiquitinating enzyme Otu1, and Rad23 and Dsk2 which are proteins that can bind both polyubiquitin chains and the proteasome (32).

A thorough understanding of mechanisms underlying ERAD of integral membrane proteins is lacking. ERAD of these proteins is complex, especially for substrates with multiple membrane-spanning regions. It is currently unknown how polytopic ERAD substrates with misfolded membrane domains are selected for ubiquitination and subsequent degradation. Does their selection involve the action of uncharacterized membrane chaperones? Some membrane bound ERAD substrates appear to become completely dislocated into the cytosol before they are degraded. This has been observed with MHC class I heavy chains and unpaired T-cell receptor subunits that contain one membrane-spanning segment as well as with proteins that contain multiple membrane-spanning segments such as cystic fibrosis transmembrane conductance regulator, Ste6p, and connexins (33-36). Does cytosolic dislocation of membrane-bound ERAD substrates require a protein-conducting channel formed by Sec61 or Derlin1? If not, what is the mechanism for dislocation of these types of substrates? How is solubility of transmembrane domains maintained during dislocation? Furthermore, how are dislocated substrates delivered to the proteasomes? Addressing these questions requires rigorous examination of a model substrate with multiple membrane-spanning segments.

1.3 Model ERAD Substrates

The central role of the ERAD pathway is cellular quality control; however, the pathway is also employed for regulatory purposes. Two prominent examples of this is lipid-regulated ERAD of polytopic membrane proteins 3-hydroxy-3-methylglutaryl

coenzyme A (HMG CoA) reductase and Insig-1, a negative regulator of reductase and another ER membrane protein called Scap. HMG CoA reductase is a rate-limiting step of the mevalonate pathway through which cholesterol and nonsterol isoprenoids are produced (37). The enzyme is anchored in the ER membrane by the hydrophobic N-terminal domain that contains eight membrane-spanning helices (38). The large C-terminal domain projects into the cytosol and catalyzes the reduction of HMG CoA to mevalonate (39, 40). Therefore HMG CoA reductase is subject to a complex feedback system through multiple mechanisms to ensure cholesterol homeostasis. When flux through the cholesterol biosynthetic pathway is high, HMG CoA reductase is subject to accelerated ERAD triggered by sterol and non-sterol isoprenoids (41).

My laboratory discovered that in mammalian cells, sterol accumulation triggers binding of ER membrane proteins Insig-1 or Insig-2 to the membrane domain of HMG CoA reductase as depicted in **Figure 1-2** (42-45). Insigs are associated with membrane-bound ubiquitin ligases gp78 and Trc8, which transfer ubiquitin from the ubiquitin conjugating enzyme Ubc7 to two lysine residues on cytosolic loops of the reductase membrane domain (46). Ubiquitination marks reductase for membrane extraction and dislocation

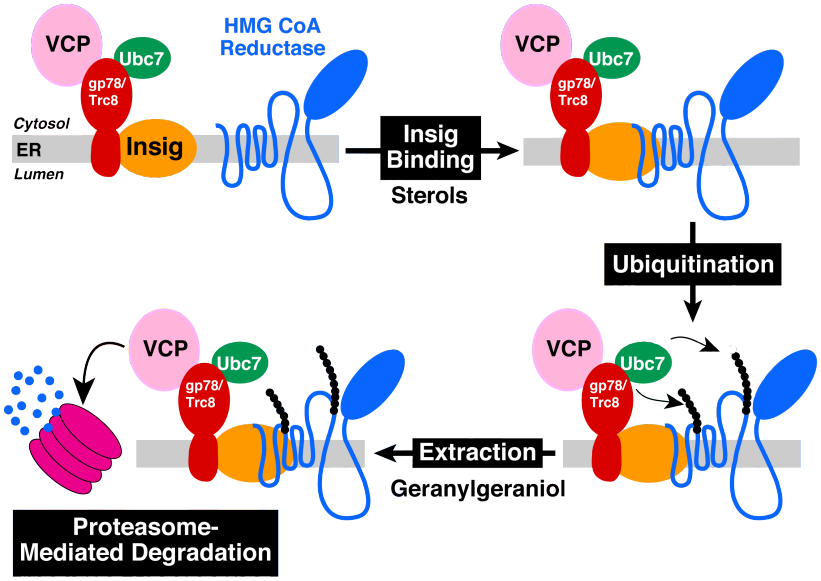

Figure 1-2. Illustration of HMG CoA reductase degradation in mammalian cells.

into the cytosol for proteasomal degradation through a reaction mediated in part by the AAA-ATPase VCP/p97 (47).

Insigs also mediate sterol regulation of Scap (48), which escorts membrane-bound transcription factors called sterol regulatory element-binding proteins (SREBPs) from the ER to the Golgi in sterol-deprived cells (49-51). In the Golgi, transcriptionally active fragments of SREBPs are proteolytically released from membranes into the cytosol, allowing them to migrate into the nucleus and activate genes encoding reductase and other cholesterol biosynthetic enzymes (52). Sterol-mediated binding of Insigs to Scap traps the protein along with its associated SREBP in the ER. Without transport to the Golgi, SREBPs do not become released from membranes and expression of SREBP target genes declines.

Although both Insigs associate with both Scap and reductase, only Insig-1 is subject to ERAD (53). In contrast to that of reductase, ERAD of Insig-1 is inhibited by sterols; the reaction is also blocked by unsaturated fatty acids as illustrated in **Figure 1-3**. In lipid-deprived cells, Insig-1 binds to gp78 rather than to reductase or Scap and thus

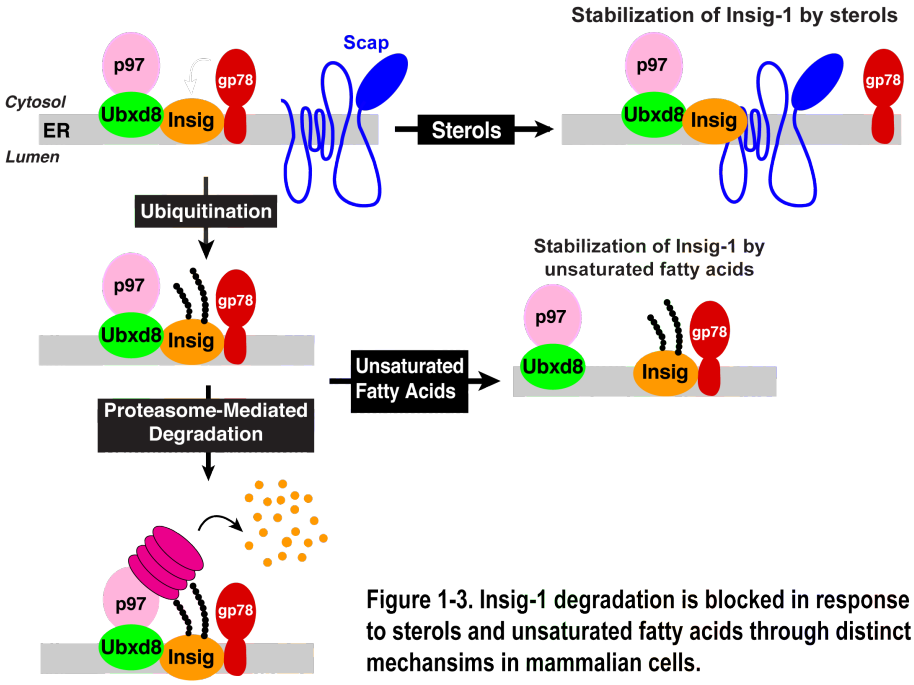

Figure 1-3. Insig-1 degradation is blocked in response to sterols and unsaturated fatty acids through distinct mechansims in mammalian cells.

becomes ubiquitinated and degraded. Sterol induced binding of Insig-1 to Scap displaces gp78, preventing Insig-1 ubiquitination and degradation. Unsaturated fatty acids block Insig-1 ERAD by inhibiting its association with ubiquitin regulatory X (Ubx) domain containing protein-8 (Ubxd8), which mediates recruitment of VCP/p97 to membranes (54). Thus, unsaturated fatty acids inhibit Insig-1 ERAD by blocking its extraction from ER membranes.

Despite recent progress in understanding lipid regulated ERAD of reductase and Insig-1, much remains to be determined. The sterol regulated ERAD of these proteins makes them ideal model substrates to elucidate mechanisms through which polytopic membrane proteins, such as reductase and Insig-1, are selected for ERAD, extracted from ER membranes into the cytosol, and delivered to proteasomes for degradation.

1.4 A Model System: *Drosophila* S2 Cells

Proteins involved in ERAD are highly conserved from yeast to mammals. To accelerate discovery of new molecules that mediate lipid-regulated degradation of HMG CoA reductase and Insig-1, I studied the reactions in *Drosophila* S2 cells. Using *Drosophila* S2 cells as a model system to study ERAD offers a number of advantages over mammalian cells. **1)** Ease of growth and maintenance; S2 cells are grown at room temperature in atmospheric CO_2 conditions. **2)** Transgenes can be easily and quickly introduced into S2 cells to study their function. **3)** RNA interference (RNAi) is simpler, more effective, and cheaper in S2 cells than in mammalian cells (55). Double-stranded RNA (dsRNA) ranging from 250-1000 bp can be used for RNAi knockdown since

Drosophila lack the interferon-response that causes many mammalian cells to shut down transcription when challenged with dsRNA >21 bp. These long dsRNAs can be quickly and affordably synthesized in a single PCR reaction using either genomic DNA or cloned cDNA as a template, followed by *in vitro* transcription. S2 cells efficiently take up these long dsRNAs eliminating the need for the expensive transfection reagents required for mammalian cells. **4)** The *Drosophila* genome is simpler and less redundant than the mammalian genome as revealed by sequencing and annotation. Thus, S2 cells are less affected by the problems of genetic redundancy, which can confound the analysis in mammalian cells. **5)** Although S2 cells express homologs for SREBP and Scap, dSREBP-dScap trafficking to the Golgi is not regulated by sterols, but a lipid derived from palmitate and ethanolamine (56, 57). Additionally, *Drosophila* cells lack a recognizable Insig gene and cannot synthesize sterols *de novo* since many enzymes in the mevalonate pathway are not present (58).

Previously, my laboratory reconstituted sterol-accelerated ERAD of mammalian reductase in *Drosophila* S2 cells (59). In these studies, S2 cells were transfected with expression plasmids encoding epitope-tagged versions of the membrane domain of hamster reductase, the minimal requirement for ERAD (40, 42), and mammalian Insig-1. ERAD of reductase in S2 cells mirrored that in mammalian cells with regard to the following requirements: dependence on the action of mammalian Insig-1 or Insig-2, stimulation by sterols plus nonsterol isoprenoids, and inhibition by the proteasome inhibitor MG-132. These findings indicate that factors mediating reductase ERAD in mammalian cells are conserved in *Drosophila*.

CHAPTER TWO:

Lipid Regulated Degradation of HMG CoA Reductase and Insig-1 through Distinct Mechanisms in Insect Cells

2.1 Abstract

In mammalian cells, levels of the integral membrane proteins 3-hydroxy-3-methylglutaryl coenzyme A reductase and Insig-1 are controlled by lipid-regulated, endoplasmic reticulum (ER)-associated degradation (ERAD). The ERAD of reductase slows a rate-limiting step in cholesterol synthesis and results from sterol-induced binding of its membrane domain to Insig-1 and the highly related Insig-2 protein. Binding to Insigs bridges reductase to ubiquitin ligases that facilitate its ubiquitination, thereby marking the protein for cytosolic dislocation and proteasomal degradation. In contrast to reductase, Insig- 1 is subjected to ERAD in lipid-deprived cells. Sterols block this ERAD by inhibiting Insig-1 ubiquitination, whereas unsaturated fatty acids block the reaction by preventing the protein's cytosolic dislocation. In previous studies, we found that the membrane domain of mammalian reductase was subjected to ERAD in *Drosophila* S2 cells. This ERAD was appropriately accelerated by sterols and required the action of Insigs, which bridged reductase to a *Drosophila* ubiquitin ligase. We now report reconstitution of mammalian Insig-1 ERAD in S2 cells. The ERAD of Insig-1 in S2 cells mimics the reaction that occurs in mammalian cells with regard to its inhibition by either sterols or unsaturated fatty acids. Genetic and pharmacologic manipulations coupled with subcellular fractionation indicate that Insig-1 and reductase are degraded through

distinct mechanisms in S2 cells that are mediated by different ubiquitin ligase complexes. Together, these results establish *Drosophila* S2 cells as a model system to elucidate mechanisms through which lipid constituents of cell membranes (i.e., sterols and fatty acids) modulate the ERAD of Insig-1 and reductase.

2.2 Introduction

In mammalian cells, the endoplasmic reticulum (ER)-associated degradation (ERAD) pathway controls levels of two integral membrane proteins that play important roles in the maintenance of lipid homeostasis, 3-hydroxy-3-methylglutaryl coenzyme A (HMG CoA) reductase and Insig-1. HMG CoA reductase catalyzes the reduction of HMG CoA to mevalonate, a rate-limiting reaction in the synthesis of cholesterol and essential nonsterol isoprenoids (37). Sterol accumulation triggers binding of reductase to either Insig-1 or its highly related isoform Insig-2 in ER membranes (42-45). Insig binding is mediated entirely by the membrane domain of reductase, which contains eight membrane-spanning helices and precedes a large C-terminal cytosolic domain containing all of the enzyme's catalytic activity (39, 40). Insigs associate with two membrane-bound ubiquitin ligases called gp78 and Trc8 that initiate ubiquitination of reductase (46). This ubiquitination marks reductase for membrane extraction and dislocation into the cytosol for proteasomal degradation through a reaction mediated by the AAA-ATPase VCP/p97 (47).

Insigs also mediate the sterol regulation of Scap (48), an ER membrane protein that like reductase contains an N-terminal membrane domain with eight membrane-

spanning helices, followed by a cytosolic C-terminal domain. The C-terminal domain of Scap mediates an association with membrane-bound transcription factors called sterol regulatory element-binding proteins (SREBPs) (60). In sterol-deprived cells, Scap mediates translocation of SREBPs from the ER to the Golgi where transcriptionally active fragments of SREBPs become proteolytically released from Golgi membranes (50, 51, 61). These fragments then migrate into the nucleus and activate transcription of target genes, which include reductase and other enzymes required for synthesis of cholesterol and fatty acids (52). Sterol-induced binding of Insigs to the membrane domain of Scap traps the protein along with its associated SREBP in the ER (62). Without transport to the Golgi, SREBPs do not become proteolytically activated and expression of SREBP target genes declines.

Topology studies indicate that the mammalian Insig proteins consist of six transmembrane helices separated by short hydrophilic loops (48). Although the transmembrane regions of Insig-1 and Insig-2 exhibit 85% amino acid identity and both proteins bind to Scap and reductase in a sterol-regulated manner, only Insig-1 is subjected to ERAD (53). In contrast to that of reductase, the ERAD of Insig-1 is inhibited by sterols and the reaction is also blocked by unsaturated fatty acids (53). When cells are deprived of lipids (i.e., cholesterol and fatty acids), Insig-1 binds to gp78 rather than to reductase or Scap and thus becomes ubiquitinated and degraded. Sterol induced binding of Insig-1 to Scap displaces gp78 and thereby prevents Insig-1 ubiquitination and degradation. Unsaturated fatty acids do not block Insig-1 ubiquitination, but they rather prevent the protein's ERAD by inhibiting its association

with ubiquitin regulatory X (Ubx) domain containing protein-8 (Ubxd8), which mediates recruitment of VCP/p97 to membranes (54, 63). Thus, unsaturated fatty acids inhibit the ERAD of Insig-1 by blocking its membrane extraction into the cytosol.

Although membrane extraction and cytosolic dislocation are well-established events in the ERAD of integral membrane proteins such as Insig-1 and reductase (64), underlying mechanisms for these reactions are not fully understood. To accelerate discovery of additional factors that mediate ERAD of integral membrane proteins, we previously examined sterol-accelerated ERAD of mammalian reductase in *Drosophila* S2 cells (59). We chose to study reductase ERAD in S2 cells because they lack a recognizable Insig gene and cannot synthesize sterols *de novo* (58, 65). In addition, general ERAD components are highly conserved from yeast to humans (see **Table 2-1**) (22). Thus, the potential role of these components in reductase ERAD can be readily determined in RNA interference (RNAi) experiments, which can be effectively executed in S2 cells (55). Our initial studies revealed that in S2 cells, ERAD of the membrane domain of mammalian reductase, the minimal requirement for sterol- accelerated ERAD (40, 42), precisely mirrored the reaction that occurs in mammalian cells with regard to: 1) dependence on the action of mammalian Insig-1 or Insig-2; 2) maximal stimulation by sterols plus nonsterol isoprenoids; and 3) inhibition by the proteasome inhibitor MG-132 (59). The *Drosophila* homolog of the yeast ubiquitin ligase Hrd1 (designated dHrd1), which exhibits significant sequence homology with gp78, was found to be required for sterol-accelerated reductase ERAD in S2 cells. These findings suggest that

mechanisms for Insig-dependent ERAD of reductase and factors that mediate these reactions are highly conserved in *Drosophila* S2 cells.

Considering that specificity of substrate ubiquitination is primarily determined by ubiquitin ligases that exist in large multiprotein complexes (22, 66, 67), we initiated the current studies by characterizing the dHrd1 ubiquitin ligase complex in S2 cells. Tandem affinity purification of dHrd1 coupled with mass spectrometry led to the identification of *Drosophila* homologs of several proteins known to associate with Hrd1 in yeast. RNA interference (RNAi) together with degradation and cytosolic dislocation assays were subsequently employed to determine a role for these newly identified components of the *Drosophila* ERAD pathway in mammalian reductase degradation. We also reconstituted the ERAD of mammalian Insig-1 in S2 cells and found that the reaction was regulated by both sterols and unsaturated fatty acids through similar mechanisms that occur in mammalian cells. Further investigation revealed that while reductase ERAD was mediated by dHrd1 in S2 cells, the ERAD of Insig-1 required another *Drosophila* ubiquitin ligase called dTeb4. The membrane-bound dTeb4 is a close homolog of mammalian Teb4 and yeast Doa10 (68). Remarkably, dHrd1 and dTeb4 degraded reductase and Insig-1 through completely distinct mechanisms. The reductase appeared to become ubiquitinated on ER membranes *prior* to its dislocation into the cytosol and proteasomal degradation. In contrast, Insig-1 became dislocated into the cytosol prior to its ubiquitination in a manner similar to that proposed for soluble ERAD substrates (5). Considered together, these results not only establish *Drosophila* S2 cells as a viable model system to elucidate general mechanisms for lipid-mediated

ERAD of reductase and Insig-1, but they also reveal that ubiquitin ligases can dictate the ERAD pathway through which integral membrane substrates become degraded.

2.3 Materials and Methods

Materials – We obtained cycloheximide, oleate, and 25-hydroxycholesterol from Sigma; fatty acid-free bovine serum albumin (BSA) from Roche Molecular Biochemicals; blasticidin from Invitrogen; MG-132 from Peptide Institute, Inc. (Osaka, Japan); digitonin from Calbiochem; Fos-choline-13 from Anatrace; anti-Myc-coupled agarose beads from Sigma; and PYR-41 from Boston Biochem. Stock solutions of oleate were prepared in 0.15 M NaCl and 10% (w/v) fatty acid-free BSA as previously described (69). Other reagents, including sodium mevalonate, lipoprotein-deficient serum (LPDS), and delipidated fetal calf serum (DFCS) were prepared as previously described (69, 70).

Expression Plasmids – The following expression plasmids have been previously described in the indicated reference: pAc-HMG-Red-T7 (TM1-8), which encodes the membrane domain (amino acids 1- 346) of hamster reductase fused to three copies of the T7 epitope under transcriptional control of the *Drosophila* actin 5c promoter (pAc) (59); pAc-Insig-1-Myc and pAc-Insig-2-Myc encoding amino acids 1-277 and 1-225 of human Insig-1 and -2, respectively, followed by six copies of the c-Myc epitope (65); pAc-Scap encoding amino acids 1-1276 of hamster Scap (65); and pAc-dHrd1-T7 encoding amino acids 1-626 of *Drosophila* Hrd1 (59). The pAc-dHrd1-TAP expression plasmid was generated by replacing the T7 epitope in pAc-dHrd1-T7 with three copies

of the FLAG epitope followed by a cleavage site for the tobacco etch virus (TEV) protease and Protein A. The open reading frame for the *Drosophila* homolog of Teb4 (designated dTeb4, CG1317) was amplified by PCR with the Phusion DNA Polymerase Kit (New England Biolabs) using first strand cDNA obtained by reverse transcription of total RNA isolated from S2 cells. Primers used in this amplification contained sequences that encode for a single epitope derived from human influenza hemagglutinin (HA). The PCR products were gel purified, subjected to restriction enzyme digest, and subcloned into the pAc5.1/V5-HisB expression vector. The QuikChangeTM Site- Directed Mutagenesis Kit (Stratagene) was used to mutate cysteine-10 in pAc-dTeb4-HA to serine, creating a catalytically inactive RING finger mutant of the enzyme. The pAc-HA-ubiquitin expression plasmid was obtained by cloning the cDNA for human ubiquitin containing a single N-terminal HA epitope into the pAc5.1/V5-HisB expression vector. The integrity of all plasmids was confirmed by DNA sequencing.

Culture and Transfection of Drosophila S2 Cells – Stock cultures of *Drosophila* S2 cells were maintained in a monolayer in medium A (Schneider's *Drosophila* medium) supplemented with 10% (v/v) heat- inactivated fetal calf serum (HI-FCS) at 23°C. The cells were set up for experiments in 6-well plates on day 0 at a density of 1 X 106 cells per well in medium A supplemented with 10% HI-FCS. On day 1 the cells were washed with medium B (Express Five Serum Free Medium) and transfected with 0.03 - 3 µg of DNA/well using Maxfect^{TM} Transfection Reagent (KD Medical) at a ratio of 1 µg DNA to 5 µl Maxfect^{TM} in 1 ml of medium B. The total amount of DNA transfected per well was

kept constant in each experiment by the addition of empty pAc5.1 vector. On day 2, each well received 1 ml of medium C (Schneider's *Drosophila* medium containing 100 units/ml penicillin and 100 µg/ml streptomycin sulfate) supplemented with 20% HI-FCS, HI-LPDS, or HI-DFCS (10% final concentration). Following incubation for 24 h at 23 °C, cells were subjected to treatments described in figure legends and harvested for analysis as described below.

Stable Transfection of Drosophila S2 Cells – *Drosophila* S2 cells were set up in 6-well plates on day 0 at a density of 1 X 10^6 cells per well in medium A supplemented with 10% HI-FCS. On day 1, cells were washed with medium B and transfected with 1 µg of pAc-dHrd1-TAP together with 50 ng of pCoBlast selection vector in medium B using MaxfectTM. On day 2, each well received 1 ml of medium C supplemented with 20% HI-FCS (final concentration 10%). Selection began on day 3 by refeeding cells with medium C containing 10% HI-FCS and 5 µg/ml blasticidin. Medium was changed as needed until colonies formed. Single cell colonies were isolated and screened for expression of dHrd1-TAP by immunoblotting detergent lysates with anti-FLAG IgG. A single colony of cells (designated S2/dHrd1- TAP) was selected and maintained in medium A supplemented with 10% (v/v) heat-inactivated fetal calf serum (HI-FCS) and 5 µg/ml blasticidin.

Tandem Affinity Purification – S2/dHrd1-TAP cells grown in suspension flasks were collected by centrifugation at 1500 X g for 5 minutes at 4°C. Cell pellets were washed

with PBS and lysed in buffer containing 10 mM HEPES-KOH pH 7.4, 10 mM KCl, 1.5 mM MgCl2, 5 mM EDTA, 5 mM EGTA, 5 mM dithiothreitol, and 0.1 mM leupeptin supplemented with 1% digitonin and a protease inhibitor cocktail (25 µg/ml *N*-acetyl-leucinal-leucinal-norleucinal, 2 µg/ml aprotinin, 0.5 mM Pefabloc, 5 µg/ml pepstatin A, 0.5 mM phenylmethylsulfonyl fluoride). Clarified lysates were subjected to immunoprecipitation with human IgG-conjugated Sepharose beads (GE Healthcare) for 16 h at 4°C. After washing the immunoprecipitates 5 times (15 minutes each) in lysis buffer containing 0.1% digitonin, precipitated proteins were eluted from the beads by treatment with AcTEV protease (Invitrogen) for 16 h at 4°C. The released proteins were subjected to a second round of immunoprecipitation with anti-FLAG- coupled agarose beads (Sigma) for 5 h at 4°C. Following extensive washes in lysis buffer containing 0.1% digitonin, bound proteins were eluted by rotating the beads with a peptide containing 5 copies of the FLAG epitope (custom synthesized by Genemed Synthesis). The eluted material was subsequently fractionated by SDS-PAGE and the proteins were visualized by Colloidal Blue (Invitrogen) staining. Segments of the gel that contained visible bands were excised and proteins were identified by tandem mass spectroscopy in the Protein Chemistry Core Facility at the University of Texas Southwestern Medical Center.

Preparation of Whole Cell Lysates – Treatment conditions prior to harvest are described in the figure legends. Following treatments, cells from triplicate wells were combined and collected by centrifugation at 1500 X g for 5 minutes at 4°C. Cell pellets were

washed with PBS and resuspended in buffer containing 50 mM Tris-HCl pH 8.0, 150 mM NaCl, 0.1% (w/v) SDS, 1.5% (w/v) Nonidet P-40, 0.5% (w/v) sodium deoxycholate, and 2 mM MgCl2 supplemented with the protease inhibitor cocktail. The cell suspension was then lysed by passage through a 22-gauage needle and subsequently rotated for 30 minutes at 4°C. Insoluble material was removed by centrifugation at 17,000 X g for 15 minutes at 4°C and clarified lysates were mixed with SDS-PAGE loading buffer.

Subcellular Fractionation – Following treatments described in the figure legends, cells from triplicate wells were scraped, washed in PBS, and the cell pellet resuspended in buffer containing 10 mM HEPES- KOH pH 7.4, 10 mM KCl, 1.5 mM MgCl2, 5 mM EDTA, 5 mM EGTA, 5 mM dithiothreitol, 0.1 mM leupeptin, and 250 mM sucrose supplemented with the protease inhibitor cocktail. The cell suspension was passed through a 22-gauage needle and centrifuged at 1000 X g for 7 minutes at 4°C. The resulting post-nuclear supernatants were further subjected to centrifugation at 100,000 X g for 1 h at 4°C. The pellet fraction obtained from this spin (designated membranes) was resuspended in buffer containing 10 mM Tris-HCl pH 6.8, 100 mM NaCl, 1% (w/v) SDS, 1 mM EDTA, 1 mM EGTA and mixed with SDS- PAGE loading buffer. The supernatant fraction obtained from the 100,000 X g spin (designated cytosol) was precipitated overnight with 5X volume of acetone at -20°C; precipitated material was pelleted by centrifugation at 17,000 X g for 10 minutes at 4°C and resuspended in buffer containing 10 mM Tris-HCl pH 6.8, 100 mM NaCl, 1% (w/v) SDS, 1 mM EDTA, and 1 mM EGTA, and subsequently mixed with SDS-PAGE loading buffer.

Immunoblot Analysis and Immunoprecipitation of Insig-1 – Aliquots of whole cell lysates, membrane, or cytosol fractions were subjected to 10% SDS-PAGE after which, the proteins were transferred to nitrocellulose membranes (GE Healthcare). Immunoblot analysis was carried out with the following primary antibodies: monoclonal anti-T7 Tag IgG (Novagen), IgG-9E10, a mouse monoclonal antibody against the c-Myc epitope purified from culture medium of hybridoma clone 9E10 (American Type Culture Collection), IgG-3B2, a mouse monoclonal antibody against *Drosophila* SREBP (57), IgG-9D5, a mouse monoclonal antibody against hamster Scap (71), monoclonal anti-HA IgG (Sigma), polyclonal anti-actin IgG (Sigma); and anti-E1 IgG (Calbiochem). Primary antibodies were detected with horseradish peroxidase-conjugated donkey anti-mouse, anti-rabbit, or anti-biotin IgG (Jackson ImmunoResearch Laboratories) using SuperSignal West Pico Chemiluminescent Substrate (Thermo Scientific).

Immunoprecipitation of transfected Insig-1-Myc from detergent lysates of S2 cells was carried out as previously described (53). Briefly, cells were harvested, lysed in PBS containing 1% Fos-choline- 13 and subjected to centrifugation at 16,000 X g for 15 min at 4 °C. The clarified lysates were adjusted to 2 M urea and immunoprecipitated with 100 µl anti-Myc-coupled agarose beads. Aliquots of the immunoprecipitates were then subjected to SDS-PAGE followed by immunoblot analysis with monoclonal anti-HA IgG (against ubiquitin) and IgG-9E10 (against Insig-1).

Production of Double-stranded (ds) RNA – Total RNA isolated from *Drosophila* S2 cells

using RNA STAT 60 (Tel-Test, Inc.) was subjected to reverse transcription PCR using the TaqMan® reagents (Applied Biosystems). DNA templates for dsRNA synthesis were amplified from first strand cDNA using the Phusion DNA polymerase (New England Biolabs) and previously described primers (59). The resulting PCR products were purified using the QIAquick PCR Purification Kit (Qiagen) and used as templates to generate dsRNAs using the MEGAscript® T7 Kit (Ambion). Resulting dsRNAs were purified from the reaction using the RNeasy Mini Kit (Qiagen).

RNA Interference (RNAi)-mediated Knockdown in Drosophila S2 Cells – S2 cells were plated on day 0 in 6-well plates at a density of 1 X 10^6 cells/well in 1 ml of medium B. Immediately after plating, 15 µg of dsRNA was added to each well and incubated for 1 h. Each well subsequently received 2 ml of medium C supplemented with either 10% HI-FCS, HI-LPDS, or HI-DFCS.

Isolation of Total RNA and Quantitative Real-time PCR Analysis – The total RNA isolated from S2 cells using STAT 60 was subjected to reverse transcription PCR as described above. Quantitative real-time PCR was performed as previously described (59, 72). The comparative C_t method was used to calculate the relative expression and the *Drosophila* Ribosomal Protein 49 was used as an internal control to account for variations in mRNA levels.

2.4 Results

In previous studies, we found that the *Drosophila* homolog of the yeast *Saccharomyces cerevisiae* ubiquitin ligase Hrd1 plays a major role in sterol-accelerated ERAD of mammalian reductase in S2 cells (59). In yeast, Hrd1 exists in a large, multiprotein complex that includes its cofactor Hrd3, the cytosolic ubiquitin-conjugating enzyme Ubc7 and its membrane receptor Cue1p, polytopic Derlin-1 and its recruitment factor Usa1, the AAA-ATPase cdc48 and its membrane anchor ubiquitin regulatory-X (ubx) domain-containing protein Ubx2, and the Hsp70 chaperone Kar2 bound to the lectin Yos9 (22). Importantly, all of these factors, except for Cue1p, are highly conserved in mammals (22) (Table 2-1). It is important to note that Hrd1 mediates regulated ERAD of the reductase isoform Hmg2p in yeast (73). However, sterols do not appear to be the major signal for Hrd1-mediated degradation of Hmg2p, and the reaction is inhibited by the yeast Insig protein (74). To identify proteins that associate with *Drosophila* Hrd1 (dHrd1), we utilized a line of S2 cells that stably overexpress the enzyme fused to a C-terminal tandem affinity purification (TAP) tag. The TAP tag is composed of three copies of the FLAG epitope and Protein A separated by a cleavage site for the tobacco etch virus (TEV) protease. Detergent lysates of S2 cells overexpressing dHrd1-TAP were subjected to affinity chromatography using IgG- and anti- FLAG-coupled agarose beads. Eluted proteins were fractionated by SDS-PAGE, visualized by Colloidal Blue staining, and identified by mass spectrometry. Precipitation of dHrd1-TAP led to the recovery of *Drosophila* homologs of known components of the yeast Hrd1 complex including Hrd3 (dSel1), Yos9 (dOs9), Kar2 (dHsc70), Usa1 (dHerp),

VCP/p97 (Ter94), Ubx2 (dUbxd8 and dUbxd2), Npl4 (dNpl4), Ufd1 (dUfd1), and Der1 (dDerlin-2/3) (Table 2-1). In addition, several chaperones, lectins, subunits of the proteasome and associated proteins, and other components of the ubiquitin/proteasome pathway were identified in the dHrd1-TAP immunoprecipitation.

In the experiment of **Fig. 2-1**, S2 cells were subjected to RNAi-mediated knockdown through incubation with dsRNAs targeting the genes encoding dHrd1, *Drosophila* homologs of two unrelated membrane-bound ubiquitin ligases (dTeb4 and dTrc8), or various proteins identified in the dHrd1 TAP experiment (see Table 2-1). The cells were then transfected with an expression plasmid encoding the entire membrane domain of hamster reductase tagged with three tandem copies of the T7 epitope together with a plasmid encoding Myc-tagged human Insig-1. Previously, we found that the membrane domain of mammalian reductase is both necessary and sufficient for Insig-mediated, sterol-accelerated ERAD in S2 as well as mammalian cells (42, 59). Following transfection, cells were treated in the absence or presence of the oxysterol 25-hydroxycholesterol (25-HC) plus mevalonate to maximally stimulate reductase ERAD (43, 75-77). The cells were subsequently harvested and lysed in detergent-containing buffer. Immunoblot analysis of the resulting lysates with anti-T7 antibody revealed that levels of the membrane domain of reductase were reduced upon treatment of control-treated cells with 25-HC plus mevalonate (Fig. 2-1, panels 1, 4, and 7, lanes 2, 14, and 26), indicating accelerated ERAD. Consistent with our previous results (59), RNAi-mediated knockdown of dHrd1 (panels 1, 4, and 7, lanes 4, 16, and 28) or its associated proteins dSel1, dUbc7, dNpl4, dUfd1, and dHerp (lanes 10, 12, 18,

20, and 24) slowed reductase ERAD. Knockdown of dUbiquilin, the *Drosophila* homolog of the yeast protein Dsk2p, or Ter94, the VCP/p97 homolog, also inhibited the reaction (panels 4 and 7, lanes 22 and 30). Knockdown of dTrc8 slightly blocked reductase dislocation (panel 1, lane 6), which may reflect a minor secondary role in the reaction. In contrast, sterol-accelerated ERAD of reductase continued in dTeb4 knockdown cells (panel 1, lane 8). Similarly, knockdown of the ubiquitination factor dUbe4a (panel 7, lane 32), DHR23 (yeast Rad23 homolog), or the chaperone dHsc70, failed to block reductase ERAD in S2 cells (data not shown). Insig-1 was stabilized by certain dsRNA treatments (panels 2 and 5); the significance of these effects will be addressed below. Levels of the loading control, E1, remained constant throughout the RNAi experiments (panels 3, 6, and 9). Quantitative real-time PCR revealed that target gene expression was reduced 70-95% by RNAi. Unfortunately, we could not determine protein levels in these experiments owing to the lack of antibodies capable of recognizing the various *Drosophila* proteins.

Our previous studies in mammalian cells indicated that following ubiquitination, reductase becomes dislocated from ER membranes into the cytosol prior to proteasome-mediated degradation (47). Considering this, we next designed an experiment to determine the genetic requirements for cytosolic dislocation of the membrane domain of reductase in S2 cells. In **Fig. 2-2**, S2 cells subjected to RNAi and transfected with the membrane domain of reductase and Insig-1 were treated with the proteasome inhibitor MG-132 (to block degradation of any dislocated reductase) in the absence or presence of 25-HC plus mevalonate. Following treatments, the cells were

harvested and lysed in the absence of detergents for the preparation of post-nuclear supernatants that were subjected to centrifugation at 100,000 X g. The resulting pellet and supernatant fractions (designated membranes and cytosol, respectively) were then analyzed by immunoblot. The results show that 25-HC plus mevalonate enhanced the appearance of the membrane domain of reductase in the cytosol fraction of transfected S2 cells (Fig. 2-2, panels 2, 5, 8, and 11, lanes 2, 10, 16, and 24). Knockdown of dHrd1 led to the reduced appearance of the protein in the cytosol of 25-HC plus mevalonate-treated cells (panels 2, 5, 8, and 11, lanes 4, 12, 18, and 26). However, reductase continued to become dislocated into the cytosol of dTrc8 (panel 2, lane 6), dTeb4 (panel 2, lane 8), and dUbe4a (panel 11, lane 30) knockdown cells. Knockdown of dSel1 (panel 5, lane 14), dHerp (panel 8, lane 22), and Ter94 (panel 11, lane 28) blunted sterol-induced cytosolic dislocation of reductase. Cytosolic dislocation of reductase continued in dUbiquilin (panel 8, lane 20) as well as in dUbe4a (panel 11, lane 30) knockdown cells.

Despite a high degree of homology, Insig-1, but not Insig-2, is subjected to lipid-regulated ERAD in mammalian cells (53, 63). Considering our successful results with reductase ERAD, we next sought to determine whether physiologically relevant ERAD of mammalian Insig-1 degradation could be reconstituted in S2 cells. **Fig. 2-3A** compares the expression of Insig-1-Myc and Insig-2-Myc in S2 cells following treatment in the absence or presence of the protein synthesis inhibitor cycloheximide. In the absence of cycloheximide, transfection of S2 cells with the appropriate plasmid led to detectable expression of Myc-tagged Insig-1 and Insig-2 (Fig. 2-3A, panels 1 and 3,

lane 2). MG-132 treatment led to a small, but detectable increase in the amount of Insig-1 (panel 1, lane 3), but the amount of Insig-2 remained unchanged (panel 3, lane 3). Expression of Insig-1 was markedly reduced following cycloheximide treatment (Fig. 2-3A, panel 1, compare lanes 2 and 5). This reduction was completely abolished when the cells were also treated with MG-132 (lane 6), indicating the proteasome-mediated degradation of Insig-1 in the absence of the inhibitor. In contrast, the level of Insig-2 was constant in cycloheximide-treated S2 cells relative to that in untreated cells, regardless of the presence or absence of MG-132 (panel 3, lanes 5 and 6).

We next evaluated the ubiquitination status of Insig-1 in S2 cells. For this purpose, we transfected S2 cells with various combinations of expression plasmids encoding Myc-tagged Insig-1 and HA-tagged ubiquitin and treated them with MG-132. Following treatments, the cells were harvested; detergent lysates were immunoprecipitated with anti-Myc, followed by immunoblot analysis of precipitated material with anti-HA to visualize ubiquitinated Insig-1. The results show that co-expression of HA-ubiquitin led to the detection of poly-ubiquitinated forms of Insig-1 in the immunoprecipitates (Fig. 2-3B, panel 1, lane 4).

To determine whether Insig-1 ERAD in S2 cells is subject to lipid-mediated regulation, we began by transfecting cells with Insig-1 and various amounts of hamster Scap and subjected them to treatment with cycloheximide in the absence or presence of 25-HC prior to harvest and lysis. Immunoblot analysis of the lysates revealed that Insig-1 protein was not detectable when expressed alone (Fig. 2-3C, panel 1, lanes 2 and 3) or together with a low level (1 ng) of plasmid encoding hamster Scap (lanes 4 and 5),

regardless of the absence or presence of 25-HC. However, a small amount of Insig-1 was detected upon co-transfection of 3 ng of the Scap-encoding plasmid, but only when the cells were also treated with 25-HC (compare lanes 6 and 7). Co-transfection of higher levels of Scap stabilized Insig-1, even in the absence of 25-HC (panel 1, lanes 8 and 10); this stabilization was further enhanced upon treatment with the sterol (lanes 9 and 11). Results of Fig. 2-3D show that in the absence of Scap co-expression, Insig-1 ERAD in S2 cells was subjected to regulation by the unsaturated fatty acid oleate. Treatment of cells with oleate stabilized Insig-1 (Fig. 2-3D, panel 1, lane 5), but to a lesser extent as that observed with MG-132 treatment (lane 8). This may reflect differences in the uptake of the two reagents by S2 cells.

To further characterize ERAD of mammalian Insig-1 in S2 cells, we next sought to identify the ubiquitin ligase required for the reaction. S2 cells were subjected first to RNAi-mediated knockdown, after which they were transfected with Insig-1-Myc, treated with cycloheximide, and harvested for preparation of detergent lysates that were analyzed by anti-Myc immunoblot. The results show that Insig-1 continued to become degraded in control cells (**Fig. 2-4A**, panel 1, lane 1) and in cells treated with dsRNA against mRNAs for dHrd1 and dTrc8 (lanes 2 and 3). However, RNAi-mediated knockdown of the dTeb4 ubiquitin ligase significantly stabilized Insig-1 (lane 4). The specificity of dTeb4 knockdown was evaluated by comparing the ability of wild type or mutant dTeb4 to restore Insig-1 ERAD in dTeb4 knockdown cells. The mutant form of dTeb4 examined in this experiment harbors a substitution of serine for cysteine-10 in the N-terminal C4HC3 RING domain, which corresponds to cysteine-9 in human Teb4

(68). Mutation of this cysteine residue in human Teb4 abolishes in vitro ubiquitin ligase activity of the enzyme (68). Consistent with results of Fig. 2-3A, Insig-1 was stabilized in dTeb4 knockdown S2 cells (Fig 2-4B, panel 1, compare lanes 2 and 3). Overexpression of wild type dTeb4 in the knockdown cells restored ERAD of Insig-1 (lanes 4-6), whereas overexpression of the C10S dTeb4 mutant failed to restore the reaction (lanes 7-9). Similarly, overexpression of dHrd1 failed to restore Insig-1 ERAD in dTeb4 knockdown cells (Fig. 2-4C, panel 1, lanes 4-6), whereas overexpression of dTrc8 unexpectedly restored the reaction (Fig. 2-4D, panel 1, lanes 3-6). Despite this, endogenous dTrc8 did not appear to contribute to degradation of Insig-1 as indicated by the observation that knockdown of dTrc8 did not appreciably stabilize Insig-1 in dTeb4 knockdown cells (Fig. 2-4E, panel 1, lanes 2 and 4).

In the absence of RNAi-mediated knockdown, overexpression of dHrd1 inhibited the ERAD of Insig-1 (**Fig. 2-5A**, panel 1, lanes 4-7). We reasoned that this inhibition resulted from titration of shared ERAD components from the dTeb4 ubiquitin ligase complex. To investigate this notion, we next examined a role for dHrd1 complex components in ERAD of Insig-1 using RNAi. The results of Fig. 2-5B show that knockdown of dTeb4 as well as dUbc6, dUbc7, dUbxd8, dHerp, dDerlin2/3, Ter94, dNpl4, and dUfd1 significantly blunted Insig-1 ERAD (panel 1, lanes 4, 6, 7, 10, 11, 16, and 18-20).

Like reductase, Insig-1 becomes dislocated from ER membranes into the cytosol of mammalian cells for proteasome-mediated ERAD (47). The RNAi experiment of **Fig. 2-6A** was designed to examine the cytosolic dislocation of mammalian Insig-1 in S2

cells. The results show that a fraction of Insig-1 appeared in the cytosol of MG-132-treated S2 cells that received control GFP dsRNA (Fig. 2-6A, panel 3, lane 1). This appearance was significantly inhibited by the RNAi-mediated knockdown of dUbc7, dUbxd8, dHerp, dDerlin2/3, Ter94, dNpl4, and dUfd1 (lanes 4-10). Surprisingly, knockdown of dTeb4 did not block the cytosolic dislocation of Insig-1 (lane 2), even though the ubiquitin ligase was found to be required for Insig-1 ERAD (see Fig. 2-4A). This result suggested that Insig-1 becomes ubiquitinated following its cytosolic dislocation. To further explore this, we next evaluated the effect of the ubiquitin-activating enzyme (E1) inhibitor PYR-41 (78) on Insig-1 dislocation. Treatment with PYR-41 led to an increase in the amount of Insig-1 detected in membranes of transfected S2 cells (Fig. 2-6B, panel 1, lanes 1- 3, 6, and 8), indicating that the inhibitor blocked ERAD of Insig-1. Insig-1 was also stabilized in dTeb4 knockdown cells, as expected (lane 5). The combination of dTeb4 knockdown and PYR-41 treatment led to an increased stabilization of Insig-1 in membranes (panel 1, lanes 5-9). Insig-1 also accumulated in the cytosol of cells that were either treated with PYR-41 (Fig. 2-6B, panel 2, lanes 3 and 8) or subjected to dTeb4 knockdown (lane 5); the combination of dTeb4 knockdown and PYR-41 treatment led to an increased amount of cytosolic Insig-1 in an additive fashion (panel 2, compare lanes 5, 6-9).

2.5 Discussion

The endoplasmic reticulum (ER)-associated degradation (ERAD) pathway is an essential, highly conserved process through which misfolded proteins, both soluble

within the ER lumen and integral to the ER membrane, are selectively degraded by proteasomes (24). Insights into the underlying mechanisms of ERAD have been traditionally provided through studies of soluble substrates. These studies disclosed that the ERAD pathway can be divided into distinct steps that include substrate recognition by molecular chaperones and ER-resident lectins, retrotranslocation across the ER membrane into the cytosol, ubiquitination, and finally, delivery of the ubiquitinated substrate to proteasomes for degradation (5). Although many concepts regarding ERAD of soluble substrates are applicable to integral membrane substrates, a thorough understanding of mechanisms underlying the ERAD of these types of substrates is lacking. In particular, how integral membrane substrates are selected for ERAD and become extracted from membranes during ERAD remains a mystery. Integral membrane ERAD substrates, especially those with multiple membrane-spanning segments, can adopt complex topologies in ER membranes and can potentially present misfolded lesions in the cytosol, the ER lumen, or within the membrane, thereby engaging distinct ERAD pathways (64). Thus, complete elucidation of mechanisms for ERAD of membrane proteins requires rigorous examination of representative model substrates.

HMG CoA reductase and Insig-1 represent ideal models of integral membrane ERAD substrates. The major virtue of studying reductase and Insig-1 is that their ERAD can be precisely controlled by the addition of sterols and other lipid constituents of cell membranes (i.e., fatty acids and nonsterol isoprenoids). This attribute ensures physiologically relevant ERAD of reductase and Insig-1 when the reactions are

reconstituted either *in vitro* or in model systems. The current study exploits these features by expanding on the previous finding that Insig-mediated, sterol-accelerated ERAD of mammalian reductase can be reconstituted in *Drosophila* S2 cells (59). We began by using tandem affinity purification to isolate a multiprotein complex containing the *Drosophila* homolog of the yeast ubiquitin ligase Hrd1 (designated dHrd1), which was previously found to mediate sterol-accelerated reductase ERAD in S2 cells (59). Protein identification by mass spectrometry revealed that the dHrd1 complex contained *Drosophila* homologs of several proteins known to associate with yeast Hrd1 including dSel1, dUbxd8, dUbxd2, Ter94, dNpl4, dUfd1, dUbc7, dDerlin-2/3, dOs9, and Bip (Table 2-1). In addition, we identified several other components of the ubiquitin/proteasome system including RE16341p (a homolog of mammalian α-mannosidase EDEM3), dUbiquilin, and DHR23 (homolog of yeast Rad23) as well as several components of the 26S proteasome. Interestingly, we also found three ubiquitin ligases and two ubiquitin conjugating enzymes of unknown function to be associated with dHrd1 (data not shown). Whether dHrd1 contributes to degradation mediated by these enzymes or whether they modulate dHrd1 function remains to be determined. To the best of our knowledge, these studies mark the first ubiquitin ligase complex characterized at the molecular level in *Drosophila*.

RNAi-mediated knockdown of dHrd1-associated proteins including dSel1, dUbc7, dNpl4, dUfd1, Ter94, dUbiquilin, and dHerp blunted the sterol-induced ERAD of reductase in S2 cells (Fig. 2-1). Similarly, knockdown of genes encoding several of these proteins also blunted another aspect of reductase ERAD, namely dislocation of

the protein into the cytosol for proteasomal degradation (47). Consistent with results in mammalian cells (47), reductase dislocation required the prior ubiquitination of reductase as indicated by the inhibition of the reaction in dHrd1 and dSel1 knockdown cells (Fig. 2-2). In addition, cytosolic dislocation of reductase required the *Drosophila* VCP/p97 homolog Ter94 (Fig. 2-2). Knockdown of dHerp also blunted reductase dislocation; however, the precise role for dHerp in reductase ERAD remains to be determined. Notably, knockdown of dUbiquilin failed to inhibit reductase dislocation (Fig. 2-2). dUbiquilin is a homolog of the yeast protein Dsk2p, which combines with another protein called Rad23 to shuttle ubiquitinated proteins to the proteasome for degradation. Thus, the possibility exists that dUbiquilin participates in delivery of cytosolic reductase to proteasomes.

Considering the successful reconstitution of reductase ERAD in S2 cells, we extended our studies to Insig-1, whose ERAD is subjected to lipid-mediated regulation in mammalian cells (53, 54). Remarkably, we found that the selectivity of Insig-1 ERAD was preserved in the *Drosophila* system. For example, Insig-1 but not its highly related isoform Insig-2, was subjected to proteasome-mediated ERAD in S2 cells (Fig. 2-3A); poly-ubiquitinated forms of Insig-1 were identified in the presence of the proteasome inhibitor MG-132 (Fig. 2-3B). Similar to the situation in mammalian cells, the ERAD of Insig- 1 was inhibited by sterols in S2 cells through a mechanism that required co-expression of the cholesterol- sensing SREBP escort protein, Scap (Fig. 2-3C). Finally, Insig-1 ERAD was inhibited by the unsaturated fatty acid oleate through a mechanism that did not require the co-expression of Scap (Fig 2-3D). Thus, reductase and Insig-1

are subjected to lipid-regulated ERAD in both *Drosophila* and mammalian systems, indicating that mechanisms underlying their selection for ERAD are highly conserved across species.

Further investigation revealed that dTeb4, the *Drosophila* homolog of the membrane-bound yeast ubiquitin ligase Doa10 and mammalian Teb4 (68), was required for Insig-1 ERAD in S2 cells (Fig. 2-4A). This finding is surprising considering that 1) Insig-1 presumably binds to dHrd1 as it bridges the ubiquitin ligase to reductase in sterol-treated cells; and 2) the same ubiquitin ligase, gp78, is required for ubiquitination and degradation of both reductase and Insig-1 in mammalian cells (63, 79). Overexpression of dHrd1 failed to rescue Insig-1 ERAD in dTeb4 knockdown cells (Fig. 2-4C); however, the reaction was fully restored upon overexpression of another membrane-bound ubiquitin ligase, dTrc8 (Fig. 2-4D). This result indicates that similar mechanisms underlie selection of Insig-1 for dTrc8- and dTeb4-mediated ERAD in S2 cells. Whether this involves direct interaction between the ubiquitin ligases and Insig-1 or whether a shared factor is involved in selection of Insig-1 for ERAD is not clear, and requires the molecular characterization of dTrc8 and dTeb4 ubiquitin ligase complexes.

In the absence of RNAi, dHrd1 overexpression blocked ERAD of Insig-1 (Fig. 2-5A), suggesting that the ubiquitin ligase sequesters components of the ERAD pathway required for dTeb4-mediated ubiquitination of Insig-1. To evaluate this possibility, we examined a role for various dHrd1 complex components in Insig-1 ERAD. The results show that several dHrd1 complex components including dUbc7, dUbxd8, dHerp, Ter94, dUfd1, and dNpl4 are required for ERAD of both Insig-1 (Fig. 2-5B) and reductase (Fig.

2-1). Interestingly, the ERAD of reductase has a specific requirement for dSel1 and dUbiquilin (Fig. 2-1), while Insig-1 ERAD specifically requires dUbc6 (Fig. 2-5B). We previously found that dDerlin 2/3 was not required for reductase ERAD in S2 cells (59), but the protein is required for the ERAD of Insig-1 (Fig. 2-5B). These differences likely reflect the differential actions of dTeb4 and dHrd1 in the ERAD of reductase and Insig-1 and indicate they may occur through distinct pathways. This notion is supported by results of experiments shown in Fig. 2-2 and 2-6A, which evaluate a role for dHrd1 complex components in cytosolic dislocation of reductase and Insig-1. Knockdown of dHrd1 and dSel1, which mediate reductase ubiquitination, blocked both the sterol-accelerated ERAD and sterol-induced cytosolic dislocation of reductase (Figs. 2-1 and 2-2). Knockdown of the ubiquitin ligase dTeb4 or the ubiquitin- conjugating enzyme dUbc6 blocked Insig-1 ERAD, but not its cytosolic dislocation (Fig. 2-6A). Instead, knockdown of genes encoding proteins involved in post-ubiquitination steps of ERAD including Ter94, dUfd1, and Np14 inhibited the reaction. Similar results were obtained in S2 cells treated with PYR-41, an inhibitor of ubiquitin-activating enzymes (78). PYR-41 treatment stabilized Insig-1 in membranes and led to the accumulation of the protein in the cytosol (Fig. 2-6B), indicating that dislocation of Insig-1 into the cytosol precedes ubiquitination.

Considered together, the current results establish that mammalian reductase and Insig-1 are degraded through distinct mechanisms in *Drosophila* S2 cells as depicted in **Fig. 2-7**. The reductase appears to become ubiquitinated through a reaction that requires the ubiquitin ligase dHrd1, its cofactor dSel1, and the ubiquitin-conjugating

enzyme dUbc7. This ubiquitination marks reductase for cytosolic dislocation, which is likely mediated by the ATPase Ter94, its membrane receptor dUbxd8, and the cofactors dUfd1 and dNpl4. Dislocation of reductase also appears to be modulated by the *Drosophila* homolog of Herp, and dUbiquilin mediates steps in reductase ERAD following dislocation of the protein into the cytosol. In contrast to reductase, Insig-1 appears to become dislocated into the cytosol prior to dTeb4-mediated ubiquitination. Importantly, this dislocation requires dDerlin-2/3, a member of the Derlin family of polytopic membrane proteins in yeast and mammals that play a key role in the ERAD of both soluble and membrane-bound ERAD substrates (25, 26). It is worth noting that although RNAi-mediated knockdown of dUbc6 or dUbc7 significantly blunted the ERAD of Insig-1 (Fig. 2-5B), dUbc7 but not dUbc6 appears to be required for cytosolic dislocation of Insig-1 (Fig. 2-6A). A likely explanation for this discrepancy is that an unknown *Drosophila* ubiquitin ligase combines with dUbc7 in the ERAD of Insig-1 in S2 cells. We postulate that this putative ubiquitin ligase directs Insig-1 through a dHrd1-like ERAD pathway in which the substrate becomes ubiquitinated prior to its cytosolic dislocation. Thus, important directions for future studies include the identification of the alternative ubiquitin ligase required for Insig-1 ERAD, examining the mechanism through which Insig-1 is selected for ERAD and dislocated into the cytosol of S2 cells; determining how Insig-1 is solubilized in the cytosol prior to ubiquitination; determining whether reductase is fully extracted from S2 cell membranes prior to cytosolic dislocation; and determining whether reductase and Insig-1 are degraded through distinct mechanisms in mammalian cells. Successful completion of these studies will

provide key insights into mechanisms that control lipid homeostasis and mechanisms for the ERAD of integral membrane proteins.

2.6 Table and Figures

Table 2-1

Components of the ER-Associated Degradation Pathway

S. cerevisiae	Mammalian	Drosophila
Hrd1	Hrd1; gp78	dHrd1*
Doa10	Teb4	dTeb4
	Trc8	dTrc8
Ubc6	Ubc6	dUbc6
Ubc7	Ube2g2 (Ubc7)	dUbc7* (courtless)
Hrd3	Sel1	dSel1* (dHrd3)
Yos9	Os9, XTP3-B	dOs-9*
Kar2	Bip	dHsc70*
Usa1	Herp	dHerp*
Der1	Derlin-1, -2, -3	Derlin-1, -2/3*
Ubx2	Ubxd2, Ubxd8	dUbxd2*, dUbxd8*
cdc48	VCP/p97	dTer94*
Npl4	Npl4	dNpl4*
Ufd1	Ufd1	dUfd1*
Dsk2	Ubiquilin-1, -2, -3, -4	dUbiquilin*
Rad23	Rad23	DHR23*
Ube4a	Ube4a	dUbe4a

* Identified in dHrd1-TAP experiments

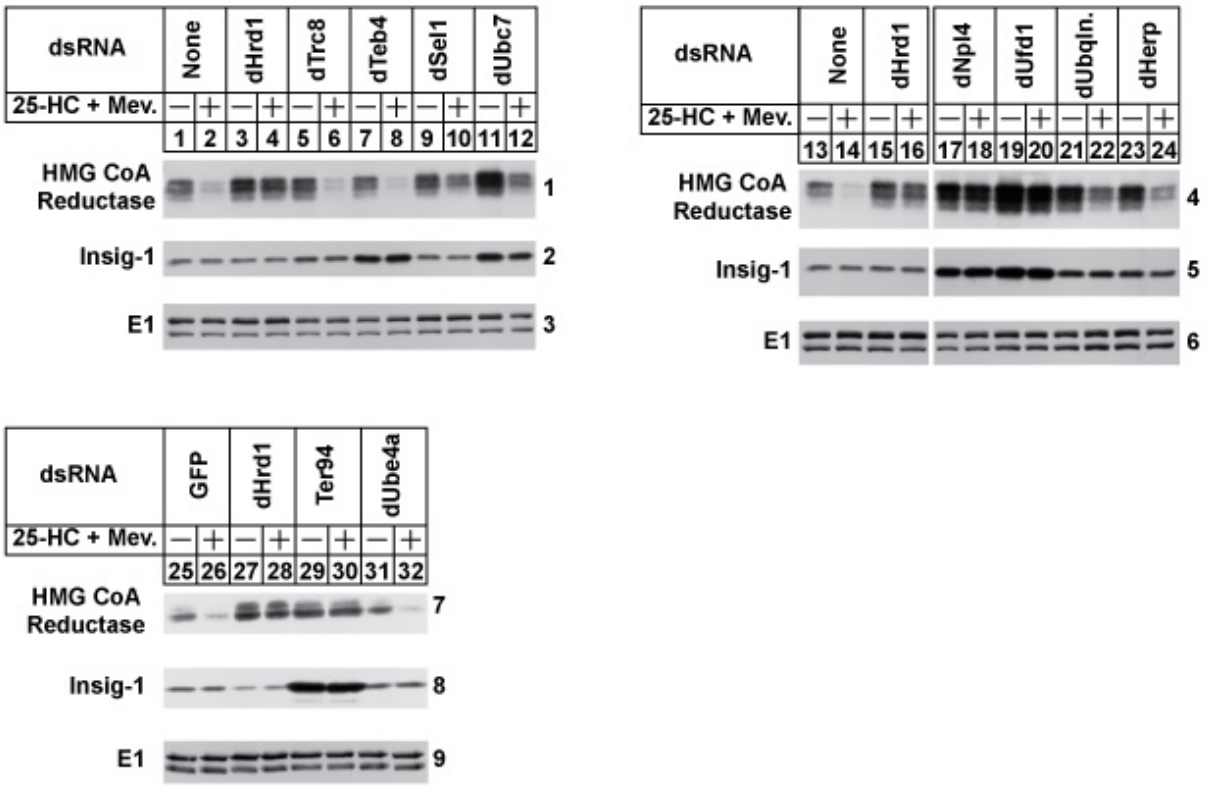

FIGURE 2-1. Components of the ER-associated degradation (ERAD) pathway required for proteasomal degradation of hamster HMG CoA reductase in *Drosophila* S2 cells. S2 cells were set up on day 0 in 6-well plates at a density of 1 X 10^6 cells per well in medium B. Immediately after plating, cells were incubated with 15 µg of dsRNA targeted against the indicated endogenous mRNAs. Following incubation for 1 h, the cells received 2 ml of medium C supplemented with 10% HI-LPDS. On day 1, cells were washed and transfected in medium B with 0.5 µg of pAc-HMG-Red-T7 (TM1-8) and 0.1 µg pAc-Insig-1-Myc in medium B using Maxfect™ Transfection Reagent as described in "Materials and Methods." On day 2, each well received 1 ml of medium B supplemented with 20% HI-LPDS. Cells were treated on day 3 with medium C supplemented with 10% HI-LPDS in the absence or presence of 2.5 µM 25-HC plus 10 mM mevalonate. Following incubation for 4 h, cells were harvested and lysed in detergent-containing buffer; aliquots of the resulting lysates (50 µg of protein/lane) were separated by 10% SDS-PAGE, the proteins were transferred to nitrocellulose membranes, followed by immunoblot analysis with anti-T7 IgG (against reductase), IgG-9E10 (against Insig-1), and anti-actin IgG. The numbers to the side of immunoblots are referred to as "panels" in the text.

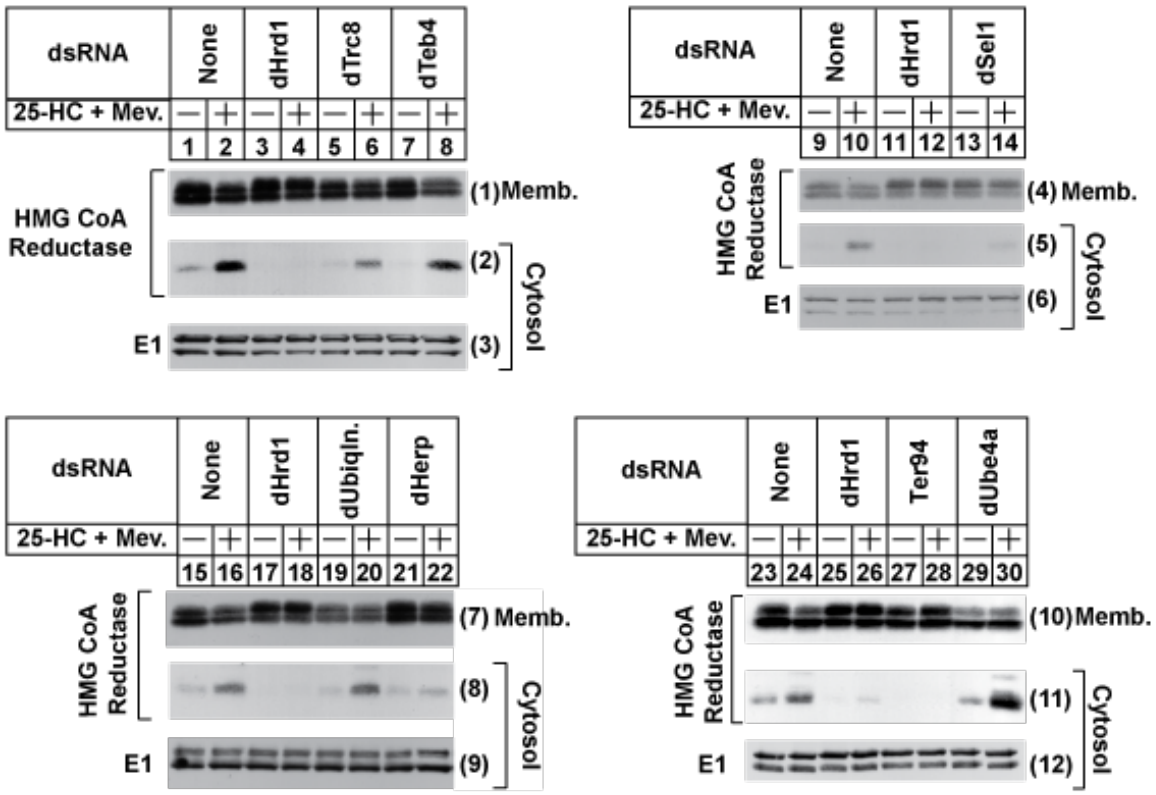

FIGURE 2-2. ERAD components required for sterol-induced cytosolic dislocation of hamster HMG CoA reductase in *Drosophila* S2 cells. S2 cells were set up for experiments and treated with dsRNA on day 0, transfected with pAc-HMG-Red-T7 (TM1-8) and pAc-Insig-1-Myc on day 1, incubated with medium B containing 10% LPDS on day 2, and subjected to treatment with 25-HC plus mevalonate on day 3 as described in the legend to Fig. 1. The cells also received 10 μM MG-132 on day 3. Following incubation for 4 h, the cells were harvested and subjected to subcellular fractionation as described in "Experimental Procedures." The resulting membrane (10 μg protein/lane) and cytosol (40 μg protein/lane) fractions were subjected to 10% SDS-PAGE followed by immunoblot analysis as described in the legend to Fig. 1. The numbers to the side of immunoblots are referred to as "panels" in the text.

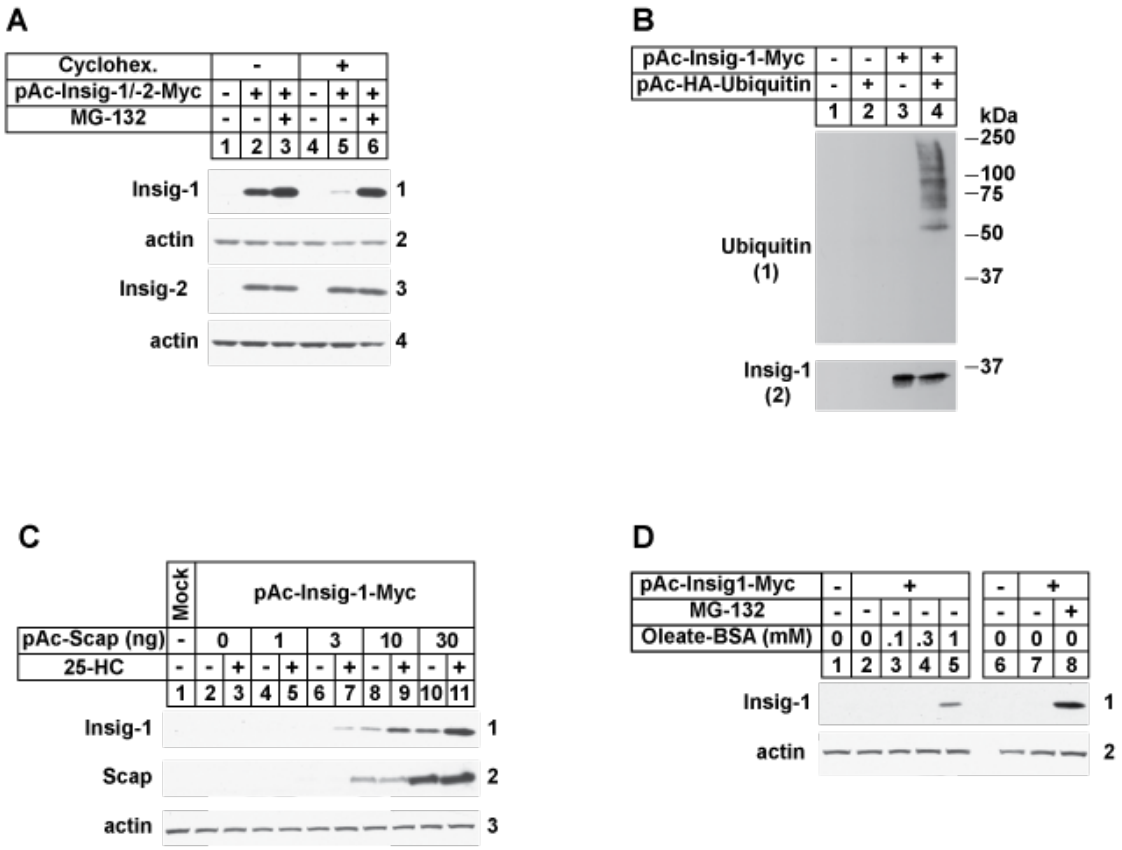

FIGURE 2-3. Reconstitution of lipid-regulated ERAD of mammalian Insig-1 in *Drosophila* S2 cells. S2 cells were set up in 6-well plates on day 0 at 1 X 10^6 cells per well in medium A supplemented with 10% HI-FCS. On day 1, cells were transfected in medium B using Maxfect™ as follows: *A*, 0.1 µg of pAc-Insig-1-myc or 0.1 µg of pAc-Insig-2-myc; *B*, 0.2 µg pAc-Insig-1-Myc in the absence or presence of 1.0 µg pAc-HA-ubiquitin; *C*, 0.1 µg of pAc-Insig-1-myc and 1, 3, 10, or 30 ng of pAc-Scap, and *D*, 0.1 of µg pAc-Insig-1-myc (total amount of DNA was adjusted to 0.1 µg (*A* and *D*), 1.2 µg (*B*), or 0.13 µg (C) using empty pAc5.1 vector). On day 2, each well received 1 ml of medium B supplemented with 20% HI-LPDS (*A*-C) or HI-DFCS (*D*). Cells were treated on day 3 with medium C supplemented with 10% HI-LPDS (*A*-*C*) or HI-DFCS (*D*) under the following conditions: *A*, in the absence or presence of 10 µM MG-132 (6 h) and 50 µM cycloheximide (2 h); *B*, in the presence of 10 µM MG-132 (2 h); *C*, in the absence and presence of 2.5 µM 25-HC and 10 mM mevalonate (4 h) together with 50 µM cycloheximide (2 h); *D*, in the absence and presence of 10 µM MG-132 (6 h) or 0.1, 0.3, or 1 mM BSA-oleate (4 h) together with 50 µM cycloheximide (2 h). *A*, *C*, and *D*, following incubations, cells were harvested and aliquots of whole cell lysates (*A*, 30 µg protein/lane; *C*, 40 µg protein/lane; *D*, 50 µg protein/lane) were subjected to 10% SDS-PAGE followed by immunoblot analysis with IgG-9E10 (against Insigs), IgG-9D5 (against hamster Scap), and anti-actin IgG. *B*, following incubation, the cells were harvested for preparation of detergent lysates that were immunoprecipitated with 60 µl anti-Myc coupled agarose beads. Aliquots of the immunoprecipitates were then subjected to SDS-PAGE followed by immunoblot analysis with anti-HA (against ubiquitin) and IgG-9E10 (against Insig-1). The numbers to the side of immunoblots are referred to as “panels” in the text.

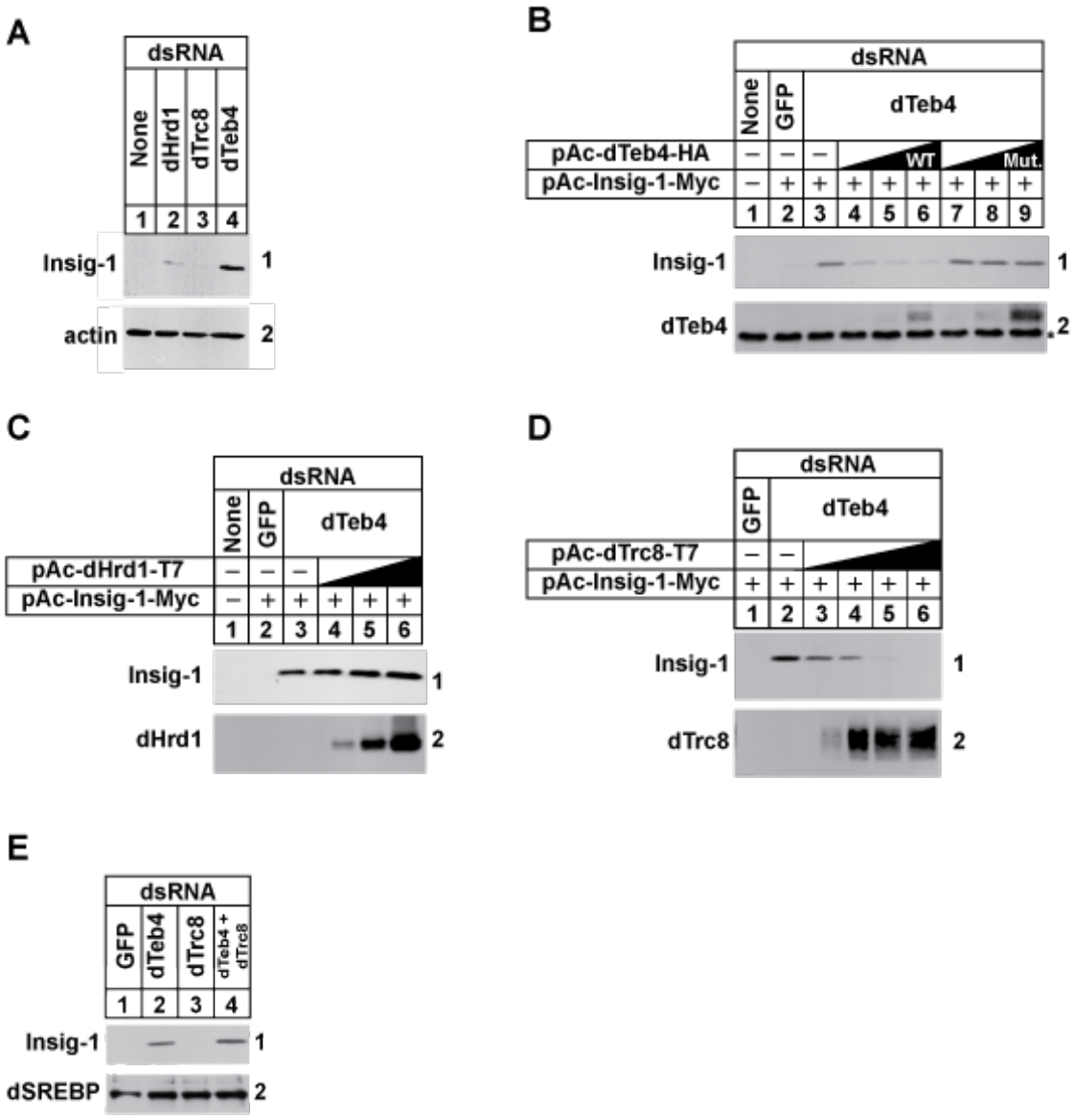

FIGURE 2-4. The dTeb4 ubiquitin ligase is required for degradation of mammalian Insig-1 in *Drosophila* S2 cells. S2 cells were set up and subjected to RNAi-mediated knockdown on day 0 and transfected with 0.5 μg of pAc-Insig-1-Myc alone (A and E) or together with 0.1, 0.3, or 1.0 μg of WT or mutant (Mut., C10S) pAc-dTeb4-HA (B); 0.1, 0.3, or 1.0 μg of pAc-dHrd1-T7 (*C*); and 0.1, 0.3, 1.0, or 3.0 μg pAc-dTrc8-T7 (*D*) on day 1 as described in the legend to Fig. 1. On day 2, each well received 1 ml of medium B supplemented with 20% HI-LPDS. The cells were subsequently switched on day 3 to medium C supplemented with 10% HI-LPDS and 50 μM cycloheximide. Following incubation for 2 h, cells were harvested for preparation of whole cell lysates that were subjected to SDS-PAGE (20 μg protein/lane) and immunoblot analysis with IgG-9E10 (against Insig-1), IgG-3B2 (against dSREBP), anti-HA IgG (against dTeb4), anti-T7 IgG (against dHrd1 and dTrc8), and anti-actin IgG. The asterisk (*) in *B* denotes a nonspecific, cross-reactive band. The numbers to the side of immunoblots are referred to as "panels" in the text.

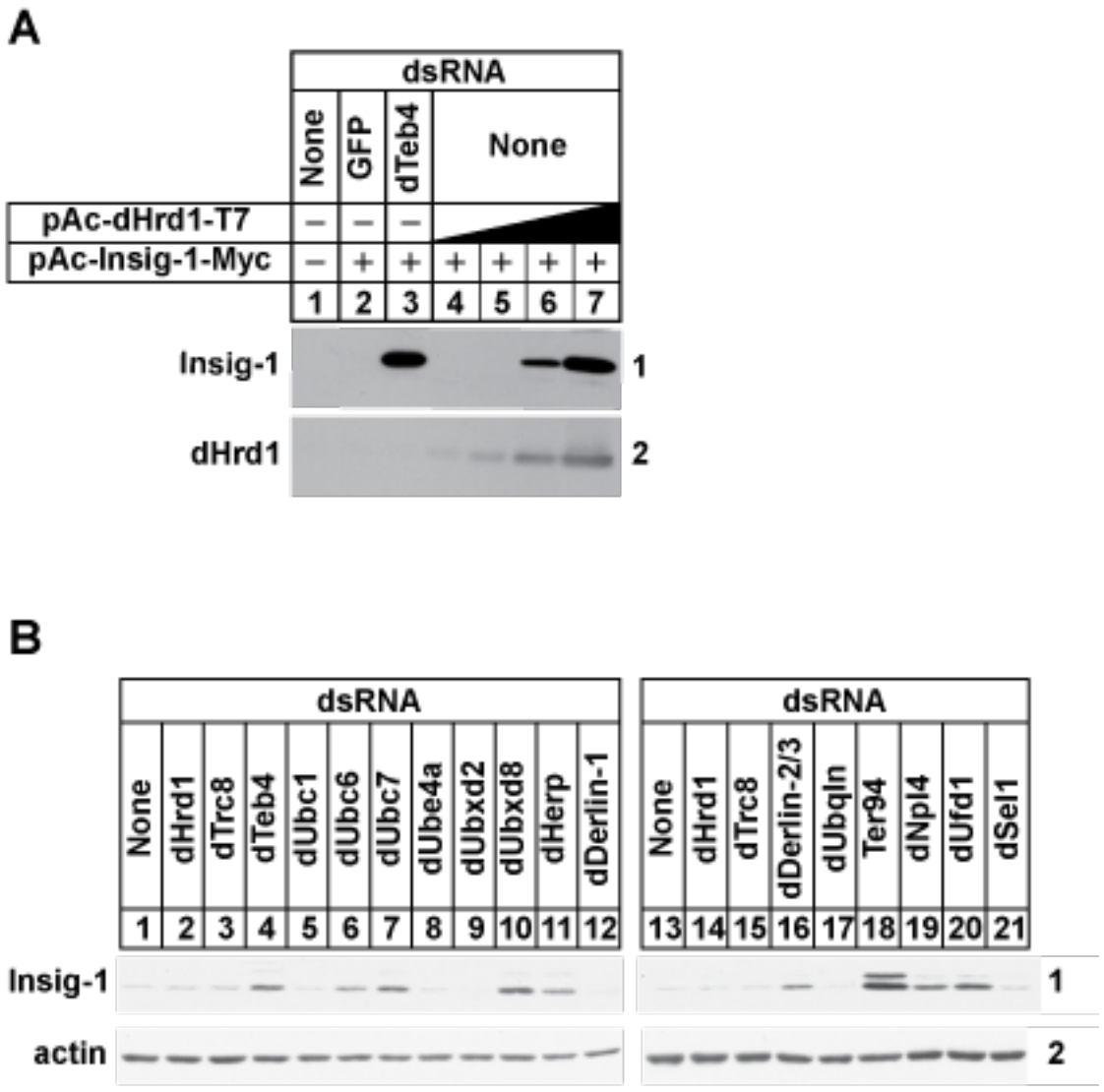

FIGURE 2-5. Components of the ERAD pathway required for degradation of mammalian Insig-1 in *Drosophila* S2 cells. S2 cells were set up and subjected to RNAi-mediated knockdown on day 0 and transfected with 0.5 μg of pAc-Insig-1-Myc alone (*B*) or together with 0.1, 0.3, 1.0, or 3.0 μg of pAc-dHrd1-T7 (*A*) on day 1 as described in the legend to Fig. 1. On day 2 each well received 1 ml of medium B supplemented with 20% HI-LPDS. On day 3, cells were incubated in medium C supplemented with 10% HI-LPDS and 50 μM cycloheximide. After 2 h, cells were harvested for preparation of detergent lysates that were subjected to SDS-PAGE (20 μg protein/lane) and immunoblot analysis with IgG-9E10 (against Insig-1), anti-T7 IgG (against dHrd1), and anti-actin IgG. The numbers to the side of immunoblots are referred to as "panels" in the text.

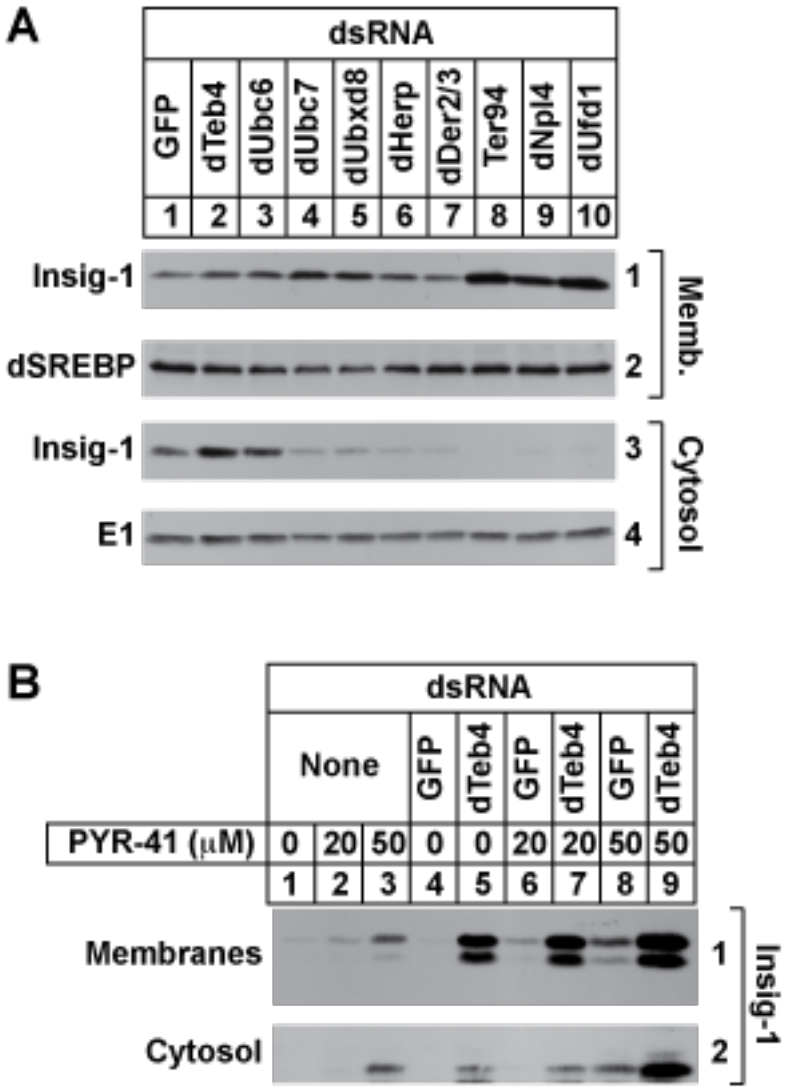

FIGURE 2-6. Components of the ERAD pathway required for cytosolic dislocation of mammalian Insig-1 in *Drosophila* S2 cells. S2 cells were set up and subjected to RNAi-mediated knockdown on day 0 and transfected on day 1 with 0.5 μg of pAc-Insig-1-Myc as described in the legend to Fig. 1. On day 2, each well received 1 ml of medium B supplemented with 20% HI-DFCS. On day 3, cells were incubated in medium C containing 10% HI-DFCS, 50 μM cycloheximide, and 10 μM MG-132 (*A*) or the indicated concentration of PYR-41 (*B*). Following incubation for 2 h, cells were harvested and subjected to subcellular fractionation. Equal proportions of membrane and cytosol fractions were subjected to SDS-PAGE, followed by immunoblot analysis with IgG-9E10 (against Insig-1), IgG-3B2 (against dSREBP), and anti-actin IgG. *C*, the gel of the cytosol shown in (*B*) was scanned and quantified by densitometry. The numbers to the side of immunoblots are referred to as "panels" in the text.

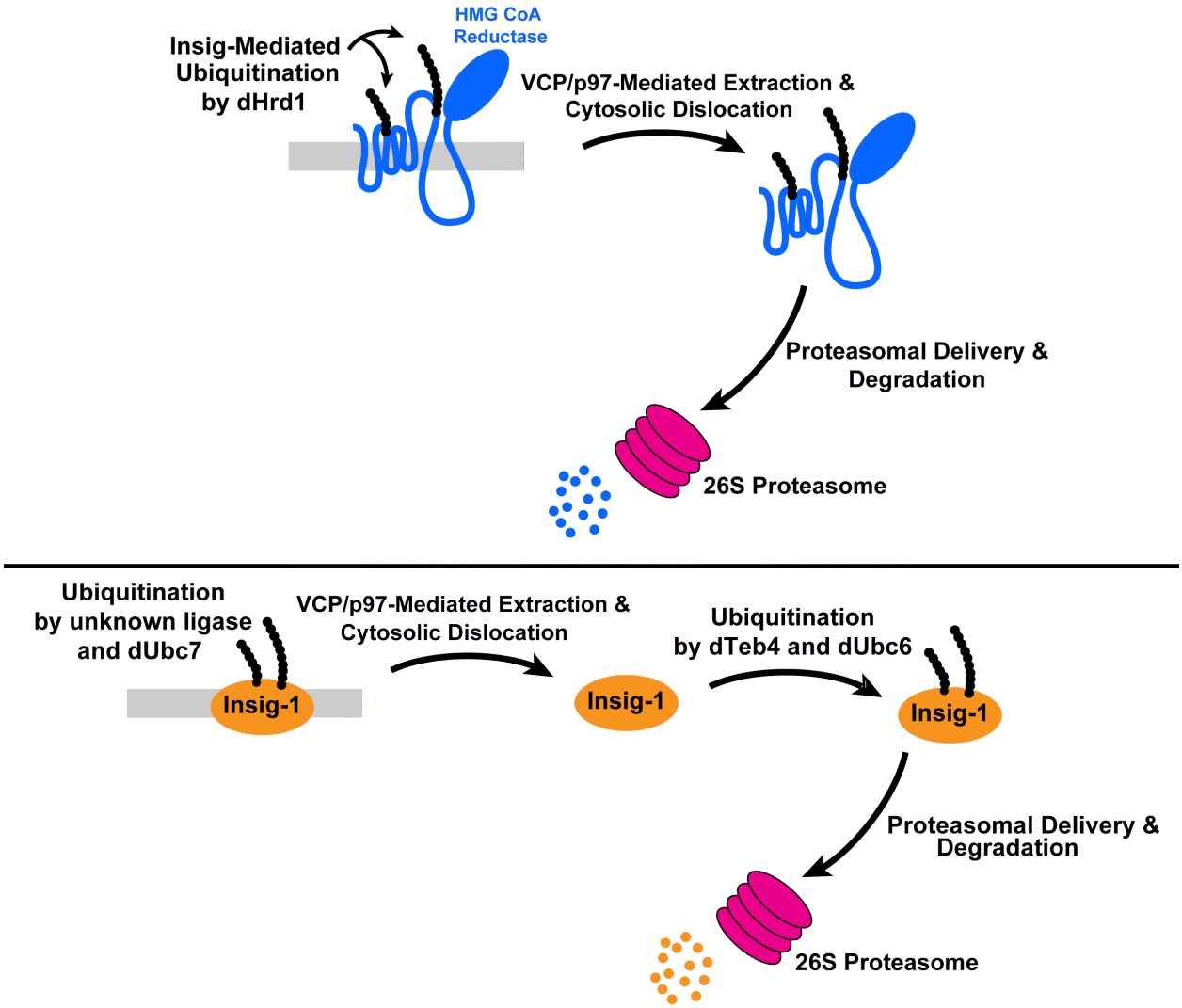

Figure 2-7. Model depicting ERAD of two integral membrane substrates, mammalian reductase and Insig-1, through distinct pathways in S2 cells. In S2 cells, mammalian reductase (shown in blue) is ubiquitinated through the actions of the ubiquitin ligase dHrd1 and the ubiquitin-conjugating enzyme dUbc7 on the ER membrane. Following ubiquitination, reductase is dislocated to the cytosol through the action of the AAA-ATPase VCP/p97. Cytosolic reductase is delivered to the 26S proteasome (shown in pink) for degradation. In contrast, data suggests Insig-1 (shown in yellow) undergoes two rounds of ubiquitination where it is first ubiquitinated by the actions of an unknown ligase and the ubiquitin-conjugating enzyme dUbc7 in the ER membrane. Next, Insig-1 is dislocated to the cytosol through the actions of VCP/p97, and undergoes a second round of ubiquitination by dTeb4 and dUbc6 prior to degradation by the 26S proteasome.

CHAPTER 3:

A Role for dSel1 in Selection of HMG CoA Reductase for Lipid-regulated, ER-associated Degradation in Insect Cells

3.1 Abstract

ER-associated degradation (ERAD) is a process through which misfolded proteins are targeted for degradation by 26S proteasomes. Newly synthesized proteins are translocated into the ER lumen where molecular chaperones assist in folding and assembly of nascent polypeptides. Molecular chaperones survey these proteins and recognize the presence of misfolded cytosolic, lumenal, or transmembrane domains, selecting them for ubiquitination and subsequent degradation. Selection of integral membrane substrates is not well understood and chaperones that mediate recognition of these regions have not yet been characterized. Our studies focus on the integral membrane substrate HMG CoA reductase, whose levels are controlled by lipid-mediated ERAD. In mammalian cells, sterol accumulation triggers the binding of the membrane domain of reductase to Insigs bridging it to an ubiquitin ligase, and thereby targeting it for ERAD. We previously established that Insig-mediated, sterol-accelerated ERAD of mammalian reductase can be reconstituted in *Drosophila* S2 cells. In this model system, ubiquitination of reductase is mediated by the *Drosophila* ubiquitin ligase dHrd1. RNAi experiments show that dSel1, a previously identified dHrd1-associated protein, is required for reductase ERAD. Here, using coimmunoprecipitation and RNAi, we show that dSel1-mediated bridging of dHrd1 to Insig-1 underlies sterol-accelerated

ERAD of HMG CoA reductase in S2 cells.

3.2 Introduction

The endoplasmic reticulum (ER)-associated degradation (ERAD) pathway constitutes a series of reactions that results in selective degradation of misfolded or unassembled secretory and integral membrane proteins by cytosolic 26S proteasomes (80). ERAD is initiated by molecular chaperones, which recognize misfolding in cytosolic, lumenal, and membrane-embedded regions of potential substrates (24). In many cases, selection leads to ubiquitination of ERAD substrates; the modification ensures efficient targeting of substrates to proteasomes for degradation. Substrate ubiquitination results from the concerted actions of E3 ubiquitin ligases and E2 ubiquitin-conjugating enzymes, which mediate transfer of ubiquitin from the E1 ubiquitin-activating enzyme to lysine residues in the substrate or in a previously attached ubiquitin of a polyubiquitin chain (81). The specificity of ubiquitination is primarily determined by ubiquitin ligases and its is widely assumed that chaperones not only mediate selection of ERAD substrates, but that they also facilitate substrate interactions with ubiquitin ligases. However, precise mechanisms through which substrates, especially those integral to the ER membrane, become ubiquitinated are poorly understood.

Hrd1, which was first discovered in the yeast Saccharomyces cerevisiae (82), is one of the most well-characterized ERAD ubiquitin ligases. The enzyme is anchored to the ER through a hydrophobic domain with multiple membrane-spanning segments and contains a cytosolic domain with a RING finger motif that directs ubiquitin ligase activity.

Co-immunoprecipitation studies reveal that yeast Hrd1 associates with a large complex containing its cofactor Hrd3, the cytosolic ubiquitin-conjugating enzyme Ubc7 and its membrane anchor Cue1, the polytopic ER membrane protein Der1 and its recruitment factor Usa1, the UBX (ubiquitin regulatory X) domain-containing protein Ubx2, which mediates recruitment of the AAA-ATPase cdc48, and the Hsp70 chaperone Kar2 bound to the lectin Yos9 (22). The mammalian and insect genomes encode homologs of all members of the yeast Hrd1 complex, except Cue1. We recently identified the *Drosophila* Hrd1 complex using co-immunoprecipitation and mass spectrometry (83) and sucrose gradient centrifugation experiments indicate mammalian Hrd1 exists in a large multi-protein complex (84).

Previously, we reconstituted ERAD of the polytopic cholesterol biosynthetic enzyme 3-hydroxy-3-methylglutaryl coenzyme A (HMG CoA) reductase in *Drosophila* S2 cells (59). This ERAD mimicked that observed in mammalian cells with respect to its requirement for mammalian ER membrane proteins called Insigs, acceleration by the oxysterol 25-hydroxycholesterol, and augmentation by the nonsterol isoprenoid geranylgeraniol. RNA interference (RNAi) studies revealed that sterol-accelerated ERAD of reductase in S2 cells required *Drosophila* Hrd1 (dHrd1) and several ERAD components found associated with the ubiquitin ligase. The requirement of dSel1 for reductase ERAD was of particular interest considering studies first established in yeast and later in mammalian cells that revealed the dSel1 homolog Hrd3 (Sel1 in mammalian cells) mediates selection of soluble ERAD substrates (22, 24, 85). This selection involves recognition of the misfolded substrates by the chaperone Kar2 (Bip in

mammalian cells), which associates with the Yos9 lectin. Substrates are then presented to Hrd1 complex for dislocation, ubiquitination, and degradation.

In the current study, we use the combination of RNAi and co-immunoprecipitation to determine the mechanism through which dSel1 arbitrates dHrd1-mediated, Insig-dependent ERAD of reductase in S2 cells. The results support a model depicted in **Fig. 3-1** in which dSel1 bridges the sterol-induced reductase-Insig complex to dHrd1 for ubiquitination and subsequent ERAD. Structure-function analysis studies show that a single domain in dSel1 mediates its binding to dHrd1 and Insig, but cannot support sterol-accelerated reductase ERAD in dSel1 knockdown cells. Thus, the possibility exists that an intermediary protein facilitates dHrd1-mediated ERAD of reductase by playing a role similar to that of Yos9 and Kar2 in ERAD of soluble substrates.

3.3 Materials and Methods

Materials − We obtained MG-132 from Peptide Institute, Inc. (Osaka, Japan); cyclohexamide and 25-hydroxycholesterol from Sigma. Sodium mevalonate and lipoprotein-deficient serum (LPDS) were prepared as previously described (70).

Expression Plasmids − The pAc-HMG-Red-T7 (TM1-8) plasmid encodes the membrane domain (amino acids 1-346) of hamster reductase fused to three copies of the T7 epitope under transcriptional control of the *Drosophila* actin 5c promoter (pAc) as previously described (59). pAc-Insig-1-Myc encodes amino acids 1-227 of human Insig-1 followed by six copies of the c-Myc epitope as described (65). pAc-Insig-1-T7

encodes amino acids 1-227 of human Insig-1 followed by three copies of the T7 epitope under transcriptional control of the *Drosophila* actin 5C promoter generated from the pAc-HMG-Red-T7 plasmid. The pAc-dSel1-Myc expression plasmid was generated by replacing Insig-1 in the pAc-Insig-1-Myc plasmid with DNA encoding *Drosophila* Sel1. This was done by amplifying the open reading frame for *Drosophila* Sel1 (designated dSel1 CG10221-RA) by PCR with the Accuprime Kit (Invitrogen) using first strand cDNA obtained by reverse transcription of total RNA purified from S2 cells. The PCR products were gel purified, subjected to restriction digests, and ligated into the digested pAc-Insig-1-Myc plasmid resulting in pAc-dSel1-Myc. The following *Drosophila* Sel1 truncated mutants were generated by restriction digests of pAc-dSel1-Myc: pAc-dSel1-702-Myc, encoding amino acids 1-702 of *Drosophila* Sel1 followed by 6 copies of the c-Myc tag; pAc-dSel1-1-331-Myc, encoding amino acids 1-331 of *Drosophila* Sel1 followed by 6 copies of the c-Myc tag; pAc-dSel1-332-702-Myc, encoding amino acids 332-702 of *Drosophila* Sel1 followed by 6 copies of the c-Myc tag. The integrity of all plasmids was confirmed by DNA sequencing.

Culture and Transfection of Drosophila S2 Cells − Stocks of *Drosophila* S2 cells were cultured in medium A, Schneider's *Drosophila* medium supplemented with 10% (v/v) heat-inactivated fetal calf serum (HI-FCS), at 23°C. Experiments were set up in 6-well plates on day 0 at a density of 1 x 10^6 cells per well in medium A. On day 1 the cells were washed with medium B (Express Five Serum Free Medium) and transfected using Maxfect™ (KD Medical) Transfection Reagent at a ratio of 1 µg DNA to 5 µl Maxfect™

in 1 ml medium B. The total amount of DNA in each experiment was kept constant by the addition of empty pAc5.1 vector. Following transfection on day 2, cells received additional medium B supplemented with 20% (v/v) heat-inactivated lipoprotein-deficient serum (HI-LPDS) resulting in a 10% final concentration. Prior to harvest on day 3, cells were treated as described in the figure legends in medium C, Schneider's *Drosophila* medium supplemented with 100 units/ml penicillin, 100 µg/ml streptomycin sulfate, and 10% HI-LPDS.

RNA Interference (RNAi)-mediated Knockdown in Drosophila S2 Cells − On day 0 S2 cells were plated in 6 well plates at a density of 1 x 10^6 cells per well in 1 ml medium B. Immediately after plating, 15 µg dsRNA was added to each well. After a 1 hour incubation each well received 2 ml medium C. The dsRNAs used were produced as previously described (59).

Preparation of Whole Cell Lysates and Membrane Fractions − Treatment conditions are described in the figure legends. After treatment, cells from triplicate wells were scraped, combined, and washed in PBS. Cell pellets were collected by centrifugation at 1,500 *g* for 5 minutes at 4°C and resuspended in buffer containing 50 mM Tris-HCl pH 8.0, 150 mM NaCl, 0.1% (w/v) SDS, 1.5% (w/v) Nonidet P-40, 0.5% (w/v) sodium deoxycholate, and 2 mM $MgCl_2$ supplemented with a protease inhibitor cocktail (25 µg/ml *N*-acetyl-leucinal-leucinal-norleucinal, 2 µg/ml aprotinin, 0.5 mM Pefabloc, 5 µg/ml pepstatin A, 0.5 mM phenylmethylsulfonyl fluoride). Next the cells were lysed by passing through a

22-gauge needle 15 times, and rotated for 30 minutes at 4°C. Lysates were clarified by centrifugation at 17,000 *g* for 15 minutes and mixed with SDS-PAGE loading buffer.

Following treatments described in the figure legends, cells from triplicate wells were scraped and combined. The cells were pelleted by centrifugation at 1,500 *g* for 5 minutes at 4°C and washed with PBS. Cell pellets were resuspended in buffer containing 10 mM HEPES-KOH pH 7.4, 250 mM sucrose, 10 mM KCl, 1.5 mM $MgCl_2$, 5 mM EDTA, 5 mM EGTA, 5 mM dithiothreitol, and 0.1 mM leupeptin supplemented with the protease inhibitor cocktail. The cells were lysed by passing the cell suspension through a 22-gauge needle 30 times and centrifuged at 1,000 *g* for 7 minutes at 4°C. The resulting postnuclear supernatants were further fractionated by centrifugation at 17,000 *g* for 15 minutes at 4°C. The pellet obtained from this spin (designated membranes) was resuspended in buffer containing 10 mM Tris-HCl pH 6.8, 100 mM NaCl, 1% (w/v) SDS, 1 mM EDTA, and 1 mM EGTA, and mixed with SDS-PAGE loading buffer.

Immunoprecipitation − Treatment conditions prior to harvest are described in the figure legends. Following treatments, cells from triplicate wells were scraped, combined, and washed in PBS. The cell pellets were resuspended in buffer containing 5 mM EDTA, 5 mM EGTA, 0.1 mM leupeptin, 1% digitonin, and a protease inhibitor cocktail. Clarified lysates were subjected to immunoprecipitation overnight at 4°C with either anti-T7 coupled agarose beads (Novagen), anti-Flag coupled agarose beads (Sigma), anti-Myc coupled agarose beads (Sigma), or anti-dHrd1 IgG plus Protein A/G agarose (Santa

Cruz Biotechnology). The beads were collected by centrifugation and washed 3 times, 15 minutes each at 4°C, in lysis buffer containing 0.1% digitonin. The bound proteins were eluted from the beads by boiling for 10 minutes in 2 x SDS loading buffer. Aliquots of supernatant and pellet fractions were subjected to SDS-PAGE and immunoblot analysis.

Immunoblot Analysis − Samples were separated by SDS-PAGE and transferred to nitrocellulose membranes for immunoblot analysis. The primary antibodies used for immunoblotting are as follows: anti-T7 tag IgG (Novagen), IgG-228D, a rabbit polyclonal antibody against *Drosophila* Hrd1, IgG-9E10, a mouse monoclonal antibody against the c-Myc epitope purified from culture medium of hybridoma clone 9E10 (American Type Culture Collection), anti-E1 IgG (Calbiochem), polyclonal anti-actin IgG (Sigma), and IgG-3B2, a mouse monoclonal antibody against *Drosophila* SREBP (57). The primary antibodies were detected using horseradish peroxidase-conjugated donkey anti-mouse or anti-rabbit (Jackson ImmunoResearch Laboratories) and SuperSignal West Pico Chemiluminescent Substrate (Thermo Scientific).

3.4 Results and Discussion

Our previous examination of mammalian reductase ERAD in *Drosophila* S2 cells supported a model in which the sterol-induced binding of reductase to Insigs bridged the enzyme to the dHrd1 ubiquitin ligase complex for ubiquitination. To appraise this model, we began by using co-immunoprecipitation to measure binding between endogenous

dHrd1 and reductase upon sterol treatment (**Fig. 3-2A**). S2 cells were transfected with an expression plasmid encoding the membrane domain of mammalian reductase, which is necessary and sufficient for accelerated ERAD, tagged with T7 epitopes together with a plasmid encoding human Insig-1 tagged with Myc. Following transfection, the cells were treated with the proteasome inhibitor MG-132 (to block ERAD of reductase) in the absence or presence of the oxysterol 25-hydroxycholersterol (25-HC) and mevalonate, which stimulates reductase ERAD. Cells were then harvested and detergent lysates were immunoprecipitated with either anti-T7 IgG to pull down transfected reductase (lanes 1-6) or control anti-Flag IgG (lanes 7 and 8). Subsequent immunoblot analysis of precipitated material revealed that in the absence of Insig-1, transfected reductase weakly co-precipitated with endogenous dHrd1 in a sterol-regulated manner (panel 3, lanes 1 and 2). This co-precipitation was significantly enhanced by the co-expression of Insig-1 (panel 3, lanes 3-6). These results considered together with those obtained previously (59), indicate that dHrd1 can associate with reductase in the presence of sterols through Insig-independent mechanisms. This association is significantly stabilized by Insigs such that reductase becomes ubiquitinated by dHrd1 and subsequently degraded from membranes.

In yeast, Hrd1 exists in a large, multiprotein complex containing components that mediate various steps in ERAD ranging from substrate recruitment and ubiquitination to membrane extraction and proteasomal delivery (22, 84, 86). Recently, we found that dHrd1 exists in a similar multiprotein complex in *Drosophila* S2 cells (83). Yeast Hrd3 (also known as Sel1 and dSel1 in mammals and *Drosophila*, respectively) is a key

component of the Hrd1 ubiquitin ligase complex. The protein facilitates transfer of misfolded lumenal substrates from chaperones to Hrd1 for ubiquitination, cytosolic dislocation, and degradation. Hrd1 likely plays a similar role in the selection of membrane-bound substrates for ERAD, but mechanisms for these reactions are not completely understood. Considering this and our previous observation that dSel1 is required for Insig-mediated, sterol-accelerated ERAD of mammalian reductase, we designed an experiment to determine whether dSel1 arbitrates an interaction between reductase/Insig-1 and dHrd1. In the experiment of Fig. 3-2B, S2 cells were transfected with various combinations of the T7-tagged membrane domain of mammalian reductase, Myc-tagged dSel1, and Myc-tagged Insig-1. Following transfection, cells were treated with MG-132 in the absence or presence of 25-HC plus mevalonate. Cells were then harvested for preparation of detergent lysates that were immunoprecipitated with anti-T7 IgG to pull down transfected reductase. Immunoblot analysis of the resulting precipitated material revealed weak, but detectable sterol-regulated co-precipitation of dSel1 with reductase in the absence of Insig-1 (panel 3, lanes 3 and 4). Similar to results obtained with dHrd1 in Fig. 3-2A, the co-precipitation of dSel1 and reductase was significantly enhanced upon the co-expression of Insig-1 (panel 3, lanes 5-8).

Considering the well-established role of Hrd3/Sel1 in recruitment of ERAD substrates to the Hrd1 ubiquitin ligase complex, we next sought to determine whether dSel1 mediates the association of Insig-1/reductase with dHrd1. **Fig. 3-3A** shows an experiment in which S2 cells were subjected to incubation with double stranded RNAs (dsRNAs) against the control GFP or dSel1 mRNAs prior to transfection with Insig-1-

Myc. Cells were then treated with MG-132 prior to harvest and preparation of detergent lysates that were immunoprecipitated with antibodies against endogenous dHrd1. Immunoblot analysis of the resulting immunoprecipitates revealed that as expected, Insig-1 co-precipitated with endogenous dHrd1 (Fig. 3-3A**,** panel 2, lane 2). Insig-1/dHrd1 co-precipitation was significantly inhibited by the RNAi-mediated knockdown of dSel1 (panel 2, lane 3). The rescue experiment shown in Fig. 3-3B was designed to demonstrate the specificity of dSel1 knockdown. As expected, Insig-1-Myc co-precipitated with dHrd1 (Fig. 3-3B, panel 2, lane 2). This co-precipitation was abolished by the RNAi-mediated knockdown of dSel1 (lane 3) and rescued by the overexpression of Myc-tagged dSel1 (lanes 4 and 5).

Having established that dSel1 mediates the association between Insig-1 and dHrd1, we next used co-immunoprecipitation to measure the association of dSel1 and either dHrd1 or Insig-1. In the experiment of **Fig. 3-4A**, detergent lysates from cells transfected with dSel1-Myc were immunoprecipitated with antibodies against endogenous dHrd1. Subsequent immunoblot analysis of the resulting immunoprecipitates revealed that dSel1 co-precipitated with dHrd1 (Fig. 3-4A, panel 2, lanes 2-4). Insig-1 co-precipitated with dSel1 in a similar manner as shown in the experiment of Fig. 3-4B (panel 2, lanes 3-5). The amino acid sequence of dSel1 predicts the protein is comprised of a large lumenal domain followed by a single membrane-spanning region and a short cytosolic tail at the C-terminus. The lumenal domain of dSel1 contains Sel1 repeats that are clustered in two regions dividing the region into an N-terminal domain (amino acids 1-331) and a C-terminal domain (amino

acids 332-702). To identify the region of dSel1 that mediates dHrd1/Insig-1 association, we began by generating three expression plasmids: dSel1 (1-702) encoding the entire lumenal domain of dSel1, dSel1 (1-331) encoding the N-terminal half of the dSel1 lumenal domain, and dSel1 (332-702) encoding the C-terminal half of the dSel1 lumenal domain. These proteins contained the Myc tag fused to their N-terminus. In the experiment of Fig. 3-4C**,** cells were transfected with wild type or truncated dSel1 and dHrd1 was subsequently immunoprecipitated from detergent lysates. The results show that dHrd1 co-precipitated with wild type dSel1 as expected (panel 2, lane 2). Similarly, dSel1 (1-702) co-precipitated with endogenous dHrd1 (panel 3, lane 5), indicating the membrane-spanning segment of dSel1 is not required for its interaction with dHrd1. The dSel1 (332-702) mutant also associated with dHrd1 (panel 4, lane 4); however, this association did not appear to be as stable as that between wild type dSel1 or dSel1 (1-702) and dHrd1. Insig-1 similarly associated with wild type dSel1 (Fig. 3-4D, panel 2, lane 3) as well as dSel1 (1-702) (panel 3, lane 4). Moreover, Insig-1 significantly co-precipitated with dSel1 (332-702) (panel 4, lane 6), but very weakly with the dSel (1-331) (panel 4, lane 5). Together, these data indicate that both dHrd1 and Insig-1 associate with dSel1 predominantly through the C-terminal half of its lumenal domain.

Experiments shown in **Fig. 3-5** were designed to determine whether binding of dSel1 to dHrd1 or Insig-1 is sufficient to confer Insig-mediated, sterol-accelerated ERAD upon mammalian reductase. Fig. 3-5A shows an experiment in which S2 cells were transfected with constructs expressing reductase and Insig-1 prior to dSel1 knockdown. The results show that reductase ERAD was accelerated by treatment of cells with 25-

HC and mevalonate (panel 1, lane 2). This accelerated ERAD was blunted in dSel1 knockdown cells (panel 1, lane 4); however, the reaction was rescued by co-expression of wild type dSel1 in the knockdown cells (panel 1, lanes 5-12). The complete lumenal domain of dSel1 (dSel1 (1-702)) similarly rescued reductase ERAD in dSel1 knockdown cells (Fig. 3-5B, panel 1, lanes 9-12). In contrast, neither dSel1 (1-331) nor dSel1 (332-702) conferred sterol-accelerated ERAD upon reductase in the knockdown cells (Fig. 3-5C, panel 1, lanes 5-8 and Fig. 3-5D, panel 1, lanes 9-12). Together these data indicate that dSel1 bridges the dHrd1 ubiquitin ligase complex to Insig-1 for sterol-accelerated ERAD of reductase. Insig-1 and dHrd1 associated with dSel1 through interactions mediated by the C-terminal half of the dSel1 lumenal domain of dSel1. However, association of dSel1 with dHrd1 is not sufficient for reductase ERAD indicating that the N-terminal half of the dSel1 lumenal domain plays a key, but unknown role in the reaction.

3.5 Figures

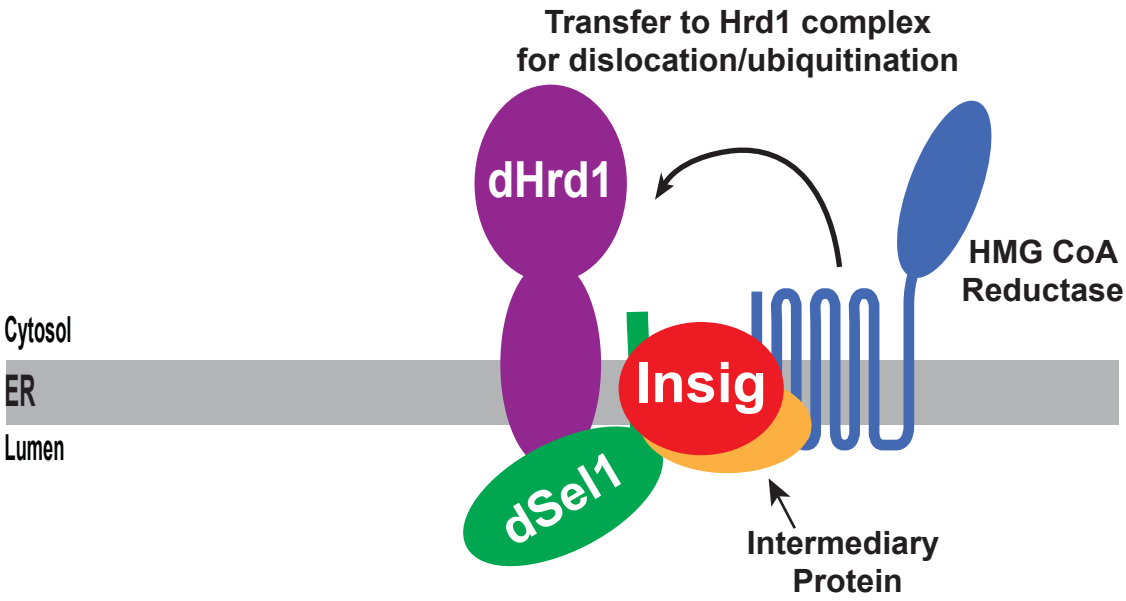

Figure 3-1. Model for dSel1-mediated recruitment of dHrd1 to mammalian reductase-Insig in response to sterols. In the presence of sterols, the ubiquitin ligase dHrd1 and its cofactor dSel1 weakly associate with reductase, sampling the protein for degradation. This association is stabilized by Insig, which interacts with both the membrane domain of reductase and the C-terminal region of the dSel1 lumenal domain. Insig-mediated stabilization of dSel1/dHrd1 and reductase binding leads to dHrd1-ubiquitination and subsequent degradation of reductase. The interaction between dSel1 and Insig-1/reductase could be mediated by direct interactions or through an unknown intermediary protein. In this case, dSel1 weakly associates with reductase through the intermediary protein, sampling it for degradation. However, in the presence of sterols, Insig binds to reductase stabilizing the complex and reductase becomes ubiquitinated by dHrd1. Alternately, the putative intermediary protein may associate with Insig and participate in stabilization of the dHrd1/dSel1/reductase complex in sterol-treated cells.

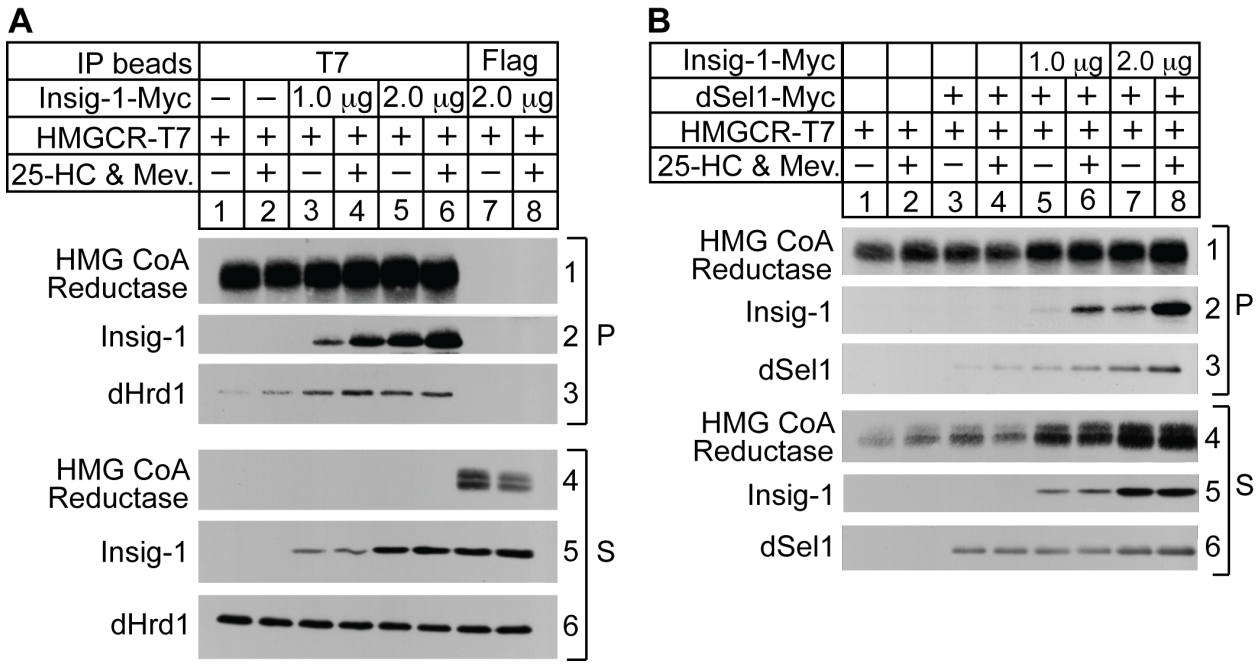

Figure 3-2. Insig-1 stabilizes binding of dHrd1 and dSel1 to HMG CoA reductase for ERAD. On day 0 S2 cells were set up in 6-well plates in medium A. On day 1, cells were washed and transfected in medium B with 2.0 μg pAc-HMG-Red-T7(TM1-8), 1.0 μg or 2.0 μg pAc-Insig-1-Myc, and 0.5 μg pAc-dSel1-Myc (A only) with Maxfect™ Transfection Reagent as described in Material and Methods. The total amount of DNA was adjusted in each sample using pAc 5.1 empty vector to 4.0 μg (A) or 4.5 μg (B). On day 2, cells were fed 1 ml medium B supplemented with 20% HI-LPDS to make the final volume 10% HI-LPDS. Prior to harvest on day 3, cells were treated for 2 hours with 10 μM MG-132 and in the absence or presence of 2.5 μM 25-HC and 10 mM mevalonate. Following treatment cell lysates were prepared in buffer containing 1% digitonin, and immunoprecipitated with either anti-T7 or anti-Flag coupled agarose beads. Aliquots of the pellet (P) and supernatant (S) fractions were subjected to SDS-PAGE followed by immunoblot analysis with anti-T7 (against reductase), IgG-9E10 (against Insig-1 and dSel1), and IgG-228D (against dHrd1).

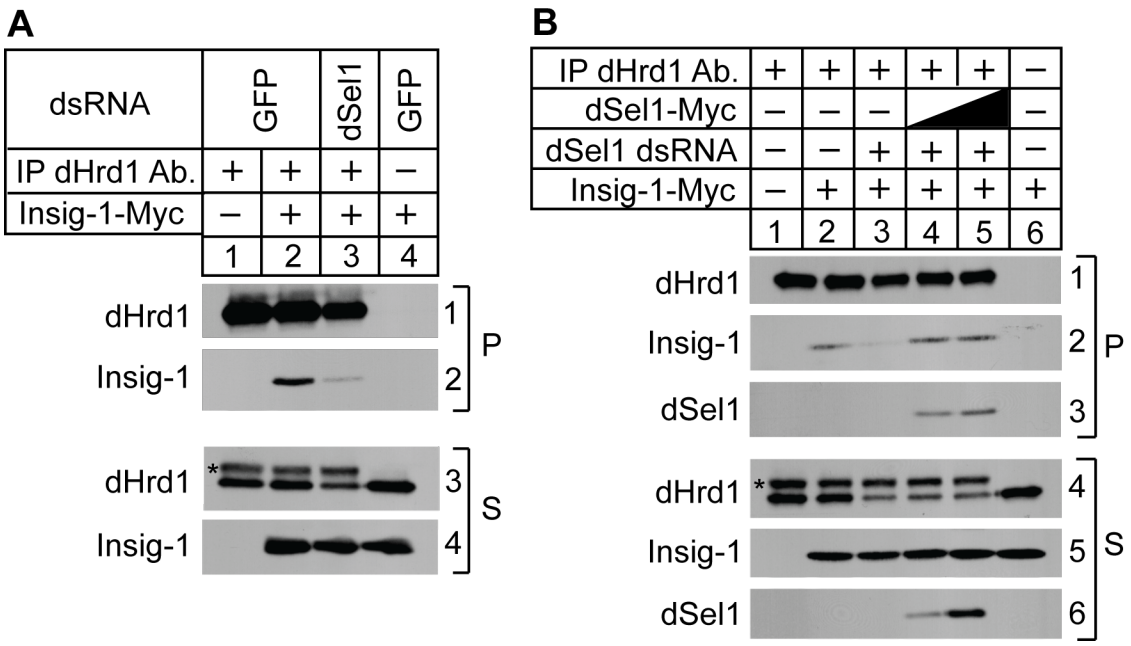

Figure 3-3. dSel1 is required for the dHrd1-Insig-1 interaction. S2 cells were set up on day 0 in medium B and incubated with 15 µg of GFP or dSel1 dsRNA targeted against the indicated endogenous mRNAs. Following incubation for 1 hr the cells received 2 ml medium C. The cells were washed and transfected on day 2 in medium B with 1.0 µg pAc-Insig-1-Myc alone (A) or together with 0.3 µg or 1.0 µg pAc-dSel1-Myc (B). The total amount of DNA was kept constant by adding empty pAc 5.1 vector. On day 2 each well received 1 ml of medium B supplemented with 20% HI-LPDS to bring the final volume to 10% HI-LPDS. On day 3, cells were treated with 10 µM MG-132 in medium C for 2 hrs, and cell lysates were prepared in buffer containing 1% digitonin. Lysates were immunoprecipitated with IgG-228D and protein A/G agarose and the resulting pellet (P) and supernatant (S) fractions were subjected to SDS-PAGE and immunoblot analysis with IgG-228D (against dHrd1) and IgG-9E10 (against Insig-1 and dSel1). The asterisk (*) denotes a nonspecific cross-reactive band.

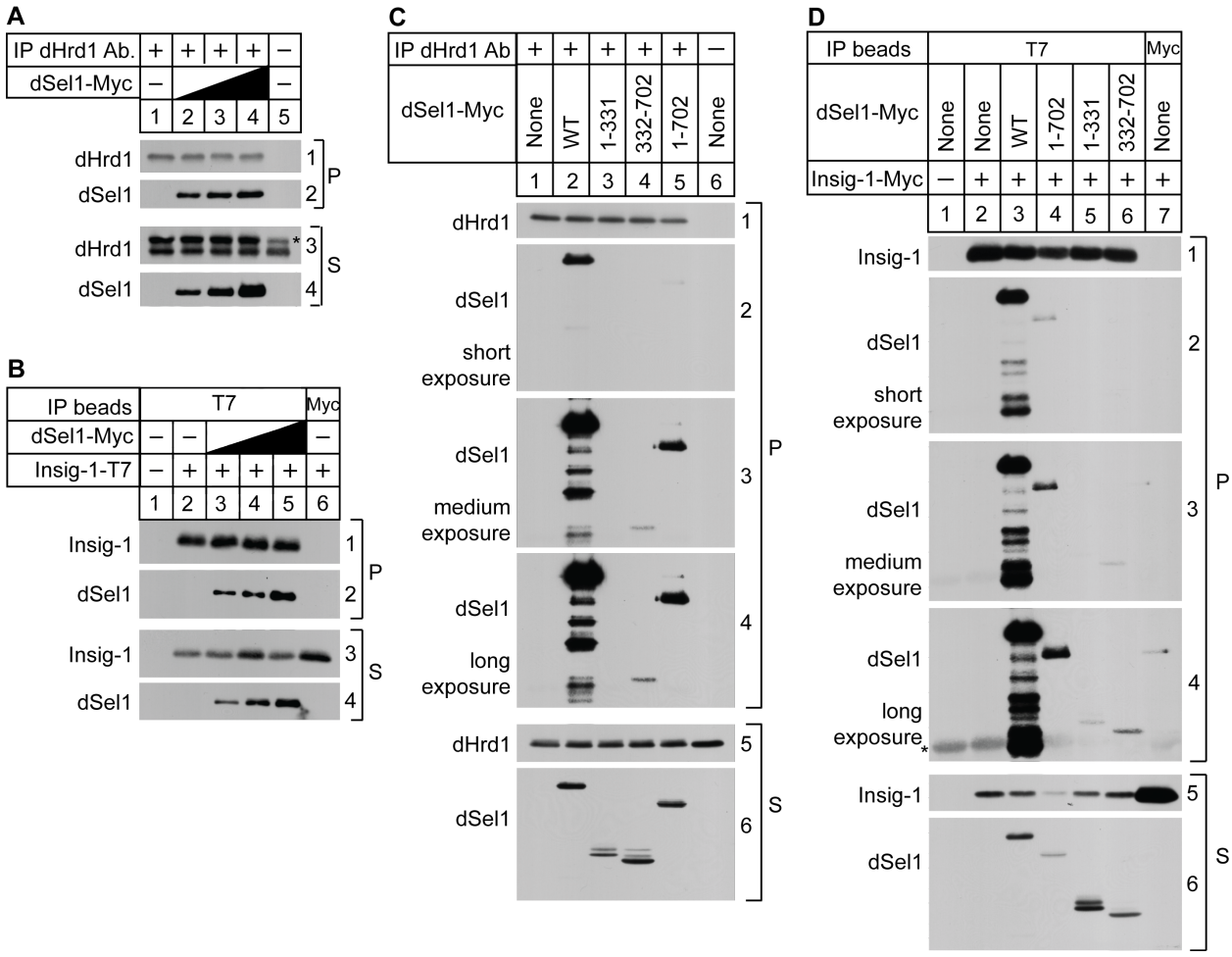

Figure 3-4. Insig-1 and dHrd1 interact predominantly with the C-terminal domain of dSel1. On day 0 S2 cells were set up in medium A in 6-well plates. On day 1 the cells were washed and transfected in medium B with 0.1 µg, 0.3 µg, or 1.0 µg pAc-dSel1-Myc (A, B) and 1.0 µg pAc-Insig-1-Myc (B). C, D: 0.5 µg pAc-dSel1-Myc, 1.0 µg pAc-dSel1-702-Myc, 0.5 µg pAc-dSel1-1-331-Myc, 1.0 µg pAc-dSel1-332-702-Myc, and 0.3 µg pAc-Insig-1-T7 (D only). The cells received an additional 1 ml of medium B supplemented with 20% HI-LPDS on day 2 to make the final volume 10% HI-LPDS. On day 3 cells were treated for 2 hrs with 10 µM MG-132 in medium C. Following treatment the cells were harvested and detergent lysates were prepared containing 1% digitonin. The lysates were immunoprecipitated with either anti-T7 conjugated agarose, anti-Flag conjugated agarose, or IgG-228D with protein A/G agarose. The pellet (P) and supernatant (S) fractions were separated by SDS-PAGE and analyzed by immunoblot using IgG-228 (against dHrd1), anti-T7 (against Insig-1), and IgG-9E10 (against dSel1). The asterisk (*) indicates a non-specific cross-reactive band.

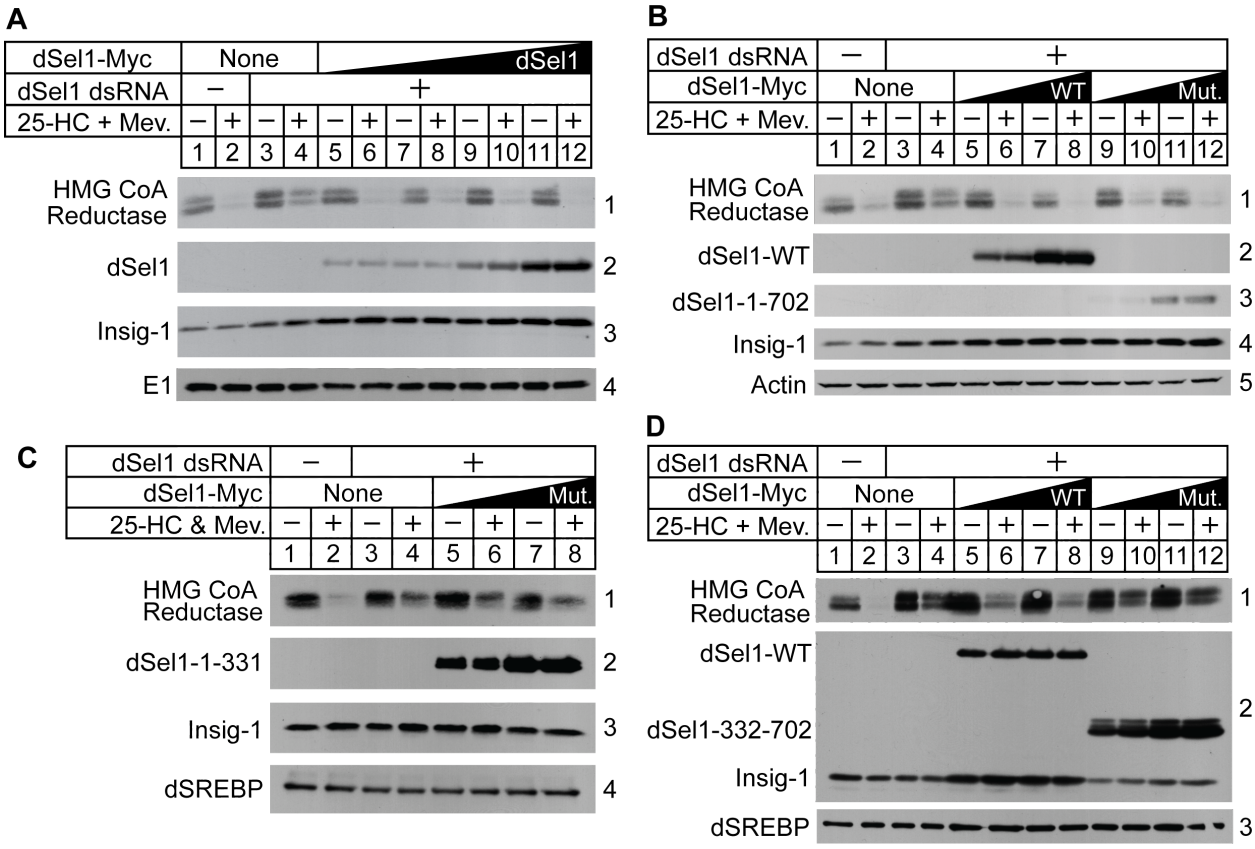

Figure 3-5. The dSel1 1-702 mutant is sufficient for reductase degradation, but not dSel1 1-331 or dSel1 332-702. S2 cells were set up on day 0 in medium B and incubated with 15 µg of GFP or dSel1 dsRNA targeted against the indicated endogenous mRNAs. On day 1 the cells were washed and transfected in medium B with 0.5 µg pAc-HMG-Red-T7, 0.3 µg pAc-Insig-1-Myc (A-D), 0.03 µg, 0.05 µg, 0.1 µg, or 0.3 µg pAc-dSel1-Myc (A, B, D), 0.3 µg or 1.0 µg pAc-dSel1-702-Myc (B), 0.1 µg or 0.3 µg pAc-dSel1-1-331-Myc (C), or 0.5 µg pAc-dSel1-332-702-Myc (D). The cells received 1 ml of medium B supplemented with 20% HI-LPDS making the final volume 10% HI-LPDS on day 2. On day 3, the cells were treated in the absence or presence of 2.5 µM 25-HC and 10 mM mevalonate for 5 hrs. Following treatment the cells were harvested and whole cell lysates (A, B) or membrane fractions (C, D) were prepared as describe in Material and Methods. The samples were separated by SDS-PAGE and subjected to immunoblot analysis with anti-T7 (against reductase), IgG-9E10 (against Insig-1, dSel1, and dSel1 mutants), anti-E1, anti-actin, and IgG-3B2 (against dSREBP).

CHAPTER 4:

Conclusions and Recommendations

4.1 Conclusions and Implications

Many insights into the underlying mechanisms of the ERAD pathway have been provided by studies that primarily focus on soluble substrates. Based on these studies, it is widely accepted that soluble substrates are selected for degradation by lumenal chaperones and transported through a channel across the ER membrane into the cytosol where they are subsequently ubiquitinated and degraded by proteasomes (5, 24). Some of what has been learned from studying soluble substrates is applicable to the ERAD of integral membrane substrates. However, ERAD of integral membrane proteins has proven to be more complex and a thorough understanding of the underlying mechanisms is lacking. To address this, I examined ERAD of two model integral membrane substrates, HMG CoA reductase and Insig-1 in which degradation can be precisely controlled by the addition of sterols or other lipids ensuring physiological relevance. These studies were initiated in *Drosophila* S2 cells taking advantage of the simpler and more effective RNAi as well as the lack of redundancy that complicates genetic knockdowns in mammalian cells. Using this system, I employed RNAi to determine the proteins that mediate key steps in the ERAD pathway of HMG CoA reductase and Insig-1. Surprisingly, mammalian reductase and Insig-1 are degraded through distinct pathways mediated by different E3 ligases in S2 cells.

The current study extends the previous finding that sterol-regulated Insig-mediated ERAD of mammalian reductase can be reconstituted in *Drosophila* S2 cells

(59). The *Drosophila* ubiquitin ligase dHrd1 was identified to be required for degradation of mammalian reductase in S2 cells (59). I used tandem affinity purification in S2 cells to purify the dHrd1 ligase complex and identified the complex components by mass spectrometry, characterizing the first ubiquitin ligase complex in *Drosophila*. This data revealed many proteins known to associate with the yeast homolog of dHrd1 including its binding partner dSel1, the dHsc70 chaperone bound to the lectin dOs9, the ubiquitin conjugating enzyme dUbc7, ubx (ubiquitin regulatory x) domain containing proteins dUbxd2 and dUbxd8, which aid in recruitment of the cytosolic AAA-ATPase Ter94 and its cofactors dNpl4 and dUfd1, as well as the polytopic membrane proteins dHerp and dDerlin-2/3. Additionally dUbiquilin, a homolog of the yeast Rad23 proteasome delivery protein, and many components of the 26S proteasome were identified (Table 2-1).

The dHrd1 complex components required for degradation of reductase were determined by RNAi-mediated knockdown to include dSel1, dUbc7, Ter94, dNpl4, dUfd1, dHerp, and dUbiquilin. In addition, I used subcellular fractionation and RNAi to determine which dHrd1-associated factors are required for the sterol-induced dislocation of reductase into the cytosol. These studies showed that knockdown of dHrd1, dSel1, Ter94, and dHerp significantly blunted cytosolic dislocation of reductase. Ter94 is the homolog of the mammalian AAA-ATPase VCP/p97, which is well known for playing a role in the extraction of ERAD substrates from the ER membrane (28). The role of dHerp in reductase degradation remains to be determined. In yeast, the proposed functional homolog of dHerp mediates recruitment of Derlins to the Hrd1

ubiquitin ligase complex (22), a conserved family of polytopic membrane proteins that play a key role in ERAD. However, dDerlins are not required for reductase degradation in S2 cells, indicating that dHerp plays a role distinct from recruitment of Derlins. A study in mammalian cells shows Herp interacts with Ubiquilins, a family of cytosolic proteasomal shuttling factors with domains that interact with both the proteasome and ubiquitin, and this interaction is required for degradation of a subset of ERAD substrates (87). Since data indicates dUbiquilin is required for reductase degradation, this implies that dHerp might be acting to recruit dUbiquilin to the complex, where dUbiquilin can associate with ubiquitinated reductase for delivery to the proteasome for degradation.

In mammalian cells, Insigs mediate degradation of reductase by binding to reductase in response to sterol treatment and thereby bridging reductase to an ubiquitin ligase marking it for degradation. Mammalian Insigs are also required in S2 cells for sterol-mediated degradation of reductase, so it is surprising that dSel1 is additionally required for reductase degradation (Fig 2-1). In yeast, dSel1 is a cofactor of dHrd1 and is known to function in the initial steps of substrate recognition and recruitment (88). I employed a series of interaction experiments to determine the role dSel1 plays in selection of mammalian reductase in S2 cells. Coimmunoprecipitation experiments establish reductase interacts with dSel1 and dHrd1 in a sterol-regulated manner that is stabilized by Insig-1 in S2 cells (Fig 3-2). Using RNAi, I focused on the interactions between Insig-1 and dHrd1 determining the interaction is mediated by dSel1 (Fig 3-3). Furthermore, the region of dSel1 that binds to both Insig-1 and dHrd1 was identified as the C-terminal half of the lumenal domain (Fig 3-4). *Drosophila* Sel1 consists of a large

lumenal domain followed by a short transmembrane domain. The lumenal domain contains 11 Sel1 repeats that are clustered into two groups, the N-terminal half (amino acids 1-331) and a C-terminal half (amino acids 332-702). Coimmunoprecipitation experiments using expression plasmids encoding either full length or fragments of dSel1 determined both Insig-1 and dHrd1 interact with the C-terminal half (332-702) of dSel1, and Insig-1 also interacts very weakly with the N-terminal half (1-331) (Fig 3-4). Since both dHrd1 and Insig-1 interact with the C-terminal half of dSel1, rescue experiments were performed to determine whether it is sufficient to degrade reductase. Neither fragment rescues degradation of mammalian reductase in dSel1-knockdown cells indicating the N-terminal half is required, but has an unknown function such as playing a structural role or interacting with an unidentified protein. The full lumenal domain (amino acids 1-702) lacking the transmembrane region is sufficient to degrade reductase further indicating the transmembrane isn't necessary for localization to the complex (Fig 3-5). This data suggests dSel1 is necessary for selection of Insig-reductase by bridging it to the ligase complex for ubiquitination and subsequent degradation (Fig 3-1).

ERAD of Insig-1 is subjected to lipid-mediated regulation in mammalian cells. The current studies establish that mammalian Insig-1 is degraded under the same physiological conditions in S2 cells as in mammalian cells, indicating that mechanisms for selection of Insig for ERAD are highly conserved. For example, Insig-1 but not its close homolog Insig-2, is subjected to proteasome-mediated degradation. Similar to mammalian cells, Insig-1 ERAD is blocked by either sterols through a mechanism that

requires Scap, or by the unsaturated fatty acid oleate through a mechanism that does not require Scap, but rather inhibits cytosolic dislocation. Finally, polyubiquitinated forms of Insig-1 accumulate in the presence of the proteasome inhibitor MG-132 (83).

RNAi experiments determined the ubiquitin ligase dTeb4 is required to degrade Insig-1 in S2 cells. Further, overexpression of dHrd1 cannot rescue Insig-1 degradation in dTeb4 knockdown cells. It is surprising that Insig-1 and reductase require different ubiquitin ligases since data indicates Insig-1 interacts with dHrd1 in a dSel1 dependent manner in S2 cells (Fig. 3-3); and in mammalian cells, reductase and Insig-1 are degraded by the same ligase, gp78. In the absence of dTeb4 knockdown, overexpression of dHrd1 blocks Insig-1 degradation suggesting the ligases share a common pool of ERAD factors. When dHrd1 is overexpressed it most likely sequesters the ERAD components leaving dTeb4 unable to degrade Insig-1. An evaluation by RNAi determined a role for dHrd1 ligase components in Insig-1 ERAD resulting in a subset of factors shared by dHrd1 and dTeb4 to degrade reductase and Insig-1 including dUbc7, dUbxd8, dHerp, Ter94, dUfd1, and dNpl4. There are also several differences in the ERAD components utilized by the ligases to degrade reductase and Insig-1. For instance, reductase degradation requires dHrd1, its cofactor dSel1, and the proteasomal shuttling protein dUbiquilin, unlike dTeb4 for Insig-1 degradation. Insig-1 ERAD specifically requires dTeb4, the ubiquitin-conjugating enzyme dUbc6, and dDerlin2/3.

The different ERAD factors utilized by dHrd1 and dTeb4 indicate they may work through distinct pathways in S2 cells. This idea is supported by experiments evaluating

the ERAD components utilized in cytosolic dislocation of reductase and Insig-1. Knockdown of dHrd1 blocks cytosolic dislocation of reductase whereas knockdown of dTeb4 does not effect dislocation of Insig-1 indicating ubiquitination by dTeb4 is not required for cytosolic dislocation of Insig-1. The differences in the ubiquitin-conjugating enzymes required further support this notion; reductase dislocation requires dUbc7 whereas Insig-1 dislocation doesn't require dUbc6. I further investigated the requirement of ubiquitination for cytosolic dislocation of Insig-1 using an inhibitor of ubiquitin-activating enzymes, PYR-41. Treatment with PYR-41 leads to an accumulation of Insig-1 in the cytosol, similar to dTeb4 knockdown, and stabilization of Insig-1 in the membranes, indicating dislocation of Insig-1 to the cytosol precedes ubiquitination by dTeb4.

Together this data indicates mammalian reductase and Insig-1 are degraded through distinct pathways in S2 cells that are mediated by the ubiquitin ligase. As sterol levels increase in the ER membrane this triggers the binding of Insig-1 to reductase targeting it for ERAD. Then reductase is selected for degradation by dSel1 that bridges reductase to the dHrd1 complex by interacting with C-terminal half of the dSel1 lumenal domain. Next reductase becomes ubiquitinated by the actions of dHrd1 and dUbc7, and dislocated to the cytosol through a mechanism that utilizes the AAA-ATPase Ter94, its membrane anchor Ubxd8, and the cofactors dUfd1 and dNpl4. Once extracted, reductase is delivered to proteasomes for degradation in a manner that requires dUbiquilin, which is most likely recruited to the complex by dHerp. In contrast, under low sterol and unsaturated fatty acids conditions Insig-1 is not bound to Scap or

reductase and is dislocated to the cytosol through a mechanism that requires dDerlin2/3, dHerp that most likely recruits dDerlin2/3, Ter94, Ubxd8, dNpl4, and dUfd1. Once dislocated Insig-1 is ubiquitinated by dTeb4 and dUbc6 and degraded by proteasomes through a mechanism that doesn't utilize the proteasomal delivery protein dUbiquilin. It is important to point out that Insig-1 degradation in S2 cells requires two ubiquitin-conjugating enzymes dUbc6 and dUbc7, however only dUbc7 is required for dislocation. This suggests there could be two rounds of ubiquitination required for Insig-1 degradation. In this case Insig-1 would be ubiquitinated by an unknown ligase that utilizes dUbc7, dislocated to the cytosol, and then undergo a second round of ubiquitination by dTeb4 and dUbc6 in the cytosol prior to degradation.

These studies establish *Drosophila* as a model system to study the underlying mechanisms of ERAD. This system can be applied to other clinically relevant ERAD substrates to accelerate the discovery of new molecules that mediate ERAD. My results contribute to understanding the ERAD of integral membrane substrates in which mutant forms result in disease.

4.2 Recommendations for Future Studies

Cytosolic dislocation of integral membrane ERAD substrates has been well documented over the past decade (33-36). One aspect that remains to be understood is how the solubility of the transmembrane domain of these substrates, such as HMG CoA reductase, are maintained during cytosolic dislocation and proteasomal delivery. One hypothesis involves reductase localizing to regions of ER membrane associated

with cytosolic organelles called lipid droplets (47, 89). Lipid droplets are lipid storage depots composed of a neutral lipid core (triacylglycerol and cholesterol esters) surrounded by a phospholipid monolayer that protrudes out of the ER membrane into the cytosol (90). They are dynamic organelles that form and change size in response to changes in lipid homeostasis. Lipids stored in the core of the droplets are mobilized when needed for cellular roles such as membrane synthesis during cell division and metabolic processes. Storage of cholesterol esters also protects the cell from the toxic effects posed by the accumulation of free cholesterol (90, 91). Proteomic studies have revealed that lipid droplets contain a distinct set of proteins some of which are unique to lipid droplets such as adipose differentiation-related protein, whereas others are associated with the plasma membrane (caveolin) or ER (Bip). The many facets lipid droplets play in cellular homeostasis are just beginning to be explored including a role in ERAD of some substrates such as HMG CoA reductase.

Several studies support that lipid droplets play a role in the ERAD of some substrates. My laboratory has identified several ERAD proteins localized to lipid droplets including p97 and its recruitment factor ubiquitin regulatory X (Ubx) domain containing protein 8 (Ubxd8) (91). Several ERAD substrates have also been found to accumulate on lipid droplets when proteasome activity is blocked such as apolipoprotein B-100, HMG CoA reductase, and Insig-1 (92). Furthermore, proteasome inhibition in sterol-deprived cells leads to the formation of lipid droplets that are closely associated with ER membranes. Isolation of lipid droplets under these conditions by sub-cellular fractionation reveals reductase co-purifies with a lipid droplet fraction when stimulated

with sterols in the presence of Insigs (47). The role lipid droplets play in ERAD seems to be specific for a subset of substrates. This conclusion comes from studies where treatment with triacsin C (inhibitor of acyl-CoA synthase) blocks lipid droplet formation while also blocking ERAD of reductase (47), but not of Insig-1 (54). ERAD components that mediate recruitment and regulation of reductase to lipid droplets, or a region of the ER closely associated with lipid droplets, remains unknown. Moreover, the role that lipid droplets play in ERAD of reductase is poorly understood.

Employing RNAi studies in *Drosophila* S2 cells will accelerate the discovery of proteins that mediate recruitment of reductase and Insig-1 to a lipid droplet region. Preliminary studies in S2 cells shown in **Fig 4-1** reconstitute co-purification of mammalian reductase with a lipid droplet fraction in a manner that mimics studies in mammalian cells. In this experiment S2 cells were transfected with expression plasmids encoding the transmembrane domain of mammalian reductase and Insig-1. The cells were treated with MG-132 to inhibit proteasomes in the absence or presence of sterols as described in the figure legend. Immunoblots reveal reductase localizes to the cytosolic and lipid droplet fractions in a sterol dependent manner in the presence of MG-132 as previous studies in mammalian cells. Using this reconstituted S2 cell system with RNAi-mediated knockdown targeting genes encoding ERAD components will determine the proteins required for sterol-mediated recruitment of reductase to lipid droplets.

My lab recently identified an intermediate in the reductase ERAD pathway that is retro-translocated across the ER membrane and peripherally associated with the

membrane prior to dislocation to the cytosol. Detection of this intermediate relies on sub-cellular fractionation followed by either a trypsin protection assay or a membrane carbonate wash assay both of which detect accumulated reductase upon proteasome inhibition. However, these assays are limited by low detection of retro-translocated reductase due to the required use of proteasome inhibitors for detection that don't provide complete inhibition, and low detection of the retrotranslocated reductase by antibodies used in immunoblot analysis. To gain insight into the mechanisms through which reductase is retro-translocated across the ER membrane a robust extraction assay is needed in combination with RNAi in the *Drosophila* system. I propose using a cytosolic biotin ligase tagging system to identify reductase that is retro-translocated, but still associated with the membrane, as previously reported for detection of retro-translocated ERAD substrates (93). This is achieved using a plasmid expressing reductase fused to a 15 amino acid long biotin acceptor peptide (BAP) placed in a lumenal loop of reductase. This construct is co-expressed with a plasmid encoding a cytosolic biotin ligase called BirA, which will biotinylate reductase once the lumenal BAP is exposed to the cytosolic side of the ER membrane. This technique will provide robust detection of retro-translocated reductase, which in combination with RNAi will determine the ERAD components required for retro-translocation. This assay can be applied to other integral membrane and lumenal ERAD substrates to better understand general mechanisms of retro-translocation, and possibly identify the proteins that compose the retro-translocation channel.

4.3 Figures

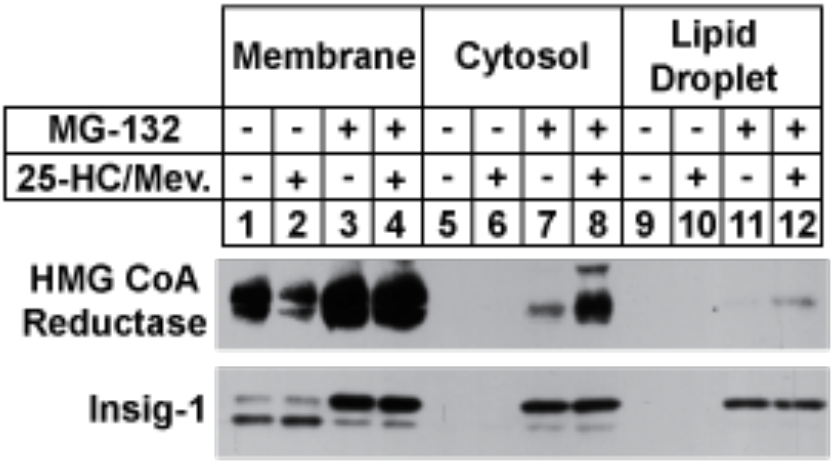

Figure 4-1. HMG CoA reductase co-purifies with a lipid droplet fraction in the presence of Insig-1 and sterols. S2 cells were set up on day 0, transfected in medium B with 0.5 μg of pAc-HMG-Red-T7 (TM1-8) and 0.1 μg pAc-Insig-1-Myc in medium B using Maxfect™ Transfection Reagent, incubated with medium B containing 10% LPDS on day 2, and subjected to treatment with 25-HC plus mevalonate on day 3 as described in the legend to Fig. 2-1. The cells also received 10 μM MG-132 on day 3. Following incubation for 4 h, the cells were harvested and subjected to subcellular fractionation as described in "Materials and Methods 2.3." The resulting membrane (10 μg protein/lane), cytosol (40 μg protein/lane), and lipid droplet (40 μg protein/lane) fractions were subjected to 10% SDS-PAGE followed by immunoblot analysis as described in the legend to Fig. 2-1.

APPENDIX A

The Primers Used for dsRNA Generation

Gene		**Nucleotides**	**Primers** (Forward and Reverse)
dHrd1	CG1937-RA	220–243	CATCTGCTGGAGCGCTTTTGGTAT
		892–915	GCAGGGCAGTTTCTTTGAGTGATT
dTeb4	CG1317-RB	823–846	GTTTTTCTGGAGCACGTCTTCTGG
		1524–1548	CAGCAATTGCAAGTTAACCGCTGAA
dTrc8	CG2304-RA	1052–1074	TCGACGGCTGTGAGACTATGACG
		1617–1638	GATGCCGAAGCAGAACTCCACT
dUbc6	CG5823-RA	48–71	GTCGCGCATGAAGCAGGACTATAT
		699–717	TCCTCCGCCGCTGGCCAAA
dUbc7	CG4443-RA	1–20	ATGGCTGGGTCCGCACTGCG
		478–504	TTACGCCGGTAAACCAAGAGTTTTGCG
dSel1	CG10221-RA	80–101	ACATTGATGGTACGGGCAGCAG
		822–842	TGGATCAGCGCCTTCTCACAG
dOs9	CG6766-RA	111–138	TGATTTCGAAGTGCCGGATTTAGATGTG
		802–825	CGCCTCGGATTCAACCCATTCCTT
dUbxd2	CG8042-RA	540–566	GGAGGCCAAGACGAATCCACCAAATTC
		1198–1218	TCGGATCTGCAGCCTCGTCTC
dUbxd8	CG10372-RA	20–42	CCAACGAACAGACGGAGAAGGTC
		654–675	GGCTACGTCGCATCCCCATAAC
dHerp	CG14536-RA	696–714	CTTGCCGCCACCGACTCAA
		1350–1373	AGCGAGGTGAAGAACGTGATGACA
dDerlin-1	CG10908-RA	33–51	CCGCTTCACCCGCTACTGG
		670–689	TGCCTAGGTGGTGCTCTGCT
dDerlin-2/3	CG14899-RA	105–127	GCCGCTGCAGCTCTACTTCAATC
		733–754	GATTCGCTGGCTCCTCATCCTG
Ter94	CG2331-RC	1713-1733	CATGTGGTTCGGCGAGTCTGA
		2452-2477	CTGTAAAGATCATCGTCGCCGTTGT
dNpl4	CG4673-RA	67–90	GTGCGCCATCGTCTGTTTGTGTTA
		810–831	GGTGCGCCAGTAGTTGAGGAAG
dUfd1	CG6233-RA	163–187	CGCCTGAATGTCGAGTATCCAATGC
		853–878	GCTACGGCATCATCTTCTTGGCTTCT
dUbiquilin	CG14224-RA	751-774	GCAAATGCATGACCTGATGCAGCG
		1477-1500	GCGCAGCGCGGCCCCAGGTCTCGT

APPENDIX B

Protein Identification from dHrd1 Purification in S2 Cells by Mass Spectrometry

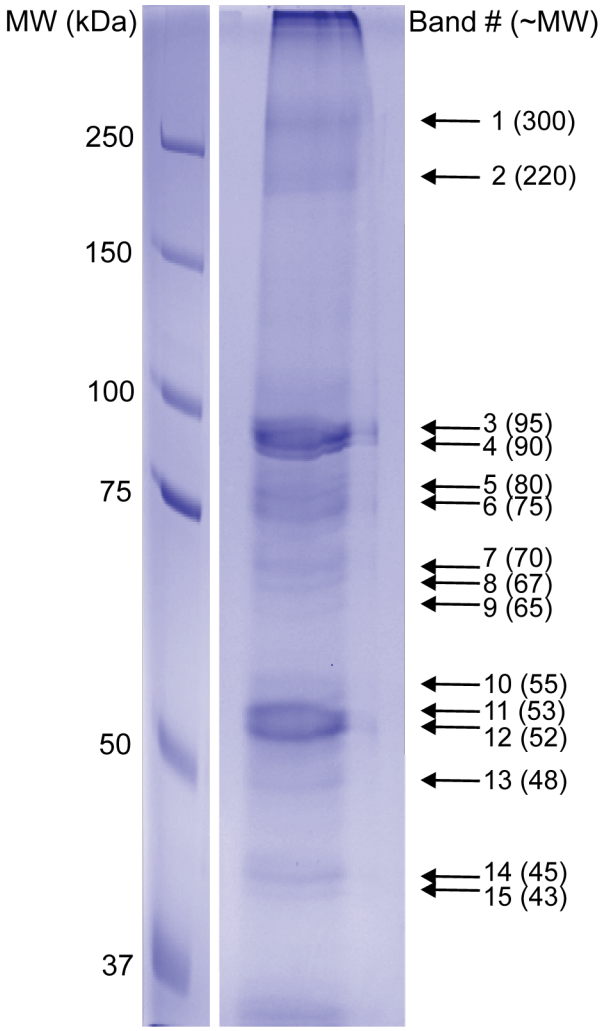

Band	#	Protein Name	Acc #	Score	MW	Description
1	1	Hrd3	gi|21355295	1417	89304	Hrd3
	2	calcium ATPase at 60A, isoform B	gi|24762445	1352	111630	Calcium ATPase
	3	septin interacting protein 3	gi|28571958	985	69228	Hrd1
	4	GM23543 [Drosophila sechellia]	gi|195331395	819	89291	SEL1
	5	GG16792 [Drosophila erecta]	gi|194900506	532	275272	Filamin-actin binding surface
	6	tiggrin [Drosophila melanogaster]	gi|493070	481	256960	
	7	GJ16071 [Drosophila virilis]	gi|195403397	427	280829	Spectrin repeats involved in cytosketetal structure
	8	GK22768 [Drosophila willistoni]	gi|195449906	404	89674	SEL1
	9	ubiquitin [Drosophila melanogaster]	gi|158765	387	8535	Ubiquitin
	10	GG11831 [Drosophila erecta]	gi|194904702	387	66620	Hrd1
	11	GG19855 [Drosophila erecta]	gi|194944118	323	36863	Polyubiquitin
	12	RecName: Full=205 kDa microtubule-associated protein	gi|126746	249	126592	microtubule-associated protein
	13	beta-spectrin [Drosophila melanogaster]	gi|157020	219	265623	Spectrin repeats involved in cytosketetal structure
	14	Derlin-2 [Drosophila melanogaster]	gi|21355437	211	29832	Derlin-2
	15	GE17676 [Drosophila yakuba]	gi|195481117	198	265331	Calponin homology domain
2	1	gp210 [Drosophila melanogaster]	gi|24585893	2380	209661	-
	2	septin interacting protein 3 [Drosophila melanogaster]	gi|28571958	1064	69228	Hrd1
	3	sarco/ER-type Ca-2+-ATPase [Drosophila melanogaster]	gi|158416	1039	109528	E1-E2_ATPase/Cation transporting ATPase
	4	Hrd3 [Drosophila melanogaster]	gi|21355295	769	89304	Hrd3
	5	ubiquitin [Drosophila melanogaster]	gi|158763	445	8558	Ubiquitin
	6	CG8858 [Drosophila melanogaster]	gi|19922080	185	211953	-
	7	RE67845p [Drosophila melanogaster]	gi|21483540	172	48177	Glucosidase II beta subunit-like protein
	8	beta-1 tubulin [Drosophila melanogaster]	gi|158739	167	50119	tubulin beta chain
3	1	Hrd3 [Drosophila melanogaster]	gi|21355295	2310	89304	Hrd3
	2	GM23543 [Drosophila sechellia]	gi|195331395	1344	89291	SEL1
	3	GE23928 [Drosophila yakuba]	gi|195503005	1102	89402	SEL1
	4	calcium ATPase at 60A, isoform B [Drosophila melanogaster]	gi|24762445	1101	111630	Calcium ATPase
	5	GK22768 [Drosophila willistoni]	gi|195449906	829	89674	SEL1
	6	septin interacting protein 3 [Drosophila melanogaster]	gi|28571958	770	69228	Hrd1
	7	GF18742 [Drosophila ananassae]	gi|194745849	663	88253	SEL1
	8	CG6766 [Drosophila melanogaster]	gi|24583799	508	59715	Os9
	9	coatomer, beta-prime subunit [Drosophila melanogaster]	gi|3204159	262	102663	WD40 domain
	10	Ref(2)P protein [Drosophila melanogaster]	gi|151175396	260	48739	PB1 domain-zinc-binding site
	11	ribosomal protein S27A [Drosophila melanogaster]	gi|17136574	239	17929	DUb80
	12	beta-coatomer protein [Drosophila melanogaster]	gi|17647193	230	107339	beta-coatamer protein/Adaptin_N
	13	protein on ecdysone puffs, isoform B [Drosophila melanogaster]	gi|17864514	174	78000	-
4	1	Hrd3 [Drosophila melanogaster]	gi|21355295	2775	89304	Hrd3
	2	calcium ATPase at 60A, isoform B [Drosophila melanogaster]	gi|24762445	2198	111630	Calcium ATPase
	3	GM23543 [Drosophila sechellia]	gi|195331395	1644	89291	SEL1
	4	GE23928 [Drosophila yakuba]	gi|195503005	1245	89402	SEL1
	5	septin interacting protein 3 [Drosophila melanogaster]	gi|28571958	932	69228	Hrd1
	6	GK22768 [Drosophila willistoni]	gi|195449906	904	89674	SEL1
	7	beta-coatomer protein [Drosophila melanogaster]	gi|17647193	512	107339	beta-coatamer protein/Adaptin_N
	8	Hsc70Cb, isoform A [Drosophila melanogaster]	gi|21357475	373	88446	Hsp70
	9	ubiquitin [Drosophila melanogaster]	gi|158767	267	8540	Ubiquitin
	10	coatomer, beta-prime subunit [Drosophila melanogaster]	gi|3204159	243	102663	WD40 domain
	11	elongation factor 2b, isoform B [Drosophila melanogaster]	gi|24585711	231	93023	elongation factor 2b

	12	GJ17974 [Drosophila virilis]	gi|195398119	230	103989	WD40 domain
	13	TER94 [Drosophila erecta]	gi|194858161	131	88765	TER94
	14	Ref(2)P protein [Drosophila melanogaster]	gi|151175378	127	31481	PB1 domain-zinc-binding site
	15	Rpn1 [Drosophila melanogaster]	gi|21356859	98	102212	26S proteasome regulatory complex component
5	1	GE19324 [Drosophila yakuba]	gi|195475210	2185	88803	TER94
	2	ER membrane fusion protein [Drosophila melanogaster]	gi|6573151	1803	88524	TER94
	3	heatshock protein cognate 70Cb [Drosophila melanogaster]	gi|4753683	1143	88518	Hsp70
	4	Hrd3 [Drosophila melanogaster]	gi|21355295	1076	89304	Hrd3
	5	septin interacting protein 3 [Drosophila melanogaster]	gi|28571958	998	69228	Hrd1
	6	glycoprotein 93 [Drosophila melanogaster]	gi|21357739	773	90182	Hsp90
	7	sarco/ER-type Ca-2+-ATPase [Drosophila melanogaster]	gi|158416	762	109528	E1-E2_ATPase/Cation transporting ATPase
	8	calnexin [Drosophila melanogaster]	gi|2213427	748	67993	Calnexin
	9	GD21603 [Drosophila simulans]	gi|195575380	555	69232	Hrd1
	10	ubiquitin [Drosophila melanogaster]	gi|158763	338	8558	Ubiquitin
	11	Rpn1 [Drosophila melanogaster]	gi|21356859	326	102212	26S proteasome regulatory complex component
	12	GG11831 [Drosophila erecta]	gi|194904702	326	66620	Hrd1
	13	GM16430 [Drosophila sechellia]	gi|195354454	317	97172	Sec21-vesicle coat complex COPI
	14	calcium-independent phospholipase isoform A [Drosophila melanogaster]	gi|45550585	299	96801	calcium-independent phospholipase
	15	CG6453 [Drosophila melanogaster]	gi|19921464	175	61501	LDL receptor class A domain
6	1	septin interacting protein 3 [Drosophila melanogaster]	gi|28571958	1116	69228	Hrd1
	2	heat shock protein 83 [Drosophila melanogaster]	gi|17647529	986	81814	Hsp83
	3	Hrd3 [Drosophila melanogaster]	gi|21355295	902	89304	Hrd3
	4	CG6453 [Drosophila melanogaster]	gi|19921464	661	61501	
	5	calnexin [Drosophila melanogaster]	gi|2213427	507	67993	calnexin
	6	ER membrane fusion protein [Drosophila melanogaster]	gi|6573151	468	88524	TER94
	7	sarco/ER-type Ca-2+-ATPase [Drosophila melanogaster]	gi|158416	457	109528	E1-E2_ATPase/Cation transporting ATPase
	8	belle [Drosophila melanogaster]	gi|17985987	379	85029	DEAD-box helicase
	9	82 kDa heat shock protein [Drosophila persimilis]	gi|2352601	349	30196	Hsp90
	10	eIF3-S9, isoform B [Drosophila melanogaster]	gi|19922458	325	80391	eIF/WD40 domain
	11	ubiquitin [Drosophila melanogaster]	gi|158771	309	8543	ubiquitin
	12	GI10230 [Drosophila mojavensis]	gi|195111735	264	84760	DEAD-box helicase
	13	RE16431p [Drosophila melanogaster]	gi|21430596	215	90469	PA_EDEM3_like: protease associated domain
	14	RNA-binding protein FMR1 [Drosophila melanogaster]	gi|10717161	192	75739	K homology RNA-binding domain, type I
	15	CG8042, isoform A [Drosophila melanogaster]	gi|21356345	174	71161	Ubxd2
7	1	heat shock protein cognate 72 [Drosophila melanogaster]	gi|157658	2338	72190	Hsp70
	2	septin interacting protein 3 [Drosophila melanogaster]	gi|28571958	1062	69228	Hrd1
	3	Hrd3 [Drosophila melanogaster]	gi|21355295	1057	89304	Hrd3
	4	GD22351 [Drosophila simulans]	gi|195577859	879	83909	3-hydroxyacyl-CoA dehydrogenase
	5	CG15118, isoform B [Drosophila melanogaster]	gi|19922584	439	71582	protein of unknown function
	6	sarco/ER-type Ca-2+-ATPase [Drosophila melanogaster]	gi|158416	349	109528	E1-E2_ATPase/Cation transporting ATPase
	7	MIP09393p [Drosophila melanogaster]	gi|237757389	331	61795	Acyl-protein synthetase
	8	withered, isoform A [Drosophila melanogaster]	gi|24652463	324	89356	Choline/Carnitine o-acyltransferase
	9	ubiquitin [Drosophila melanogaster]	gi|158767	319	8540	ubiquitin
	10	CG11984, isoform D [Drosophila melanogaster]	gi|281361403	239	62359	Zinc finger present in K+ channel modulatory factor
	11	CG10824 [Drosophila melanogaster]	gi|24648649	229	62109	unknown
	12	CG6904, isoform B [Drosophila melanogaster]	gi|21357845	151	79184	Glycogen Synthase
8	1	heat shock protein cognate 72 [Drosophila melanogaster]	gi|157658	2591	72190	Hsp70

	2	Hrd3 [Drosophila melanogaster]	gi|21355295	1045	89304	Hrd3
	3	growl, isoform A [Drosophila melanogaster]	gi|21355167	897	59706	5-formyltetrahydrofolate cyclo-ligase
	4	septin interacting protein 3 [Drosophila melanogaster]	gi|28571958	864	69228	Hrd1
	5	unnamed protein product [Drosophila melanogaster]	gi|8170	742	60359	Zinc finger present in K+ channel modulatory factor
	6	NADPH--ferrihemoprotein reductase [Drosophila melanogaster]	gi|1296517	740	76359	NADPH-ferrihemoprotein reductase
	7	withered, isoform A [Drosophila melanogaster]	gi|24652463	624	89356	Choline/Carnitine o-acyltransferase
	8	CG4389, isoform B [Drosophila melanogaster]	gi|24583077	559	79588	3-hydroxyacyl-CoA dehydrogenase
	9	SD01152p [Drosophila melanogaster]	gi|16769794	421	77296	Acyl-protein synthetase
	10	sarco/ER-type Ca-2+-ATPase [Drosophila melanogaster]	gi|158416	415	109528	E1-E2_ATPase/Cation transporting ATPase
	11	ubiquitin [Drosophila melanogaster]	gi|158763	361	8558	ubiquitin
	12	TER94 [Drosophila erecta]	gi|194858161	359	88765	TER94
	13	lethal (1) G0193, isoform A [Drosophila melanogaster]	gi|18858077	351	77091	-
	14	GF18742 [Drosophila ananassae]	gi|194745849	291	88253	SEL1
	15	CG15118, isoform B [Drosophila melanogaster]	gi|19922584	223	71582	protein of uknown function
	16	CG3702 [Drosophila melanogaster]	gi|19920668	188	73553	Cleft lip and palate transmembrane protein 1
	17	CG2118, isoform A [Drosophila melanogaster]	gi|24651757	153	76467	Acetyl/propionyl-CoA carboxylase
9	1	heat shock protein cognate 4, isoform A [Drosophila melanogaster]	gi|17737967	1997	71087	Hsp70
	2	Hrd3 [Drosophila melanogaster]	gi|21355295	998	89304	Hrd3
	3	NADPH--ferrihemoprotein reductase [Drosophila melanogaster]	gi|1296517	980	76359	NADPH-ferrihemoprotein reductase
	4	septin interacting protein 3 [Drosophila melanogaster]	gi|28571958	708	69228	Hrd1
	5	CG4673, isoform A [Drosophila melanogaster]	gi|62484318	479	73315	NPL4
	6	growl, isoform A [Drosophila melanogaster]	gi|21355167	475	59706	5-formyltetrahydrofolate cyclo-ligase
	7	sarco/ER-type Ca-2+-ATPase [Drosophila melanogaster]	gi|158416	462	109528	E1-E2_ATPase/Cation transporting ATPase
	8	lethal (1) G0193, isoform A [Drosophila melanogaster]	gi|18858077	459	77091	-
	9	TER94 [Drosophila erecta]	gi|194858161	439	88765	TER94
	10	ubiquitin [Drosophila melanogaster]	gi|158763	331	8558	ubiquitin
	11	GTP-binding protein [Drosophila melanogaster]	gi|24641198	330	67753	signal recognition particle-docking protein FtsY
	12	CG3702 [Drosophila melanogaster]	gi|19920668	293	73553	Cleft lip and palate transmembrane protein 1
	13	GG19855 [Drosophila erecta]	gi|194944118	280	36863	polyubiquitin
	14	poly(A)-binding protein [Drosophila melanogaster]	gi|495594	257	69658	RNA binding protein
	15	Homocysteine-induced ER protein, isoform A [Drosophila melanogaster]	gi|24582606	256	50030	Herp
	16	GM16531 [Drosophila sechellia]	gi|195353788	252	73167	transglutaminase-like domain
	17	GM10754 [Drosophila sechellia]	gi|195343415	250	59608	5-formyltetrahydrofolate cyclo-ligase
	18	CG8237 [Drosophila melanogaster]	gi|20129803	237	36560	
	19	CG9281, isoform B [Drosophila melanogaster]	gi|18859989	230	69458	Elongation Factor 3
	20	IGF-II mRNA-binding protein, isoform A [Drosophila melanogaster]	gi|17530887	202	62091	K homology RNA-binding domain
	21	yolk protein factor 1 beta subunit [Drosophila melanogaster]	gi|450857	182	72390	ATP-dependent DNA helicase
10	1	Hrd3 [Drosophila melanogaster]	gi|21355295	805	89304	Hrd3
	2	septin interacting protein 3 [Drosophila melanogaster]	gi|28571958	790	69228	Hrd1
	3	Homocysteine-induced ER protein, isoform A [Drosophila melanogaster]	gi|24582606	768	50030	Herp
	4	serine palmitoyl transferase LCB2 subunit [Drosophila melanogaster]	gi|5821160	495	65935	serine palmitoyl transferase
	5	GF22986 [Drosophila ananassae]	gi|194764893	481	70104	Hrd1
	6	coro, isoform A [Drosophila melanogaster]	gi|24586098	476	57233	protein of unknown function
	7	CG6766 [Drosophila melanogaster]	gi|24583799	463	59715	Os9
	8	eukaryotic initiation factor 4B, isoform B [Drosophila melanogaster]	gi|62862344	432	52171	eukaryotic initiation factor 4B
	9	GM17026 [Drosophila sechellia]	gi|195345035	380	63819	Aspartyl/asparaginyl-tRNA synthetases
	10	sarco/ER-type Ca-2+-ATPase [Drosophila melanogaster]	gi|158416	368	109528	E1-E2_ATPase/Cation transporting ATPase

	11	ubiquitin [Drosophila melanogaster]	gi|158763	336	8558	ubiquitin
	12	RH21402p [Drosophila melanogaster]	gi|28557577	320	72069	Hsp70
	13	fatty acid (long chain) transport protein [Drosophila melanogaster]	gi|24583463	319	70119	Acyl-protein synthetase
	14	GK22768 [Drosophila willistoni]	gi|195449906	316	89674	SEL1
	15	GG17187 [Drosophila erecta]	gi|194901932	260	61920	RNA binding protein
	16	CG6370 [Drosophila melanogaster]	gi|19922486	254	69187	Oligosaccharyltransferase subunit Ribophorin II
	17	T-cp1zeta [Drosophila melanogaster]	gi|18859933	191	58210	TCP-1/cpn60 chaperonin family/Hsp60
11	1	CG6766 [Drosophila melanogaster]	gi|24583799	1465	59715	Os9
	2	Homocysteine-induced ER protein, isoform A [Drosophila melanogaster]	gi|24582606	767	50030	Herp
	3	coro, isoform A [Drosophila melanogaster]	gi|24586098	757	57233	unknown function
	4	septin interacting protein 3 [Drosophila melanogaster]	gi|28571958	677	69228	Hrd1
	5	GD22141 [Drosophila simulans]	gi|195578651	650	58906	Glucosidase II beta subunit-like protein
	6	CG6370 [Drosophila melanogaster]	gi|19922486	553	69187	Oligosaccharyltransferase subunit Ribophorin II
	7	Rpn5 [Drosophila melanogaster]	gi|21357319	540	57711	Proteasome component
	8	Hrd3 [Drosophila melanogaster]	gi|21355295	537	89304	Hrd3
	9	RH10980p [Drosophila melanogaster]	gi|261338785	492	70151	Very long chain acyl-CoA dehydrogenase
	10	ubiquilin [Drosophila melanogaster]	gi|20129061	395	58798	ubiquilin
	11	proteasome 26S subunit subunit 4 ATPase [Drosophila melanogaster]	gi|24649446	312	49293	proteasome 26S subunit subunit 4 ATPase
	12	pendulin (NLS-receptor) [Drosophila melanogaster]	gi|555821	288	57770	Transporter/Armadillo/beta-catenin-like repeats
	13	phosphatase 2A 65 kDa regulatory subunit [Drosophila melanogaster]	gi|156723	284	65396	protein phosphatase 2A 65 kDa regulatory subunit
	14	CG5642 [Drosophila melanogaster]	gi|21358039	265	63182	RNA polymerase I-associated factor PAF67
	15	GF18742 [Drosophila ananassae]	gi|194745849	244	88253	SEL1
	16	CCT-gamma protein [Drosophila melanogaster]	gi|1199816	220	59472	Involved in productive folding of proteins
	17	RecName: Full=Ubiquitin	gi|51701999	209	8560	ubiquitin
	18	regulatory particle non-ATPase 3 [Drosophila melanogaster]	gi|17137450	174	55970	Proteasome regulatory subunit C-terminal
12	1	CG6766 [Drosophila melanogaster]	gi|24583799	1524	59715	Os-9
	2	proteasome 26S subunit subunit 4 ATPase [Drosophila melanogaster]	gi|24649446	892	49293	proteasome 26S subunit subunit 4 ATPase
	3	ubiquilin [Drosophila melanogaster]	gi|20129061	849	58798	ubiquilin
	4	regulatory particle non-ATPase 3 [Drosophila melanogaster]	gi|17137450	810	55970	Proteasome regulatory subunit C-terminal
	5	GD22141 [Drosophila simulans]	gi|195578651	723	58906	Glucosidase II beta subunit-like protein
	6	eukaryotic initiation factor 4B, isoform B [Drosophila melanogaster]	gi|62862344	644	52171	eukaryotic initiation factor 4B
	7	septin interacting protein 3 [Drosophila melanogaster]	gi|28571958	548	69228	Hrd1
	8	Hrd3 [Drosophila melanogaster]	gi|21355295	499	89304	Hrd3
	9	Rpn5 [Drosophila melanogaster]	gi|21357319	447	57711	Proteasome component
	10	pendulin (NLS-receptor) [Drosophila melanogaster]	gi|555821	445	57770	Transporter/Armadillo/beta-catenin-like repeats
	11	CG6370 [Drosophila melanogaster]	gi|19922486	431	69187	Oligosaccharyltransferase subunit Ribophorin II
	12	GG10283 [Drosophila erecta]	gi|194861414	427	60381	Glucosidase II beta subunit-like protein
	13	alpha-Tubulin at 84B [Drosophila melanogaster]	gi|17136564	423	49876	tubulin alpha chain
	14	Ugt58Fa [Drosophila melanogaster]	gi|22024248	279	59090	UDP-glucoronosyl and UDP-glucosyl transferase
	15	ubiquitin [Drosophila melanogaster]	gi|158763	234	8558	ubiquitin
	16	Homocysteine-induced ER protein, isoform B [Drosophila melanogaster]	gi|19920894	225	27368	Herp
	17	CG5642 [Drosophila melanogaster]	gi|21358039	209	63182	RNA polymerase I-associated factor PAF67
	18	CG8258 [Drosophila melanogaster]	gi|19921848	175	59396	Involved in productive folding of proteins
	19	GF15494 [Drosophila ananassae]	gi|194760539	164	60159	Glucosidase II beta subunit-like protein
	20	GK14262 [Drosophila willistoni]	gi|195453308	147	57517	Pyruvate kinase
13	1	eukaryotic initiation factor 4B, isoform B [Drosophila melanogaster]	gi|62862344	1701	52171	eukaryotic initiation factor 4B
	2	Hrd3 [Drosophila melanogaster]	gi|21355295	1053	89304	Hrd3
	3	beta-Tubulin at 56D, isoform B [Drosophila melanogaster]	gi|24655737	1013	50115	tubulin beta chain

	4	DHR23 [Drosophila melanogaster]	gi|4928709	812	45767	Has ubiquitin associated domain
	5	Fas-associated factor [Drosophila melanogaster]	gi|17137596	661	52928	Ubxd8
	6	supercoiling factor, isoform A [Drosophila melanogaster]	gi|17137602	571	37969	EF-hand, calcium binding motif
	7	60C beta tubulin [Drosophila melanogaster]	gi|860916	552	48805	tubulin beta chain
	8	oligosaccharyltransferase 48kD subunit [Drosophila melanogaster]	gi|24640745	492	49950	Oligosaccharyltransferase 48 kDa subunit beta
	9	GK22768 [Drosophila willistoni]	gi|195449906	433	89674	SEL1
	10	CaBP1 [Drosophila melanogaster]	gi|19921434	346	46723	Protein disulfide isomerase related protein
	11	CG6766 [Drosophila melanogaster]	gi|24583799	332	59715	Os9
	12	GM26527 [Drosophila sechellia]	gi|195331393	327	47763	ATP-dependent 26S proteasome regulatory subunit
	13	aldehyde dehydrogenase [Drosophila melanogaster]	gi|20129399	274	56983	aldehyde dehydrogenase family 2 member
	14	GG11976 [Drosophila erecta]	gi|194905813	266	51791	Acetyl-CoA hydrolase
	15	septin interacting protein 3 [Drosophila melanogaster]	gi|28571958	261	69228	Hrd1
	16	serine palmitoyltransferase subunit I, isoform A [Drosophila melanogaster]	gi|24653276	250	52500	serine palmitoyltransferase subunit I
	17	RecName: Full=Ubiquitin	gi|51701999	249	8560	ubiquitin
	18	Homocysteine-induced ER protein, isoform A [Drosophila melanogaster]	gi|24582606	227	51653	Herp
	19	CG9723 [Drosophila melanogaster]	gi|18860005	216	51653	uncharacterized conserved protein
	20	GK25161 [Drosophila willistoni]	gi|195447816	212	50267	Oligosaccharyltransferase 48 kDa subunit beta
	21	Rpt1 [Drosophila melanogaster]	gi|17137738	208	48511	ATP-dependent 26S proteasome regulatory subunit
	22	RE73786p [Drosophila melanogaster]	gi|25012813	198	50601	Rpt1 subunit of 19S
	23	gamma-tubulin [Drosophila melanogaster]	gi|157570	196	53278	tubulin gamma chain
	24	actin [Drosophila melanogaster]	gi|156750	193	41797	Actin
	25	pontin [Drosophila melanogaster]	gi|7243680	183	50184	beta-catenin binding
	26	CG10616 [Drosophila melanogaster]	gi|24663300	154	54553	protein of unknown function
	27	EF-1-alpha [Drosophila melanogaster]	gi|7915	153	50250	elongation factor 1- alpha
	28	nucleosome assembly protein NAP-1 [Drosophila melanogaster]	gi|1072120	149	42755	nucleosome assembly protein NAP-1
	29	CG8237 [Drosophila melanogaster]	gi|20129803	128	36560	protein of unknown function
14	1	GG12513 [Drosophila erecta]	gi|194911038	569	45288	26S proteasome regulatory complex component
	2	proteasome p44.5 subunit, isoform B [Drosophila melanogaster]	gi|17137740	549	47234	26S proteasome regulatory complex component
	3	GL16409 [Drosophila persimilis]	gi|195164327	548	30017	ATPase associated with wide variety of celluar functions
	4	CG13349, isoform A [Drosophila melanogaster]	gi|19922206	485	41986	Proteasome complex subunit Rpn13 ubiquitin receptor
	5	Rpt6R [Drosophila melanogaster]	gi|24651451	427	45141	ATP-dependent 26S proteasome regulatory subunit
	6	skpA associated protein, isoform A [Drosophila melanogaster]	gi|24645208	305	54773	Carbamoyl-phosphate synthase/succinyl-CoA ligase
	7	actin related protein [Drosophila melanogaster]	gi|558568	293	47032	Actin
	8	isocitrate dehydrogenase, isoform D [Drosophila melanogaster]	gi|24660856	277	48934	Isocitrate/isopropylmalate dehydrogenase
	9	CG8735 [Drosophila melanogaster]	gi|19921826	221	43610	Predicted integral membrane metal-binding protein
	10	ubiquitin [Drosophila melanogaster]	gi|158763	215	8558	ubiquitin
	11	septin interacting protein 3 [Drosophila melanogaster]	gi|28571958	178	69228	Hrd1
	12	hormone epoxide hydrolase 2, isoform A [Drosophila melanogaster]	gi|24655327	171	51972	Predicted hydrolases or acyltransferases
	13	Homocysteine-induced ER protein, isoform A [Drosophila melanogaster]	gi|24582606	169	50030	Herp
	14	CG14969 [Drosophila melanogaster]	gi|28574983	164	34871	Osteopetrosis-associated transmembrane protein1
	15	CG2604, isoform A [Drosophila melanogaster]	gi|21356081	143	47226	uncharacterized conserved protein
15	1	proteasome p44.5 subunit, isoform B [Drosophila melanogaster]	gi|17137740	1182	47234	26S proteasome regulatory complex component
	2	actin [Drosophila melanogaster]	gi|156750	1109	41797	Actin
	3	Rpn7 [Drosophila melanogaster]	gi|21355773	985	45352	26S proteasome regulatory complex component
	4	Rpt4 [Drosophila melanogaster]	gi|24640100	969	44181	ATP-dependent 26S proteasome regulatory subunit
	5	RE23388p [Drosophila melanogaster]	gi|17945503	897	44797	ATP-dependent 26S regulatory subunit/Rpt1
	6	eukaryotic initiation factor 4B, isoform B [Drosophila melanogaster]	gi|62862344	695	52171	eukaryotic initiation factor 4B
	7	Rpt6R [Drosophila melanogaster]	gi|24651451	586	45141	ATP-dependent 26S proteasome regulatory subunit

8	CG13349, isoform A [Drosophila melanogaster]	gi|19922206	561	41986	Proteasome complex subunit Rpn13 ubiquitin receptor
9	GD24111 [Drosophila simulans]	gi|195579768	549	34469	-
10	GI10792 [Drosophila mojavensis]	gi|195113761	479	45405	26S proteasome regulatory complex component
11	Int6 homologue [Drosophila melanogaster]	gi|17137592	353	51129	eIF3 subunit 6 N terminal domain
12	hormone epoxide hydrolase 2, isoform A [Drosophila melanogaster]	gi|24655327	333	51972	Predicted hydrolases or acyltransferases
13	CG5028, isoform A [Drosophila melanogaster]	gi|24650122	321	44404	Isocitrate/isopropylmalate dehydrogenase
14	RE36666p [Drosophila melanogaster]	gi|19528495	319	46774	-
15	Homocysteine-induced ER protein, isoform A [Drosophila melanogaster]	gi|24582606	304	50030	Herp
16	GI10644 [Drosophila mojavensis]	gi|195113257	278	45429	ATP-dependent 26S proteasome regulatory subunit
17	GF11152 [Drosophila ananassae]	gi|194757784	257	41797	Proteasome complex subunit Rpn13 ubiquitin receptor
18	septin interacting protein 3 [Drosophila melanogaster]	gi|28571958	249	69228	Hrd1
19	CG2211 [Drosophila melanogaster]	gi|28575005	218	37857	-
20	CG4164 [Drosophila melanogaster]	gi|19920464	206	40186	DnaJ-class molecular chaperone w/ C-terminal Zn finger
21	ribosomal protein L40 [Drosophila melanogaster]	gi|17136570	199	14720	Ubq - CUE interaction site
22	CG14969 [Drosophila melanogaster]	gi|28574983	198	34871	Osteopetrosis-associated transmembrane protein1
23	GM14611p [Drosophila melanogaster]	gi|17861924	197	31247	Pex19 protein family
24	CG8237 [Drosophila melanogaster]	gi|20129803	197	36560	-
25	CG8735 [Drosophila melanogaster]	gi|19921826	197	43610	Predicted integral membrane metal-binding protein
26	CG32528 [Drosophila melanogaster]	gi|24643390	181	41837	actin binding domain
27	transport and golgi organization 7 [Drosophila melanogaster]	gi|19922220	130	44059	transport and golgi organization 7
28	CG33462 [Drosophila melanogaster]	gi|85816286	93	34644	Trypsin-like serine protease
29	Derlin-2 [Drosophila melanogaster]	gi|21355437	85	29832	Derlin 2

BIBLIOGRAPHY

1. Huh, W.K., Falvo, J.V., Gerke, L.C., Carroll, A.S., Howson, R.W., Weissman, J.S., and O'Shea, E.K. 2003. Global analysis of protein localization in budding yeast. *Nature* 425:686-691.
2. Buck, T.M., Wright, C.M., and Brodsky, J.L. 2007. The activities and function of molecular chaperones in the endoplasmic reticulum. *Semin Cell Dev Biol* 18:751-761.
3. Ellgaard, L., and Helenius, A. 2003. Quality control in the endoplasmic reticulum. *Nat Rev Mol Cell Biol* 4:181-191.
4. Helenius, A., and Aebi, M. 2004. Roles of N-linked glycans in the endoplasmic reticulum. *Annu Rev Biochem* 73:1019-1049.
5. Meusser, B., Hirsch, C., Jarosch, E., and Sommer, T. 2005. ERAD: the long road to destruction. *Nat Cell Biol* 7:766-772.
6. Romisch, K. 2005. Endoplasmic reticulum-associated degradation. *Annu Rev Cell Dev Biol* 21:435-456.
7. Aridor, M. 2007. Visiting the ER: the endoplasmic reticulum as a target for therapeutics in traffic related diseases. *Adv Drug Deliv Rev* 59:759-781.
8. Hebert, D.N., and Molinari, M. 2007. In and out of the ER: protein folding, quality control, degradation, and related human diseases. *Physiol Rev* 87:1377-1408.
9. Liu, Y., Choudhury, P., Cabral, C.M., and Sifers, R.N. 1997. Intracellular disposal of incompletely folded human alpha1-antitrypsin involves release from calnexin and post-translational trimming of asparagine-linked oligosaccharides. *J Biol Chem* 272:7946-7951.
10. Qu, D., Teckman, J.H., Omura, S., and Perlmutter, D.H. 1996. Degradation of a mutant secretory protein, alpha1-antitrypsin Z, in the endoplasmic reticulum requires proteasome activity. *J Biol Chem* 271:22791-22795.
11. Kopito, R.R. 1999. Biosynthesis and degradation of CFTR. *Physiol Rev* 79:S167-173.
12. Varon, R., Magdorf, K., Staab, D., Wahn, H.U., Krawczak, M., Sperling, K., and Reis, A. 1995. Recurrent nasal polyps as a monosymptomatic form of cystic fibrosis associated with a novel in-frame deletion (591del18) in the CFTR gene. *Hum Mol Genet* 4:1463-1464.
13. Molinari, M., Calanca, V., Galli, C., Lucca, P., and Paganetti, P. 2003. Role of EDEM in the release of misfolded glycoproteins from the calnexin cycle. *Science* 299:1397-1400.
14. Molinari, M., Galli, C., Piccaluga, V., Pieren, M., and Paganetti, P. 2002. Sequential assistance of molecular chaperones and transient formation of covalent complexes during protein degradation from the ER. *J Cell Biol* 158:247-257.
15. Koulen, P., Cai, Y., Geng, L., Maeda, Y., Nishimura, S., Witzgall, R., Ehrlich, B.E., and Somlo, S. 2002. Polycystin-2 is an intracellular calcium release channel. *Nat Cell Biol* 4:191-197.

16. Imamura, T., Takata, Y., Sasaoka, T., Takada, Y., Morioka, H., Haruta, T., Sawa, T., Iwanishi, M., Hu, Y.G., Suzuki, Y., et al. 1994. Two naturally occurring mutations in the kinase domain of insulin receptor accelerate degradation of the insulin receptor and impair the kinase activity. *J Biol Chem* 269:31019-31027.
17. Tolleshaug, H., Hobgood, K.K., Brown, M.S., and Goldstein, J.L. 1983. The LDL receptor locus in familial hypercholesterolemia: multiple mutations disrupt transport and processing of a membrane receptor. *Cell* 32:941-951.
18. Cooper, A.A., Gitler, A.D., Cashikar, A., Haynes, C.M., Hill, K.J., Bhullar, B., Liu, K., Xu, K., Strathearn, K.E., Liu, F., et al. 2006. Alpha-synuclein blocks ER-Golgi traffic and Rab1 rescues neuron loss in Parkinson's models. *Science* 313:324-328.
19. Payne, A.S., Kelly, E.J., and Gitlin, J.D. 1998. Functional expression of the Wilson disease protein reveals mislocalization and impaired copper-dependent trafficking of the common H1069Q mutation. *Proc Natl Acad Sci U S A* 95:10854-10859.
20. De Jaco, A., Comoletti, D., Kovarik, Z., Gaietta, G., Radic, Z., Lockridge, O., Ellisman, M.H., and Taylor, P. 2006. A mutation linked with autism reveals a common mechanism of endoplasmic reticulum retention for the alpha,beta-hydrolase fold protein family. *J Biol Chem* 281:9667-9676.
21. VanSlyke, J.K., Deschenes, S.M., and Musil, L.S. 2000. Intracellular transport, assembly, and degradation of wild-type and disease-linked mutant gap junction proteins. *Mol Biol Cell* 11:1933-1946.
22. Carvalho, P., Goder, V., and Rapoport, T.A. 2006. Distinct ubiquitin-ligase complexes define convergent pathways for the degradation of ER proteins. *Cell* 126:361-373.
23. Vashist, S., and Ng, D.T. 2004. Misfolded proteins are sorted by a sequential checkpoint mechanism of ER quality control. *J Cell Biol* 165:41-52.
24. Vembar, S.S., and Brodsky, J.L. 2008. One step at a time: endoplasmic reticulum-associated degradation. *Nat Rev Mol Cell Biol* 9:944-957.
25. Ye, Y., Shibata, Y., Yun, C., Ron, D., and Rapoport, T.A. 2004. A membrane protein complex mediates retro-translocation from the ER lumen into the cytosol. *Nature* 429:841-847.
26. Lilley, B.N., and Ploegh, H.L. 2004. A membrane protein required for dislocation of misfolded proteins from the ER. *Nature* 429:834-840.
27. Kostova, Z., Tsai, Y.C., and Weissman, A.M. 2007. Ubiquitin ligases, critical mediators of endoplasmic reticulum-associated degradation. *Semin Cell Dev Biol* 18:770-779.
28. Ye, Y., Meyer, H.H., and Rapoport, T.A. 2001. The AAA ATPase Cdc48/p97 and its partners transport proteins from the ER into the cytosol. *Nature* 414:652-656.
29. Schuberth, C., and Buchberger, A. 2008. UBX domain proteins: major regulators of the AAA ATPase Cdc48/p97. *Cell Mol Life Sci* 65:2360-2371.
30. Nakatsukasa, K., Huyer, G., Michaelis, S., and Brodsky, J.L. 2008. Dissecting the ER-associated degradation of a misfolded polytopic membrane protein. *Cell* 132:101-112.

31. Koegl, M., Hoppe, T., Schlenker, S., Ulrich, H.D., Mayer, T.U., and Jentsch, S. 1999. A novel ubiquitination factor, E4, is involved in multiubiquitin chain assembly. *Cell* 96:635-644.
32. Raasi, S., and Wolf, D.H. 2007. Ubiquitin receptors and ERAD: a network of pathways to the proteasome. *Semin Cell Dev Biol* 18:780-791.
33. Wiertz, E.J., Jones, T.R., Sun, L., Bogyo, M., Geuze, H.J., and Ploegh, H.L. 1996. The human cytomegalovirus US11 gene product dislocates MHC class I heavy chains from the endoplasmic reticulum to the cytosol. *Cell* 84:769-779.
34. Huppa, J.B., and Ploegh, H.L. 1997. The alpha chain of the T cell antigen receptor is degraded in the cytosol. *Immunity* 7:113-122.
35. Wiertz, E.J., Tortorella, D., Bogyo, M., Yu, J., Mothes, W., Jones, T.R., Rapoport, T.A., and Ploegh, H.L. 1996. Sec61-mediated transfer of a membrane protein from the endoplasmic reticulum to the proteasome for destruction. *Nature* 384:432-438.
36. VanSlyke, J.K., and Musil, L.S. 2002. Dislocation and degradation from the ER are regulated by cytosolic stress. *J Cell Biol* 157:381-394.
37. Goldstein, J.L., and Brown, M.S. 1990. Regulation of the mevalonate pathway. *Nature* 343:425-430.
38. Roitelman, J., Olender, E.H., Bar-Nun, S., Dunn, W.A., Jr., and Simoni, R.D. 1992. Immunological evidence for eight spans in the membrane domain of 3-hydroxy-3-methylglutaryl coenzyme A reductase: implications for enzyme degradation in the endoplasmic reticulum. *J Cell Biol* 117:959-973.
39. Liscum, L., Finer-Moore, J., Stroud, R.M., Luskey, K.L., Brown, M.S., and Goldstein, J.L. 1985. Domain structure of 3-hydroxy-3-methylglutaryl coenzyme A reductase, a glycoprotein of the endoplasmic reticulum. *J Biol Chem* 260:522-530.
40. Gil, G., Faust, J.R., Chin, D.J., Goldstein, J.L., and Brown, M.S. 1985. Membrane-bound domain of HMG CoA reductase is required for sterol-enhanced degradation of the enzyme. *Cell* 41:249-258.
41. Brown, M.S., and Goldstein, J.L. 1980. Multivalent feedback regulation of HMG CoA reductase, a control mechanism coordinating isoprenoid synthesis and cell growth. *J Lipid Res* 21:505-517.
42. Sever, N., Yang, T., Brown, M.S., Goldstein, J.L., and DeBose-Boyd, R.A. 2003. Accelerated degradation of HMG CoA reductase mediated by binding of insig-1 to its sterol-sensing domain. *Mol Cell* 11:25-33.
43. Sever, N., Song, B.L., Yabe, D., Goldstein, J.L., Brown, M.S., and DeBose-Boyd, R.A. 2003. Insig-dependent ubiquitination and degradation of mammalian 3-hydroxy-3-methylglutaryl-CoA reductase stimulated by sterols and geranylgeraniol. *J Biol Chem* 278:52479-52490.
44. Sever, N., Lee, P.C., Song, B.L., Rawson, R.B., and Debose-Boyd, R.A. 2004. Isolation of mutant cells lacking Insig-1 through selection with SR-12813, an agent that stimulates degradation of 3-hydroxy-3-methylglutaryl-coenzyme A reductase. *J Biol Chem* 279:43136-43147.

45. Lee, P.C., Sever, N., and Debose-Boyd, R.A. 2005. Isolation of sterol-resistant Chinese hamster ovary cells with genetic deficiencies in both Insig-1 and Insig-2. *J Biol Chem* 280:25242-25249.
46. Jo, Y., Lee, P.C., Sguigna, P.V., and DeBose-Boyd, R.A. 2011. Sterol-induced degradation of HMG CoA reductase depends on interplay of two Insigs and two ubiquitin ligases, gp78 and Trc8. *Proc Natl Acad Sci U S A* 108:20503-20508.
47. Hartman, I.Z., Liu, P., Zehmer, J.K., Luby-Phelps, K., Jo, Y., Anderson, R.G., and DeBose-Boyd, R.A. 2010. Sterol-induced dislocation of 3-hydroxy-3-methylglutaryl coenzyme A reductase from endoplasmic reticulum membranes into the cytosol through a subcellular compartment resembling lipid droplets. *J Biol Chem* 285:19288-19298.
48. Feramisco, J.D., Goldstein, J.L., and Brown, M.S. 2004. Membrane topology of human insig-1, a protein regulator of lipid synthesis. *J Biol Chem* 279:8487-8496.
49. Nohturfft, A., Brown, M.S., and Goldstein, J.L. 1998. Topology of SREBP cleavage-activating protein, a polytopic membrane protein with a sterol-sensing domain. *J Biol Chem* 273:17243-17250.
50. Espenshade, P.J., Li, W.P., and Yabe, D. 2002. Sterols block binding of COPII proteins to SCAP, thereby controlling SCAP sorting in ER. *Proc Natl Acad Sci U S A* 99:11694-11699.
51. Sun, L.P., Li, L., Goldstein, J.L., and Brown, M.S. 2005. Insig required for sterol-mediated inhibition of Scap/SREBP binding to COPII proteins in vitro. *J Biol Chem* 280:26483-26490.
52. Horton, J.D., Goldstein, J.L., and Brown, M.S. 2002. SREBPs: transcriptional mediators of lipid homeostasis. *Cold Spring Harb Symp Quant Biol* 67:491-498.
53. Gong, Y., Lee, J.N., Lee, P.C., Goldstein, J.L., Brown, M.S., and Ye, J. 2006. Sterol-regulated ubiquitination and degradation of Insig-1 creates a convergent mechanism for feedback control of cholesterol synthesis and uptake. *Cell Metab* 3:15-24.
54. Lee, J.N., Zhang, X., Feramisco, J.D., Gong, Y., and Ye, J. 2008. Unsaturated fatty acids inhibit proteasomal degradation of Insig-1 at a postubiquitination step. *J Biol Chem* 283:33772-33783.
55. Clemens, J.C., Worby, C.A., Simonson-Leff, N., Muda, M., Maehama, T., Hemmings, B.A., and Dixon, J.E. 2000. Use of double-stranded RNA interference in Drosophila cell lines to dissect signal transduction pathways. *Proc Natl Acad Sci U S A* 97:6499-6503.
56. Dobrosotskaya, I.Y., Seegmiller, A.C., Brown, M.S., Goldstein, J.L., and Rawson, R.B. 2002. Regulation of SREBP processing and membrane lipid production by phospholipids in Drosophila. *Science* 296:879-883.
57. Seegmiller, A.C., Dobrosotskaya, I., Goldstein, J.L., Ho, Y.K., Brown, M.S., and Rawson, R.B. 2002. The SREBP pathway in Drosophila: regulation by palmitate, not sterols. *Dev Cell* 2:229-238.
58. Clark, A.J., and Block, K. 1959. The absence of sterol synthesis in insects. *J Biol Chem* 234:2578-2582.

59. Nguyen, A.D., Lee, S.H., and DeBose-Boyd, R.A. 2009. Insig-mediated, sterol-accelerated degradation of the membrane domain of hamster 3-hydroxy-3-methylglutaryl-coenzyme A reductase in insect cells. *J Biol Chem* 284:26778-26788.
60. Sakai, J., Nohturfft, A., Cheng, D., Ho, Y.K., Brown, M.S., and Goldstein, J.L. 1997. Identification of complexes between the COOH-terminal domains of sterol regulatory element-binding proteins (SREBPs) and SREBP cleavage-activating protein. *J Biol Chem* 272:20213-20221.
61. Nohturfft, A., Yabe, D., Goldstein, J.L., Brown, M.S., and Espenshade, P.J. 2000. Regulated step in cholesterol feedback localized to budding of SCAP from ER membranes. *Cell* 102:315-323.
62. Yang, T., Espenshade, P.J., Wright, M.E., Yabe, D., Gong, Y., Aebersold, R., Goldstein, J.L., and Brown, M.S. 2002. Crucial step in cholesterol homeostasis: sterols promote binding of SCAP to INSIG-1, a membrane protein that facilitates retention of SREBPs in ER. *Cell* 110:489-500.
63. Lee, J.N., Song, B., DeBose-Boyd, R.A., and Ye, J. 2006. Sterol-regulated degradation of Insig-1 mediated by the membrane-bound ubiquitin ligase gp78. *J Biol Chem* 281:39308-39315.
64. Brodsky, J.L., and Skach, W.R. 2011. Protein folding and quality control in the endoplasmic reticulum: Recent lessons from yeast and mammalian cell systems. *Curr Opin Cell Biol* 23:464-475.
65. Dobrosotskaya, I.Y., Goldstein, J.L., Brown, M.S., and Rawson, R.B. 2003. Reconstitution of sterol-regulated endoplasmic reticulum-to-Golgi transport of SREBP-2 in insect cells by co-expression of mammalian SCAP and Insigs. *J Biol Chem* 278:35837-35843.
66. Deshaies, R.J., and Joazeiro, C.A. 2009. RING domain E3 ubiquitin ligases. *Annu Rev Biochem* 78:399-434.
67. Denic, V., Quan, E.M., and Weissman, J.S. 2006. A luminal surveillance complex that selects misfolded glycoproteins for ER-associated degradation. *Cell* 126:349-359.
68. Hassink, G., Kikkert, M., van Voorden, S., Lee, S.J., Spaapen, R., van Laar, T., Coleman, C.S., Bartee, E., Fruh, K., Chau, V., et al. 2005. TEB4 is a C4HC3 RING finger-containing ubiquitin ligase of the endoplasmic reticulum. *Biochem J* 388:647-655.
69. Hannah, V.C., Ou, J., Luong, A., Goldstein, J.L., and Brown, M.S. 2001. Unsaturated fatty acids down-regulate srebp isoforms 1a and 1c by two mechanisms in HEK-293 cells. *J Biol Chem* 276:4365-4372.
70. Goldstein, J.L., Basu, S.K., and Brown, M.S. 1983. Receptor-mediated endocytosis of low-density lipoprotein in cultured cells. *Methods Enzymol* 98:241-260.
71. Herz, J., Kowal, R.C., Ho, Y.K., Brown, M.S., and Goldstein, J.L. 1990. Low density lipoprotein receptor-related protein mediates endocytosis of monoclonal antibodies in cultured cells and rabbit liver. *J Biol Chem* 265:21355-21362.

72. Liang, G., Yang, J., Horton, J.D., Hammer, R.E., Goldstein, J.L., and Brown, M.S. 2002. Diminished hepatic response to fasting/refeeding and liver X receptor agonists in mice with selective deficiency of sterol regulatory element-binding protein-1c. *J Biol Chem* 277:9520-9528.
73. Hampton, R.Y., and Garza, R.M. 2009. Protein quality control as a strategy for cellular regulation: lessons from ubiquitin-mediated regulation of the sterol pathway. *Chem Rev* 109:1561-1574.
74. Theesfeld, C.L., Pourmand, D., Davis, T., Garza, R.M., and Hampton, R.Y. 2011. The sterol-sensing domain (SSD) directly mediates signal-regulated endoplasmic reticulum-associated degradation (ERAD) of 3-hydroxy-3-methylglutaryl (HMG)-CoA reductase isozyme Hmg2. *J Biol Chem* 286:26298-26307.
75. Correll, C.C., and Edwards, P.A. 1994. Mevalonic acid-dependent degradation of 3-hydroxy-3-methylglutaryl-coenzyme A reductase in vivo and in vitro. *J Biol Chem* 269:633-638.
76. Roitelman, J., and Simoni, R.D. 1992. Distinct sterol and nonsterol signals for the regulated degradation of 3-hydroxy-3-methylglutaryl-CoA reductase. *J Biol Chem* 267:25264-25273.
77. Nakanishi, M., Goldstein, J.L., and Brown, M.S. 1988. Multivalent control of 3-hydroxy-3-methylglutaryl coenzyme A reductase. Mevalonate-derived product inhibits translation of mRNA and accelerates degradation of enzyme. *J Biol Chem* 263:8929-8937.
78. Yang, Y., Kitagaki, J., Dai, R.M., Tsai, Y.C., Lorick, K.L., Ludwig, R.L., Pierre, S.A., Jensen, J.P., Davydov, I.V., Oberoi, P., et al. 2007. Inhibitors of ubiquitin-activating enzyme (E1), a new class of potential cancer therapeutics. *Cancer Res* 67:9472-9481.
79. Jo, Y., Sguigna, P.V., and DeBose-Boyd, R.A. 2011. Membrane-associated ubiquitin ligase complex containing gp78 mediates sterol-accelerated degradation of 3-hydroxy-3-methylglutaryl-coenzyme A reductase. *J Biol Chem* 286:15022-15031.
80. Brodsky, J.L. 2012. Cleaning up: ER-associated degradation to the rescue. *Cell* 151:1163-1167.
81. Pickart, C.M. 2001. Mechanisms underlying ubiquitination. *Annu Rev Biochem* 70:503-533.
82. Hampton, R.Y., Gardner, R.G., and Rine, J. 1996. Role of 26S proteasome and HRD genes in the degradation of 3-hydroxy-3-methylglutaryl-CoA reductase, an integral endoplasmic reticulum membrane protein. *Mol Biol Cell* 7:2029-2044.
83. Faulkner, R.A., Nguyen, A.D., Jo, Y., and DeBose-Boyd, R.A. 2013. Lipid-regulated degradation of HMG-CoA reductase and Insig-1 through distinct mechanisms in insect cells. *J Lipid Res* 54:1011-1022.
84. Schulze, A., Standera, S., Buerger, E., Kikkert, M., van Voorden, S., Wiertz, E., Koning, F., Kloetzel, P.M., and Seeger, M. 2005. The ubiquitin-domain protein HERP forms a complex with components of the endoplasmic reticulum associated degradation pathway. *J Mol Biol* 354:1021-1027.

85. Christianson, J.C., Shaler, T.A., Tyler, R.E., and Kopito, R.R. 2008. OS-9 and GRP94 deliver mutant alpha1-antitrypsin to the Hrd1-SEL1L ubiquitin ligase complex for ERAD. *Nat Cell Biol* 10:272-282.
86. Bays, N.W., Gardner, R.G., Seelig, L.P., Joazeiro, C.A., and Hampton, R.Y. 2001. Hrd1p/Der3p is a membrane-anchored ubiquitin ligase required for ER-associated degradation. *Nat Cell Biol* 3:24-29.
87. Kim, T.Y., Kim, E., Yoon, S.K., and Yoon, J.B. 2008. Herp enhances ER-associated protein degradation by recruiting ubiquilins. *Biochem Biophys Res Commun* 369:741-746.
88. Gardner, R.G., Swarbrick, G.M., Bays, N.W., Cronin, S.R., Wilhovsky, S., Seelig, L., Kim, C., and Hampton, R.Y. 2000. Endoplasmic reticulum degradation requires lumen to cytosol signaling. Transmembrane control of Hrd1p by Hrd3p. *J Cell Biol* 151:69-82.
89. Ploegh, H.L. 2007. A lipid-based model for the creation of an escape hatch from the endoplasmic reticulum. *Nature* 448:435-438.
90. Martin, S., and Parton, R.G. 2006. Lipid droplets: a unified view of a dynamic organelle. *Nat Rev Mol Cell Biol* 7:373-378.
91. Liu, P., Ying, Y., Zhao, Y., Mundy, D.I., Zhu, M., and Anderson, R.G. 2004. Chinese hamster ovary K2 cell lipid droplets appear to be metabolic organelles involved in membrane traffic. *J Biol Chem* 279:3787-3792.
92. Ohsaki, Y., Cheng, J., Fujita, A., Tokumoto, T., and Fujimoto, T. 2006. Cytoplasmic lipid droplets are sites of convergence of proteasomal and autophagic degradation of apolipoprotein B. *Mol Biol Cell* 17:2674-2683.
93. Petris, G., Vecchi, L., Bestagno, M., and Burrone, O.R. 2011. Efficient detection of proteins retro-translocated from the ER to the cytosol by in vivo biotinylation. *PLoS One* 6:e23712.